Science of the Total Environment 579 (2017) 1000–1034

Contents lists available at ScienceDirect

Science of the Total Environment

journal homepage: www.elsevier.com/locate/scitotenv

Review

A review of biomass burning: Emissions and impacts on air quality, health and climate in China

Jianmin Chen [a,h,*], Chunlin Li [a], Zoran Ristovski [b], Andelija Milic [b], Yuantong Gu [b], Mohammad S. Islam [b], Shuxiao Wang [c], Jiming Hao [c,**], Hefeng Zhang [d], Congrong He [b], Hai Guo [e], Hongbo Fu [a], Branka Miljevic [b], Lidia Morawska [b,**], Phong Thai [b], Yun Fat LAM [f], Gavin Pereira [g], Aijun Ding [h], Xin Huang [h], Umesh C. Dumka [a,i]

[a] Shanghai Key Laboratory of Atmospheric Particle Pollution and Prevention, Department of Environmental Science and Engineering, Institute of Atmospheric Sciences, Fudan University, Shanghai 200433, China
[b] International Laboratory for Air Quality and Health, Queensland University of Technology, Brisbane, QLD 4001, Australia
[c] State Key Joint Laboratory of Environment Simulation and Pollution Control, School of Environment, Tsinghua University, Beijing 100084, China
[d] State Key Laboratory of Environmental Criteria and Risk Assessment, Chinese Research Academy of Environmental Sciences, Beijing 100012, China
[e] Department of Civil and Environmental Engineering, Hong Kong Polytechnic University, Hong Kong, China
[f] School of Energy and Environment, City University of Hong Kong, Hong Kong, China
[g] School of Public Health, Curtin University, Perth, WA, 6000, Australia
[h] Collaborative Innovation Center of Climate Change, School of Atmospheric Sciences, Nanjing University, Nanjing 210023, China
[i] Aryabhatta Research Institute of Observational Sciences, Manora Peak, Nainital 263001, India

HIGHLIGHTS

- This review discusses wildfire and anthropogenic emission from biomass burning in China.
- Field observations and laboratory studies on public health and climate impacts of biomass burning
- Atmospheric process of biomass burning plumes and their transport
- Proposed research priorities and insights about biomass burning in China

GRAPHICAL ABSTRACT

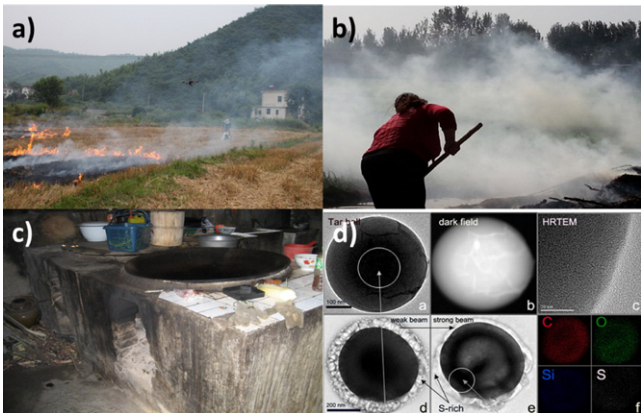

Open field biomass burning causes severe air pollution, public health risk and potential climate impact. a) Photo taken in Changzhou rural area on June 10, 2015; b) Photo taken in Hebei rural area on October 23, 2013; c) A traditional indoor burner in rural area in China; d) Tar ball emitted from biomass burning.

ARTICLE INFO

Article history:
Received 1 September 2016
Received in revised form 4 November 2016
Accepted 4 November 2016
Available online 29 November 2016

ABSTRACT

Biomass burning (BB) is a significant air pollution source, with global, regional and local impacts on air quality, public health and climate. Worldwide an extensive range of studies has been conducted on almost all the aspects of BB, including its specific types, on quantification of emissions and on assessing its various impacts. China is one of the countries where the significance of BB has been recognized, and a lot of research efforts devoted to investigate it, however, so far no systematic reviews were conducted to synthesize the information which has been

* Corresponding author at: Shanghai Key Laboratory of Atmospheric Particle Pollution and Prevention, Department of Environmental Science and Engineering, Institute of Atmospheric Sciences, Fudan University, Shanghai 200433, China.
** Corresponding authors.
E-mail addresses: jmchen@fudan.edu.cn (J. Chen), hjm-den@tsinghua.edu.cn (J. Hao), l.morawska@qut.edu.au (L. Morawska).

http://dx.doi.org/10.1016/j.scitotenv.2016.11.025

Editor: D. Barcelo

Keywords:
Biomass burning
Emission
Air quality
Health
Climate
China

emerging. Therefore the aim of this work was to comprehensively review most of the studies published on this topic in China, including literature concerning field measurements, laboratory studies and the impacts of BB indoors and outdoors in China. In addition, this review provides insights into the role of wildfire and anthropogenic BB on air quality and health globally. Further, we attempted to provide a basis for formulation of policies and regulations by policy makers in China.

Contents

1. Introduction

Traditionally, Chinese families used to collect and store the biomass of crop residues, weeds, branches and leaves as irreplaceable fuel for cooking or heating, and there are still some rural areas where this practice continues (Fig. 1a, b). Usually, this does not produce distinct air pollution events as the BB emissions are similar through the year. Recently, due to rapid economic growth and urbanization in China, crop residues have been often field burnt post harvests in a couple of days to prepare for planting the next season's crops (Fig. 1c, d). Rice, wheat and corn straws are the top three crop residues in China, which make up 75% of total straw productions. Usually, there are three concentrated periods of BB: i) rice/wheat straw field burning from South to North of China, which is called summer harvest season (some reports call this spring harvest) in the late of May to the end of June; ii) crop residue burning in October, mainly corn residue burning in North China, and second

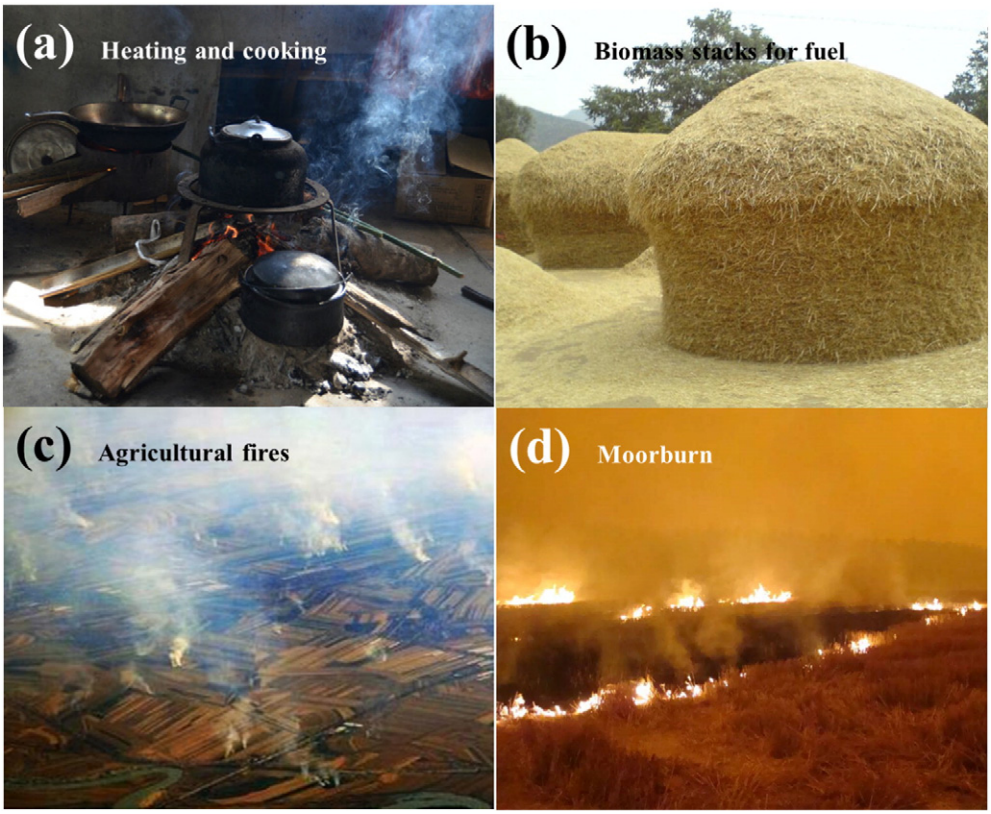

Fig. 1. Representative figures for biomass burning in China.

season rice straw burning in South China; iii) heating in winter in North China. This seasonality in BB was observed by Cheng et al. (2014a). They monitored air pollution in five cities (Shanghai, Hangzhou, Ningbo, Suzhou and Nanjing) of the Yangtze River delta (YRD), and found a ten days heavy haze episode with visibility of 2.9–9.8 km from 28 May to 6 June 2011. The average and maximum daily $PM_{2.5}$ concentrations during the episode were 82 and 144 μg/m^3, respectively. Estimation based on observation data and Community Multi-scale Air Quality (CMAQ) model simulation indicated that biomass open burning contributed 37% of ambient $PM_{2.5}$ in the harvest period in YRD (Cheng et al., 2014a). An on-line study on water-soluble potassium ion (K^+) in PM_{10} and trace gaseous pollutants revealed that BB had a significant impact on Shanghai air quality from 22 May to 30 June during the summer harvest time of 2009 (Li et al., 2010a). The average K^+ concentration (3.96 μg/m^3) of severely polluted days within 2.0–8.5 μg/m^3 was more than 24 times that of clear days, in the range of 0.0–0.3 μg/m^3 (Li et al., 2010a). Three-year on-line measurements of $PM_{2.5}$ chemical compositions have shown that $PM_{2.5}$ mass concentration could increase because of BB to a high level with an average of 134 μg/m^3, being three times higher than that of clear days from 2011 to 2013 in Shanghai (Wang et al., 2015a).

BB has played a noticeable role in unexpected severe haze episodes that overlapped with the primary and secondary pollutants derived from engine exhausts and coal combustion. Huang et al. (2014) investigated the chemical components and sources of $PM_{2.5}$ in Beijing, Shanghai, Guangzhou and Xi'an upon a severe and persistent haze pollution, which affected 1.3 million km^2 and 800 million people in January 2013. The calculated contributions of fossil origin secondary organic aerosol (SOA) to the total organic aerosol (OA) mass were 1.1–2.4 times larger for high pollution events than for clear or less polluted days, highlighting the importance of fossil-derived SOA, or fossil SOA, to particulate pollution. Fossil SOA accounts for 25–40% of OA mass or 45–65% of SOA mass in Shanghai and Beijing, consistent with the large emissions of SOA precursors from high traffic flow and/or large coal usage for domestic heating/cooking at these locations. The fossil SOA fraction decreases to 10–20% of OA mass in Guangzhou and Xi'an, with the non-fossil SOA fraction increasing to 30–60% of the OA mass or 65–85% of the SOA mass, mostly due to the enhanced BB activities (Huang et al., 2014).

Agricultural residues burning calls for close attention in China as it emits significant amounts of greenhouse gases such as CO_2, CO and hydrocarbons, other gaseous pollutants such as SO_2 and NO_x, and smoke particles carrying carcinogenic substances with a wide size distribution (Li et al., 2007; Zhang et al., 2008a; Zhang et al., 2011a; Li et al., 2016a; Sun et al., 2016a). A significant amount of toluene, isoprene, and propene (active volatile organic components (VOCs) and O_3 precursors (Mellouki et al., 2015)), have been detected with high total ozone formation potential (OFP) values from BB observation at a rural site in Northern China during summer 2013 (Zhu et al., 2016b). The spatial–temporal variation of BB in June from 2005 to 2012 has revealed that the wheat harvest season in the North China has a significant influence on the regional aerosol optical depth (AOD) and the chemical compositions of size-segregated aerosols (Wang et al., 2015b). Under high relative humidity and south winds, emissions from straw burning combined with high urban/industrial emissions to produce intensive regional haze pollution in the North Plain. The formation of secondary inorganic particles was intensified due to the interactions of smoke plumes of BB and urban/industrial pollutants in an urban environment (Wang et al., 2015b).

Polycyclic aromatic hydrocarbons (PAHs) are typical carcinogenic substances. As a respiratory exposure health care, laboratory studies are conducted to determine PAHs emissions from the burning of rice, wheat, and corn straws in China (Zhang et al., 2011a). PAHs in both particulate and gaseous phases were simultaneously collected and analyzed. It shows that PAHs emission factors of rice, wheat, and corn straws were 5.26, 1.37, and 1.74 mg/kg, respectively. The total PAHs emissions from the burning of three agricultural crop residues in China were estimated to be 1.09 Gg for the year 2004 (Zhang et al.,

2011a). However, there are only a handful of reports on the impact of BB on health in China (Zhang et al., 2011a; Lin et al., 2015a).

BB is of global concern, particularly in recent years due to its link to climate changes. BB emits significant amounts of short-living global warming substances (Gustafsson et al., 2009; Ramana et al., 2010; Lack et al., 2012; Victor et al., 2015) such as black carbon, and also significantly contributes to ozone formation by photochemical reactions among its precursor VOCs and NO_x. An excellent review has covered optical properties of smoke particles relative to radiative forcing (Reid et al., 2005a). It included available data from published sensitivity studies, field campaigns, and inversions from the Aerosol Robotic Network (AERONET) of Sun photometer sites (Reid et al., 2005a). So far, there has been less work conducted on this aspect in China.

Here, we include advances on BB emissions and their impacts on air quality, public health and climate in China. This may be helpful to assess the regional emissions of BB and its connection and role on a global scope.

2. Monitoring of biomass burning

2.1. Field observations

Field observation is a practical way to characterize properties and dynamic changes of BB pollutants (Reid et al., 2005a, b). Outdoor studies concerning BB try i) to depict the contribution of smoke plumes to regional or global reactive trace gases, $PM_{2.5}$, and cloud condensation nuclei (CCN) concentrations lifting via transportation (Du et al., 2011; Rose et al., 2011; Wang et al., 2013; Zauscher et al., 2013; Ding et al., 2015; Bougiatioti et al., 2016), ii) to elucidate the role of smoke aerosol in triggering haze and new particle formation (NPF) (Ding et al., 2013a; Wang et al., 2013; Yang et al., 2015; Sun et al., 2016b), iii) to figure out the relationship between smoke aerosol emissions and social welfare loss (e.g., air quality deterioration in visibility decrease, public health hazard, etc.) (Lai and Sequeira, 2001; Fullerton et al., 2008; Bølling et al., 2009; Saffari et al., 2013), iv) to explain the mechanism of smoke particles aging and internal mixing with ambient aerosols (Capes et al., 2008; Jolleys et al., 2012; Zauscher et al., 2013), and v) to describe the influence of smoke particle emission and aging on the physiochemical property changes of ambient aerosols (e.g., chemical compositions, redox activity, morphology, light scattering-absorption, hygroscopicity, etc.) and also the influence on the atmospheric chemical process (e.g., diurnal O_3 formation, nocturnal chloride and NO_y chemistry, HONO chemistry, etc.) (Cape et al., 2011; Jaffe and Wigder, 2012; Saffari et al., 2013; Li et al., 2015; Nie et al., 2015; Bougiatioti et al., 2016; Hu et al., 2016). Field observations have a definite advantage over laboratory study, as the investigations are conducted on-site close to the actual burning (Li et al., 2007; Ding et al., 2013a, 2013b; Brito et al., 2014; Liu et al., 2014). However, some unfavorable factors such as variable environmental conditions, random burning process, inevitable chemical contaminations and ultra-low concentration of target components due to atmospheric dilution also add the challenges to the practical work, and the deviations between field research and laboratory study were also reported (Dhammapala et al., 2007; Mohr et al., 2009; Aurell et al., 2015; Carrico et al., 2016). Actually, results from field investigation incorporated with laboratory studies and numerical simulations would supply more precise and thorough results (Huang et al., 2012a; Calfapietra et al., 2016; Huo et al., 2016; Pokhrel et al., 2016).

Field fire can be classified as agricultural open burning, forest and basin fire in term of burning activity, scales, and fuel issues (e.g., straw stack burning, residue field burning, grassland fire, forest fire, biofuel waste open burning) (Li et al., 2003, 2007; Martins et al., 2009; Huang et al., 2012b; Da Rocha et al., 2005). In China, in-situ fire studies have mainly focused on the agricultural straw burning, and field observations monitor and discriminate pollutants from BB via the methods including but not limited to instrumental on-line measurements and offline analysis of PM and gas samples (Du et al., 2011; Rose et al., 2011; Ding et al., 2013a; Huang et al., 2014; Wang et al., 2015a; Yao et al., 2016a). Chemical markers or signals (e.g., potassium, levoglucose, mannosan, galactosan, and some non-methane VOCs), diagnostic ratios (e.g., K^+/EC, OC/EC, char-EC/soot-EC, ratios of PAHs and some gaseous species), and specific target particles (e.g., soot, tar ball, crystal KCl particles) are commonly used to trace BB in the field and help make source apportionment of BB emissions (Guo et al., 2004; Bo et al., 2008; Han et al., 2009; Li and Shao, 2009; Wang et al., 2011; Fu et al., 2012; Saffari et al., 2013; Li et al., 2015; Li et al., 2016a). BB as a potential source of ambient primary and secondary carbonaceous aerosol has been widely reported, and BB events have also been found to be highly correlated with heavy pollution events like haze, fog, NPF, and photochemical smog (Kaul et al., 2011; Li et al., 2011b; Wang et al., 2013; Yang et al., 2015; Wang et al., 2016a).

By a synergy of ground-based monitoring and satellite-lidar observation, three typical haze types in Shanghai are identified as the secondary inorganic aerosol (SIA) pollution, dust, and BB (Du et al., 2011; Huang et al., 2012d). Even in the dust haze (dust storm) episode, soot and tar ball internally mixing with K-rich particles are encountered frequently, and heterogeneous reactions occur to convert Cl^- into SO_4^{2-} and NO_3^- during smoke plume transportation, while BB emissions also facilitate solubility of iron in dust (Fu et al., 2012; Fu et al., 2014). Field studies in multi-cities over China suggest that severe haze episodes are driven to a large extent, by secondary organic and inorganic aerosols (SIA and SOA are of similar importance). BB primary emissions contributed 5–20% of $PM_{2.5}$ mass generally during haze episodes, while VOCs and SO_2-NO_x-NH_3 from BB may present even more contribution to SOA and SIA (Streets et al., 2003; Huang et al., 2014). Apart from elevating aerosol mass concentration, BB plume suppresses nucleation mode and CCN activity of ambient particles, while increases field AOD and absorption angstrom exponent (AAE) in mixing and transportation process (Agus et al., 2008; Nowak et al., 2010; He et al., 2015).

2.2. Satellite remote sensing

The ground-based instruments are very useful for continuous measurements of local and regional properties of atmospheric aerosols, which play an important role in the estimation of BB aerosol's impact on the Earth's radiation budget and, hence, local and regional climate (e.g. Badarinath et al., 2009; Mielonen et al., 2013). However, for the global monitoring of the BB aerosol properties, in general, and fire spots, emissions, concentrations, distribution, vertical profiles and long-range transport, in particular, multiple satellite sensors such as MODIS (Moderate Resolution Imaging Spectroradiometer), MISR (Multi-Angle Imaging Spectroradiometer), CALIPSO (Cloud-Aerosol Lidar Infrared Pathfinder Satellite Observation), OMI (Ozone Monitoring Instrument), MOPITT (Measurements of Pollution in the Troposphere) and AIRS (Atmospheric Infrared Sounder), among others are commonly used. These sensors help in studying the BB aerosols by retrieving various products of aerosol optical and physical properties, precursors and trace gases, vertical profiles, fire count, Fire Radiative Power (FRP), smoke-plume characteristics and long-range transport and mapping of the burned areas (e.g. Guan et al., 2010; Kaskaoutis et al., 2011; Witte et al., 2011; Giglio et al., 2013; Kumar et al., 2011, 2013; Mielonen et al., 2013; Qin et al., 2014; Kumar et al., 2015; Vadrevu et al., 2015; Zhu et al., 2016a). The satellite monitoring over the vulnerable regions of the Earth for any kind of burning (i.e. tropical wildfires, boreal forest fires, peat fires, agricultural burning, waste-material burning, biofuel burning, etc.) gives important information about the number of fire count (FC), location of fires, smoke-plume distribution and its injection height, which are the key factors for local/regional meteorology and climate, as well as for ecosystems, socio-economic and human health-related issues (Barnaba et al., 2011; Hodnebrog et al., 2012; Kaskaoutis et al., 2012, 2014; Chakrabarty et al., 2016).

The MODIS on-board the Terra (known as EOS AM-1) and Aqua (known as EOS PM-1) satellites is a key instrument for identification

of the BB activities over the globe. The MODIS (Terra + Aqua) retrievals provide daily global AOD, fine mode fraction (FMF) and Ångström exponent (AE) over land (0.47, 0.55 and 0.66 μm) and Ocean (0.47, 0.55, 0.65, 0.86, 1.20, 1.60 and 2.10 μm). Based on the relationship between AOD vs FMF and AOD vs AE, several researchers have investigated the aerosol types such as urban/industrial, BB, dust, urban mixed one, etc. (Kaskaoutis et al., 2012; Pathak et al., 2012; Levy et al., 2013; Kumar et al., 2015; Zhu et al., 2016a). Furthermore, the MODIS global monthly fire location product (MCD14ML; spatial resolution 1 × 1 km) is available from the University of Maryland website (*ftp://fuoco.geog.umd.edu*), and contains the information about the geographical location of fires and their intensity (Giglio, 2010). The fire-detection algorithm (Giglio et al., 2003) uses the variation in the brightness temperatures obtained from the MODIS measurements of 4 and 11 μm channels (Matson and Dozier, 1981; Dozier, 1981) in order to detect the fire locations over the globe. The fire detection strategy is based on the absolute detection in the cases when fire strength is sufficiently high and on the detection relative to the background thermal emissions of the surrounding pixels (Justice et al., 2002). This algorithm examines each pixel of the MODIS swath and assigns them into the following classes: i) missing data, ii) cloud, iii) water, iv) non-fire, v) fire and vi) unknown. MODIS provides data for fire location, fire count detection confidence and FRP. Further details about the data description and validation are presented in the literature (Giglio, 2010; Giglio et al., 2013; Justice et al., 2006). In the present study, we have used the FC retrievals from Terra-MODIS during January 2001–December 2015 and analyzed their seasonal spatial distribution over south, southeast and east Asia (Fig. 2) with 80% confidence level. Furthermore, the seasonal mean MODIS AOD_{550} spatial distributions from Terra (MOD08_D03.006) and Aqua (MYD03_D3.006) are examined over the same area in order to reveal the influence of BB on seasonal variability of AOD_{550} (Fig. 3).

As shown in Fig. 2, the fire counts cover nearly the whole South and Southeast Asian region in winter and spring due to extensive forest fires during the dry seasons. During the summer monsoon, the fire counts are much less over India and Indochina due to extensive rainfall, while they significantly increase over Siberia due to the seasonal forest and peat fires. Over eastern part of China, the fire counts are really large, especially in winter and spring. Arid regions like Tibetan Plateau, central and western China exhibit very fewer fire counts as shown in Fig. 3 (Huang et al., 2012b). The seasonal-mean spatial distributions of AOD_{550} from Terra and Aqua MODIS retrievals exhibit great similarities for each month, with the highest AODs in winter to be detected over the densely-populated regions of Indo-Gangetic Plains (IGP), central and eastern parts of China. The large anthropogenic emissions from the highly urbanized and industrialized centers over this region contribute to the high AODs, which are the highest over the globe. During spring,

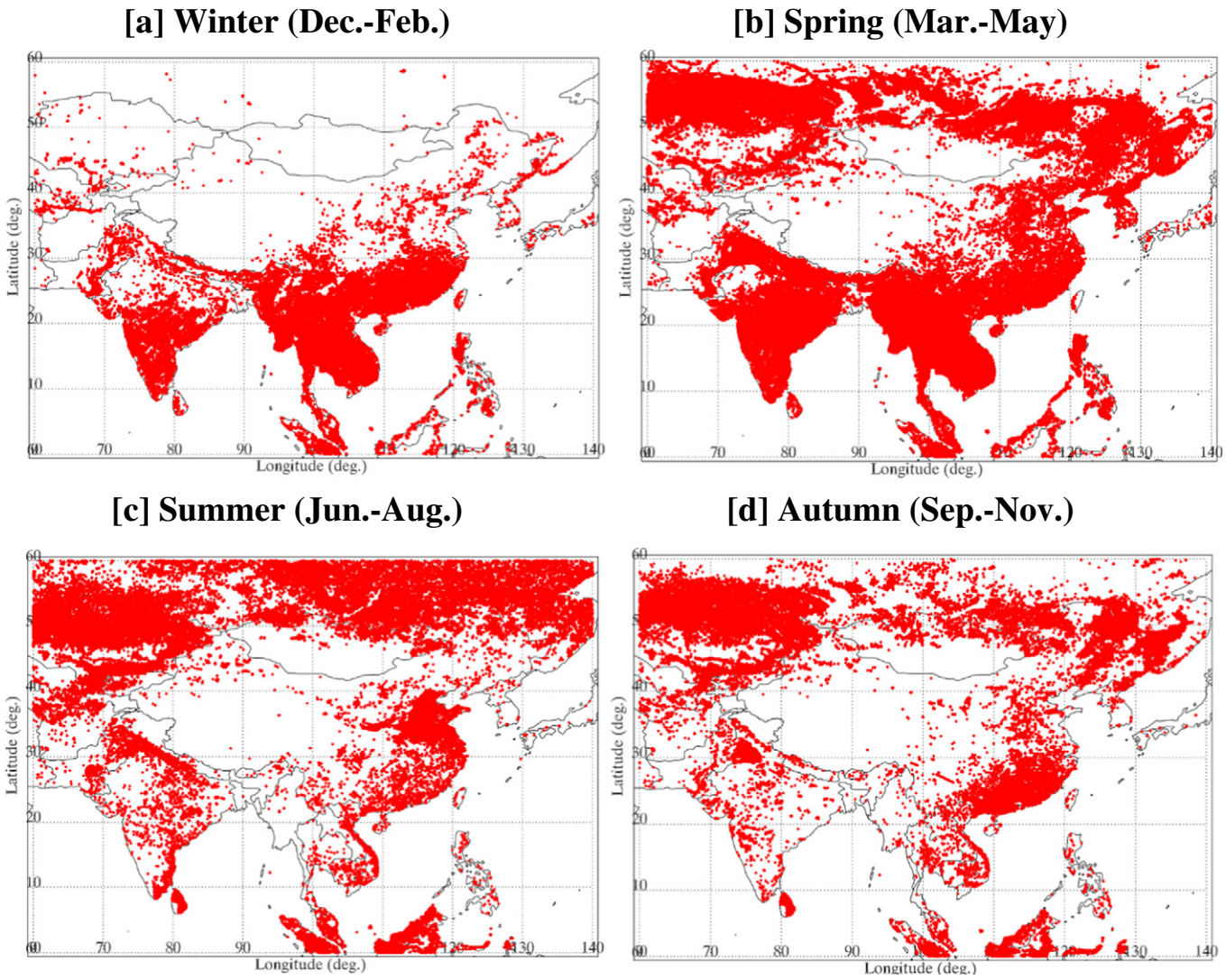

Fig. 2. Seasonal distribution of MODIS (Terra + Aqua) forest fire counts at 80% confidence level during January 2001 to December 2015. (Source: ftp://fuoco.geog.umd.edu)

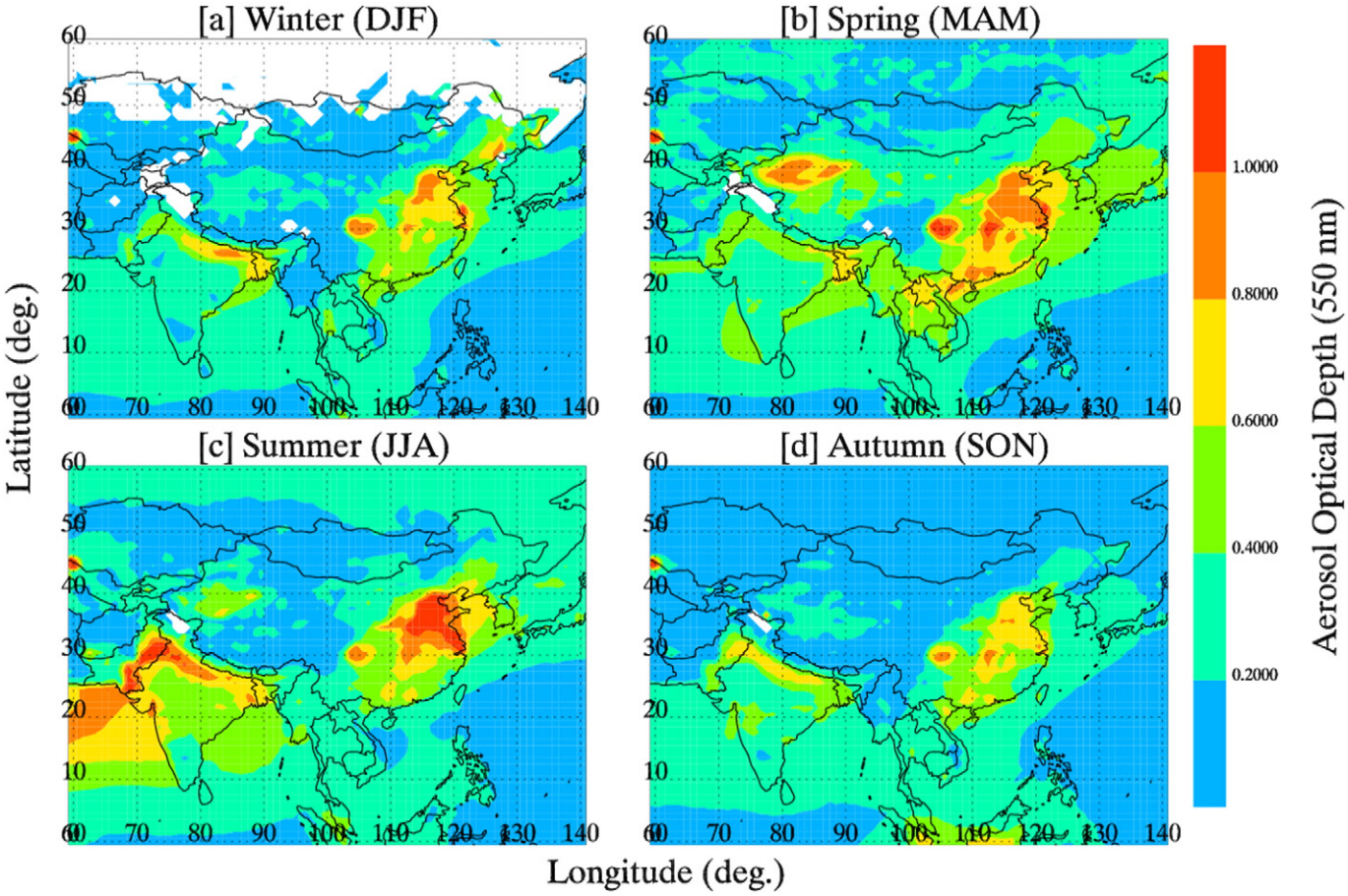

Fig. 3. Seasonal distribution of aerosol optical depth (AOD) at 550 nm during January 2000 to December 2015 via using the Moderate Resolution Imaging Spectroradiometer (MODIS) Terra + Aqua satellite.
(Source: http://giovanni.gsfc.nasa.gov/giovanni/)

high AODs are also shown over the Taklimakan desert in western China, while in summer the AOD increases significantly over the western IGP and the Arabian Sea due to enhanced desert-dust emissions. In general, autumn is characterized with the lowest AODs over the region, with the same hot-spot areas. The seasonal-mean spatial distribution of AOD_{550} shows that the fire counts do not seem to affect the aerosol loading and distribution of seasonal scales. Sparse fire and the associated plumes on certain days have been shown to strongly affect the local/regional AODs (Arola et al., 2007; Kaskaoutis et al., 2011), but without a strong influence on seasonal aerosols. Therefore, the seasonal mean AOD spatial distribution over the South and East Asia is mostly controlled by the local anthropogenic emissions and the large influence of sand and dust storms during the spring and summer. However, at local scales, and especially over the Indochina, the increased BB during the winter and spring seems to affect the AOD distribution (note also the lower AODs associated with much lesser fire counts during the summer).

The CALIOP (Cloud-Aerosol Lidar with Orthogonal Polarization) is an instrument onboard the CALIPSO satellite, which provides new insight into observing the vertical profile of aerosols and clouds at 532 and 1064 nm, and the linear depolarization profile at 532 nm (Winker et al., 2003; Omar et al., 2009; Winker et al., 2009). The CALIPSO level 1 profiles at 532 nm (version 3.30) are commonly used to monitor the long-range transport of the BB aerosols, providing information mainly on the concentrations and shape (via attenuated backscatter coefficient and Volume Depolarization Ratio, VDR), vertical profiles and injection height of the smoke plumes (Turquety et al., 2009; Guan et al., 2010; Kaskaoutis et al., 2014). Furthermore, the CALIOP products can differentiate the aerosol types, by considering "smoke" in their retrievals for the easier monitoring of the biomass-burning aerosols.

The AIRS are on board the Aqua satellite (with MODIS) and part of the A-Train constellation, covering the entire Earth from pole to pole twice a day (*http://airs.jpl.nasa.gov/mission/description/*). It provides very high spectral resolution measurements of emitted radiation in three spectral bands (3.74–4.61, 6.20–8.22 and 8.80–15.40 μm) using 2378 channels. In addition, four channels in the visible/near infrared range (between 0.4 and 1 μm) are used for detecting the cloud cover and its spatial variability. The spatial resolution of the measurements is 13.5 km at nadir. AIRS standard products include temperature, water vapor mixing ratios and trace-gas concentrations (e.g., O_3, CO, CO_2, CH_4), which are usually products or by-products from biomass-burning processes (Galanter et al., 2000; Lawrence and Lelieveld, 2010; Mielonen et al., 2013; Kumar et al., 2013). In the present study, level 3 daily carbon monoxide (CO) data from both daytime ascending orbit of AIRS with a spatial resolution of $1° \times 1°$ in order was used to assess the spatial distribution of CO over south and East Asia on a seasonal basis during 2003–2015 (Fig. 4). In accordance with the FC, the highest CO levels were found in spring over the tropical regions of India and Indochina, eastern China and Siberia. However, the high CO concentrations over the same regions in winter did not coincide with the very fewer fire counts in Siberia. Also, the CO is less during the summer monsoon over the tropical regions due to extensive rainfall and less number of fires, while low level also exhibited over Siberia, despite the tremendous increase in fire counts. Thus, on the seasonal basis, the CO does not coincide so well with the fire counts, especially over Siberia, while better correspondence is shown over the tropical regions of southern India and Indochina.

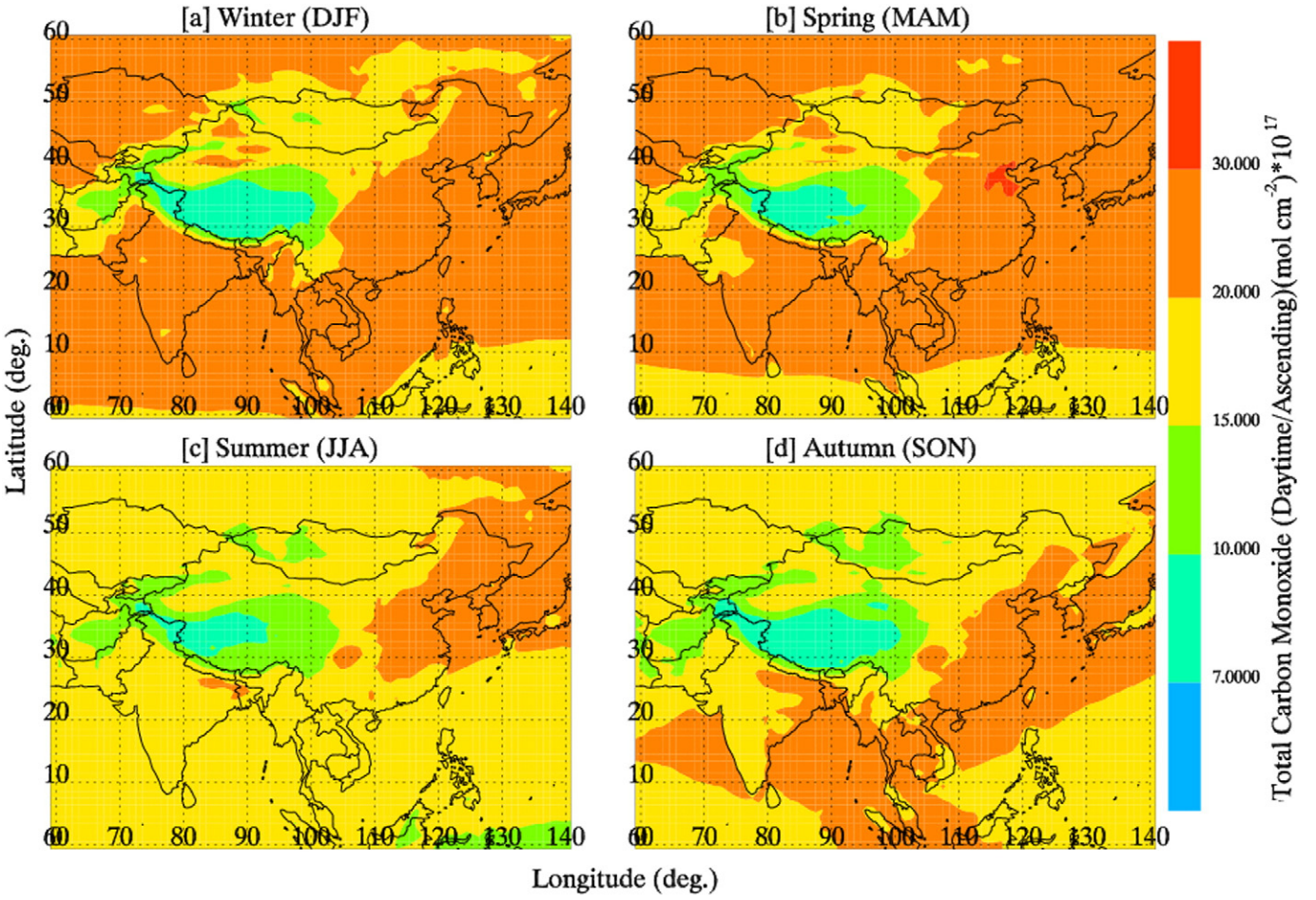

Fig. 4. Seasonal distribution of total carbon monoxide (daytime/ascending) during January 2003 to December 2015. (Source: http://giovanni.gsfc.nasa.gov/giovanni/)

In addition to AIRS, continuous measurements of regional and global observations of CO are taken from MOPITT, a sun-synchronous polar orbit satellite. The MOPITT makes 14–15 daytime and nighttime passes per day and crosses the equator around 10:45 and 22:45 local time (*http://www.atmosp.physics.utoronto.ca/MOPITT/MOPoverview.html*). The MOPITT retrieval provides the near surface, total column, and vertical profiles of CO at 10 pressure levels between the surface and 100 hPa with a resolution of 100 Pa, which has extensively been used for monitoring of BB emissions (Liu et al., 2006; Kaskaoutis et al., 2011; Kumar et al., 2013; Ding et al., 2015).

2.3. Laboratory studies

Laboratory experiments to investigate BB are typically conducted to characterize the performance of domestic heaters, and in particular to quantify emission factors of the heaters operating in different conditions (in terms of burning rate), fueled by different types of wood fuels, and the condition of the wood (dry or wet). As such they are not designed to establish burning conditions similar to those of wide, open fires. Since combustion process is very sensitive to the burning conditions, and a small change in the conditions may results in large variation in the emission factors, it cannot be considered that emission factors obtained from such investigation could be utilized in the qualification of emissions from wild fires.

Several examples of the studies on various types of heaters were reported in the literature since 2000. McDonald et al. (2000) characterized emissions from wood burnings in a fireplace and found that $PM_{2.5}$ emission factors ranged from 2.9 to 9 g/kg for softwoods and 2.3 to 8.3 g/kg for hardwoods. In another study, $PM_{2.5}$ emission factors of birch wood burned in a stove ranged from 0.1 to 2.6 g/kg (Hedberg et al., 2002). Burning wood logs in several combustion systems resulted in $PM_{2.5}$ emission factors ranging from 0.13 to 1.68 g/kg and particle number emission factors, from 3×10^{15} to 40×10^{16} particles/cm^3 (Wieser and Gaegauf, 2000). Calvo et al. (2015) comprehensively investigated combustion of three common southern and mid-European woods, burned in a fireplace and a stove and found that emission factors of some pollutants were similar for both devices for the same woods, but some differed. For example, mean $PM_{2.5}$ emission factor of the fireplace operating on *P. nigra* as a fuel was 14.0 ± 5.1 g/kg, while of the stove operating on the same fuel, 4.4 ± 1.4 g/kg.

In general, the studies reported in literature showed that the majority of particles resulting from BB were less than 2.5 μm in diameter (Wieser and Gaegauf, 2000; Hays et al., 2002; Hedberg et al., 2002; Ferge et al., 2005). The $PM_{2.5}$ emission factors have been measured in the range of 0.2 to 12 g/kg (McDonald et al., 2000; Fine et al., 2002; Hays et al., 2002).

Somewhat different was the study conducted by Wardoyo et al. (2006) with an aim to quantify emission factors under laboratory conditions, but to capture the maximum number of parameters which could be controlled in such conditions, and to maintain them at the levels similar to these of wide fires. To do this, Wardoyo et al. (2006) used a commercial stove, but modified for the purpose of these experiments. Therefore the focus was not on the operation of the stove, but on establishing the wide fires burning conditions. Five common tree species found in South East Queensland (Australia) forests: Spotted Gum (*Corymbia citriodora*), Blue Gum (*Eucalyptus tereticornis*), Bloodwood

(*Eucalyptus intermedia*), Iron Bark (*Eucalyptus crebra*), and Stringybark (*Eucalyptus umbra*) have been studied (Wardoyo et al., 2006). The results demonstrated that $PM_{2.5}$ and particle number emission factors depend on the type of tree and the burning rate. The average particle number emission factors for fast burning conditions are in the range of 3.3 to 5.7 $\times$ 10^{15} particles/kg for woods and 0.5 to 6.9 $\times$ 10^{15} particles/kg for leaves and branches (Wardoyo et al., 2006). The $PM_{2.5}$ emission factors are in the range of 0.14 to 0.21 g/kg for woods and 0.45 to 4.70 g/kg for leaves and branches (Wardoyo et al., 2006). For slow burning conditions, the average particle number emission factors are in the range of 2.8 to 44.8 $\times$ 10^{13} particles/kg for woods and 0.5 to 9.3 $\times$ 10^{13} particles/kg for leaves and branches (Wardoyo et al., 2006). And the $PM_{2.5}$ emissions factors are in the range of 0.12 to 0.48 g/kg for woods and 3.30 to 4.90 mg/kg for leaves and branches (Wardoyo et al., 2006).

2.4. Campaigns for biomass burning

Serveral campaigns (e.g., CARE-Beijing, PRIDE-PRD, and PEACE-YRB) have been programmed and conducted to investigate regional and large-scale air quality systematically, provided detail information about pollution conditions, physiochemical profile, sources, and atmospheric chemistry. The research supported establishment and enforcement of some environmental policy, and the sound database which accumulated from these campaigns also helped numerical model simulation and further studies.

CARE-Beijing campaigns (Campaign of Air Quality Research in Beijing and Surrounding Region) have been operated several times (e.g., CARE-Beijing 2006, 2008, 2013, North China Plain) to help get full view of air pollution in the North China Plain, which highlighted local and transported BB pollutants as a potential source in Beijing and surrounding areas (Ho et al., 2010; Wu et al., 2011; Liu et al., 2012; Zhang et al., 2014b; Zhang et al., 2015b; George et al., 2016).

PRIDE-PRD campaigns (Program of Regional Integrated Experiments of Air Quality over the Pearl River Delta) conducted in 2004 concentrated on in depth characterization of the pollution, and on improvement of the understanding of chemical and radiative process in the atmosphere of the Pearl River Delta region. PRIDE-PRD 2006 focused on the CCN in polluted air and BB smoke near the megacity of Guangzhou. Severe haze episodes were observed in PRIDE-PRD from October 4th to November 5th in 2004, and chemical profile of the haze aerosol indicated a great contribution from BB (Andreae et al., 2008; Zhang et al., 2008d). Efficiency spectra, size-resolved chemical composition, mixing state, optical scattering coefficient, and CCN effective activity of aerosol particles were measured online using various online measurement techniques from 1 to 30 July 2006 at a rural site of Guangzhou. The study found that strong local BB emissions and mixing decreased ambient average hygroscopicity parameter κ from 0.3 to 0.2, which is similar to the characteristic value for freshly emitted smoke from agricultural fires, of which soot particles with low hygroscopicity contribute a substantial portion. Moreover, CCN activity for aerosol was parameterized with volatility and chemical characters, binary function between bulk κ and number fraction of low volatility particles or ensemble particle chemical mass fraction was extrapolated from the linear relationship of size-dependent CCN activity and volatile fraction or chemical compositions, and the functions fitted well for aerosol particles, including or excluding BB plume. The results confirmed that κ value can be more simplified in global and climate modeling (Nowak et al., 2010; Gunthe et al., 2011; Rose et al., 2011).

PEACE-YRB 2015 (Program of Extensive Air Quality Research Campaign over the Yangtze River Basin in 2015) organized by the Fudan University in collaboration with many international institutions, including Queensland University of Technology, Cambridge University, Manchester University and Nanjing University was conducted from November 20th to December 5th, 2015. The campaign was carried out both on board and land using the well-equipped ship, which sailed from Shanghai Port to Wuhan City in round trip through a total distance of 2150 km, as well as a mobile van, which followed on the ground. Extensive smoke emissions from domestic use and field burning were distinguished by preliminary analysis, and were showed to make up a considerable contribution to the Yangtze River Basin pollution in mixing with engine exhaust from vehicle and ship (Morawska et al., 2016; Ouyang et al., 2016). Detailed emissions and pollution conditions will be elucidated in the later publications.

3. Types of biomass burning

3.1. Forest fire

Forests are the main part of the terrain ecosystem and play an important role in maintaining the balance of terrain ecosystem. The forest coverages are very limited and it accounts for only 21% of the mainland of the nation (Zhang et al., 2011b; Li et al., 2011a). The seventh National Forest Resources Inventory during 2004–2008 shows that the forest area was enhanced at ~200 million ha stocking ~14/m^3 billion and ranking fifth in the world after Russia, Brazil, Canada and USA (Li et al., 2004; Li et al., 2011a). During the last few decades, due to the deforestation, number of forest fires and burned area has drastically increased (Zhou and Lu, 2000; Shao, 2000). One of the largest forest fire, well known as black dragon fire, occurred in northeast China during May 1987, where the areas over 1.3 million ha (Cahoon et al., 1994) of forest were charred. The forest fire or wildland fires have become an important and more frequent issue in China (Kong et al., 2003), and the Indo-China peninsula is one of the most active fire hotspots in the world, which is a matter of great concern because of the high population densities (Gautam et al., 2013; Johnston et al., 2015). Prior to the onset of monsoon, the Indo-China Peninsula region is the witness of intense BB in the form of forest fires, which significantly increase the aerosol concentration (Gautam et al., 2013).

Forest fires have had impact on biosphere-atmosphere interface, atmospheric chemistry, composition of ecosystem system and its distribution, environmental degradation and air quality monitoring (Crutzen and Andreae, 1990; Penner et al., 1992; Costanza et al., 1997; Bond and Keeley, 2005; Randerson et al., 2006; Zhang et al., 2011b). They emit large amounts of trace gases (both chemically active and greenhouse gases), non-methane hydrocarbons, and aerosols (Crutzen and Andreae, 1990). These aerosols and pollutants are significantly affecting atmospheric chemistry, cloud properties, Earth radiation budget and climate change, global carbon cycle, ecosystem and biodiversity, vegetation, rainfall, air quality and atmospheric circulation (Crutzen and Andreae, 1990; Ramanathan et al., 2001; Andreae et al., 2004; Liu, 2005; IPCC, 2013). A recent study by Johnston et al. (2015) shows that the forest fire/BB was responsible for about 339,000 premature deaths per year. The increasing intensity and spread of forest fires in Asian countries, and their impact on ecosystems and climate change suggest that the real-time monitoring of forest fire activities is essential. Fire monitoring due to high potential hazards associated with forest fires, the ground-based and airborne fire monitoring, space-borne satellite sensors have been widely used to detect and monitor the forest fires (Prins et al., 1998; Justice et al., 2002). Fire monitoring via satellite remote sensing such as MODIS Rapid Response System Global Fire Maps, GLOBSCAR, European Forest Fire Information System, NOAA/AVHRR (the National Oceanic and Atmospheric Administration/the Advance Very High Resolution Radiometer), Landsat, Chinese Feng-Yun series have been widely used to detect the forest fire hot spots and burned areas across China (Zhang et al., 2011b). The MODIS data sets provide a vast temporal coverage along-with high spectral (36 bands total) and spatial resolution (250, 500, and 1000 m). In general MODIS provides information on the burned areas and smoke, and is used to detect active fires.

3.2. Agricultural straw open burning

China is among the major agricultural nations in the world. Agricultural crop production generates tremendous amounts of agricultural

crop residues such as rice, wheat, and corn straws etc., which account for 17.3% of the global crop residues production and rank the first in the world (Bi et al., 2010). During the summer/autumn harvest season, a large amount of agricultural straws are removed by burning in a short period in order to prepare the next crop planting. Open burning is the most convenient and less expensive way to eliminate agricultural straw.

In China, studies on gaseous and particulate pollutant emissions from open burning of agricultural straw have been presented in previous publications (Li et al., 2007; Zhang and Smith, 2007; Zhang et al., 2008a; Zhang et al., 2011a; Huang et al., 2012a; Tian et al., 2015). Efforts have been also made to characterize particle number emission factors and size distributions from agricultural straw burning in the laboratory simulation experiments (Hays et al., 2005; Zhang et al., 2008a; Zhang et al., 2011a). Particle size distribution from agricultural straw open burning is mainly dominated by an accumulation mode, with a count median diameter of 0.10–0.15 μm (Zhang et al., 2011a). In addition, trace gas emission inventories (CO_2, CO, NO_x and BC etc.) from agricultural straw open burning had been estimated in China (Zhang et al., 2008a; Huang et al., 2016; Sun et al., 2016a).

In addition to emission characteristics, understanding of the impact of agricultural straw open burning on urban and regional air quality is essential. In China, especially during and shortly after the harvest seasons, open burning of agricultural straw has a significant impact on urban and regional air quality. In extreme cases, agricultural straw open burning would trigger the explosive growth of secondary $PM_{2.5}$ and accelerate the heavy haze formation in the urban and regional atmosphere (Nie et al., 2015; Xie et al., 2015). However, detailed information on the effects of smoke from agricultural straw open burning on urban and regional air quality is still rare (Zhang et al., 2010a; Li et al., 2010a). It is well known that the impact of agricultural straw open burning on heavy haze formation during and shortly after the harvest seasons is complex, and not only contributes to primary $PM_{2.5}$ emissions but also includes the potential contribution to secondary $PM_{2.5}$ formation. For instance, during the process of smoke plume transport, organic compounds (such as VOCs) in the presence of NO_x can be oxidized to generate secondary organic aerosol (SOA) (Wang et al., 2009a, 2009b; Li et al., 2014a). Similarly, atmospheric gases, such as SO_2 and NO_x, can also be oxidized to form the secondary inorganic aerosol (SIA, such as sulfate and nitrate) (Cheng et al., 2013; Zha, 2013; Tao et al., 2013; Cheng et al., 2014a, 2014b; Chen and Xie, 2014; Zhang et al., 2016a, 2016b, 2016c). Heterogeneous reactions in BB plume also played important roles in the formation of HONO (Nie et al., 2015). High concentration of NO_2 together with high concentration of NH_3 in the BB plume has been found to enhance sulfate formation through aqueous-phase reactions and to produce HONO as a by-product (Nie et al., 2015). Both SOA and SIA are the most important components of secondary $PM_{2.5}$. Therefore, when smoke plume is transported to the urban atmosphere, secondary $PM_{2.5}$ can rapidly increase in a short time under the stagnant weather conditions, and can further aggravate haze pollution and/or result in increase of the frequency of heavy haze pollution through the interactions between physical and chemical processes (Ding et al., 2013a; Huang et al., 2016; Ding et al., 2016a). That is why the heavy haze pollution often happened in North, Central and eastern China, especially during and shortly after the harvest season.

3.3. Wood and straw combustion as fuel

Approximately half of China's population lives in rural areas and use biomass fuels (such as wood and straw) as the domestic fuel for cooking/heating. Biomass fuels burnt in low-efficient stoves would produce substantial air pollutants and increase fine particulate matter ($PM_{2.5}$) exposure in the indoor environment (Wei et al., 2014), which is associated with adverse health impacts such as pneumonia, tuberculosis and chronic obstructive pulmonary disease (Pope et al., 2002). In China, household combustion of wood and straw, is the dominant source of indoor air pollution in rural areas and contribute significantly to human health burden (Zhang et al., 2012, 2014a). Household combustion methods of both wood and straw in rural China are of low energy conversion efficiency and result in high pollutant emissions (Zeng et al., 2007).

Characteristics of pollutants from wood and crop straw combustion as domestic fuel have been studied in China by several research groups (He et al., 2005; Jin et al., 2005; Shen et al., 2010; Zhang et al., 2012; Zhang et al., 2014a). Jin et al. (2005) monitored indoor air pollutant (respirable particles, CO and SO_2) emissions from wood and straw burning in the rural households of Inner Mongolia and Gansu provinces of China. He et al. (2005) measured multiple pollutant emissions from wood and straw burning in the rural household of Guizhou and Shaanxi provinces of China. Shen et al. (2010) calculated emission factors of particulate matter (PM) and elemental carbon (EC) from domestic crop straw burning in typical household stoves. Zhang et al. (2012) measured chemical and size characteristics of particulate matter from domestic wood burning in rural areas of southwestern China. Zhang et al. (2014a) conducted field experiments to measure indoor emissions of carbonaceous aerosols (OC and EC) and other air pollutants (CO, PM_1, $PM_{2.5}$ and PM_{10}) from household wood burning in southwest China.

As noted by a number of studies (Zhang et al., 2012; Zhang et al., 2014a), low combustion efficiency leads to high emission factors for wood and straw burning. High emissions do not necessarily mean high exposures unless they reach human breathing zones. However, available evidence indicates that total exposure to combustion-derived fine particles from domestic use of wood and straw in indoor environment is larger than that from all outdoor sources (Zhang and Smith, 2007; Fullerton et al., 2008). Epidemiological studies have shown that exposure to high levels of indoor $PM_{2.5}$ contributed to a consistent increase in cardiac and respiratory morbidity and mortality (Pope et al., 2002). For instance, pulmonary effects of indoor $PM_{2.5}$ include the triggering of inflammation in the smaller airways, which can result in the exacerbation of asthma and chronic bronchitis, airway obstruction, and decreased gas exchange (Nel, 2005). Moreover, high concentrations of $PM_{2.5}$ in the indoor environment have been regarded as a cardiovascular risk factor that is associated with heart attacks, stroke, heart rhythm disturbances, and sudden death. Inhalation of fine particles elicits proinflammatory effects, cytokine production, and enhancement of allergic responses in the upper and lower airways (Perez-Padilla et al., 2010).

3.4. Miscellaneous

In China, annual biomass waste productions contain ~2.6×10^5 GWh energy that equals to the energy storage of ~3.65×10^8 tons coal (Chen et al., 2009; Zhang, 2011; Koppejan et al., 2012). Apart from traditional field burning and domestic use of biomass waste, co-firing with coal or municipal solid waste (MSW) in power stations or incineration plants is indeed a practical method to deal with biomass waste, and many studies have focused on the development of combustion technologies and emission control of pyrogenic pollutants (Waldheim et al., 2000; Nussbaumer, 2003; Tian et al., 2005). Somewhat comparable heat density of biomass to fossil fuels such as coal and petrochemical products implies that biomass fuel represents a considerable amount of renewable energy (Zhang et al., 2005), and scientific utilization of biomass energy would partly relieve shortage of fossil fuels and ameliorate the serious atmospheric pollution (Baxter, 2005; Koppejan and Van Loo, 2012). Robinson et al. (2003) suggested that biomass co-firing with coal is a possible way to achieve significant near-term CO_2 emission mitigation through economic analysis. Ross et al. (2002) found that co-combustion of coal and biomass can decrease emission factors of multiple gaseous and particulate pollutants. However, a mixture of pollutants from the co-firing process can be more complex. Zhang et al. (2009c) observed Pb-chlorine co-enriched particles that are formed from waste incineration, as high concentrated HCl in the gas stream from the combustion of garbage (chlorine-rich plastic, biomass, etc.) has volatile effect on Pb to form $PbCl_2$. Wang et al. (2006, 2007b) and Jiménez and Ballester (2005) found distinctly different particle size distribution

and PM chemical profiles from co-firing of coal and biomass compared to that from the sole fuel combustion.

4. Pollutants from biomass burning

4.1. Particulate matter

PM refers to a mixture of solid particles and liquid droplets in the air (Hinds, 2012), with a varying physical and chemical properties. PM is a dominant contributor to the air pollution in China (Fang et al., 2009). In particular, Beijing-Tianjin-Hebei (BTH) Province, the Yangtze River Delta (YRD) and the Pearl River Delta (PRD) are subject to severe PM pollution. Daily average $PM_{2.5}$ concentrations during severe haze periods in 2013 are 159, 91, 69 and 345 μg/m^3 for Beijing, Shanghai, Guangzhou and Xi'an, respectively (Huang et al., 2014). All $PM_{2.5}$ values are significantly higher than mean concentration of 25 μg/m^3, recommended by the World Health Organization (WHO). In order to address serious PM pollution issue, the Chinese government announced the long-term plan to reduce the $PM_{2.5}$ concentration by 25%, 20%, 15% and 10% compared to 2012 levels by 2017, in BTH, YRD, PRD and other cities, respectively (*http://www.gov.cn/zwgk/2013-09/12/content_2486773.htm)*. For instance, annual value for $PM_{2.5}$ in Beijing is targeted as 60 μg/m^3, which would be still high compared to the values recommended by WHO (annual mean of 10 μg/m^3), but a big step in air pollution regulation in China. It will certainly be a challenge to achieve this level because of the heavy pollution prevailing currently, for example, it was observed in Beijing in 2014 that $PM_{2.5}$ mean annual value was 86 μg/m^3 (Zhang et al., 2016a).

4.1.1. Carbonaceous material

Dominant PM fraction emitted into the atmosphere is carbonaceous material (Chan and Yao, 2008), which is composed of organic carbon (OC) and EC. Carbonaceous species influences earth's radiation balance. While BC absorbs incoming solar radiation contributing to increased atmospheric temperatures, OC cools the atmosphere by scattering the solar radiation (Penner et al., 1998; Haywood and Boucher, 2000). Carbonaceous particles can efficiently act as CCN, having an influence on cloud formation and their properties (Hallett et al., 1989; Roberts et al., 2002; Reid et al., 2005b). They can also contribute to various health issues (Pope and Dockery, 2006). Emissions of carbonaceous matter in China have increased by approximately 20% from 1996 to 2010 (Lu et al., 2011). It is estimated that a portion of this fraction can vary between 20% and 50% of $PM_{2.5}$ mass (Cao et al., 2007).

In general, the dominant particle-phase fraction detected in BB emissions is found to be carbonaceous matter (Formenti et al., 2003; Bond et al., 2004; Reid et al., 2005b; Hallquist et al., 2009; Fu et al., 2012, 2014; Li et al., 2016a, b). In fact, BB combustion sources are considered as the largest contributors to the primary carbonaceous particles in the atmosphere (Hallquist et al., 2009; Bond et al., 2004; Crutzen and Andreae, 1990). Many studies investigated the dominant sources of $PM_{2.5}$ and carbonaceous species in China, mostly using the offline sampling technique in urban Beijing region (Zheng et al., 2005; Song et al., 2006; Song et al., 2007; Wang et al., 2007a, 2007b; Wang et al., 2009a; Cheng et al., 2013; Yu et al., 2013a; Cheng et al., 2014a) with some of them illustrated in Table 1. For instance, Positive Matrix Factorization (PMF) source apportionment performed on data collected over the whole year 2000 in Beijing, shows that on average 11% of $PM_{2.5}$ was influenced by BB activities (Song et al., 2006). Using the same source apportionment method, Yu et al. (2013a) observe a similar contribution in Beijing in 2010. According to studies summarized in Table 1, the contribution of BB activities can go up to 19%, 25% and 37% in autumn, winter and summer months, respectively. It is observed that BB is one of the main sources that contribute to fine particle and carbonaceous emissions (besides traffic and coal combustion sources) in China (Chan and Yao, 2008). Moreover, in recent years source apportionment has been performed on the organic aerosol (OA) data collected by Aerosol mass spectrometer (AMS) using mostly PMF. The significance of BB emissions (mainly due to burning of crop residues during harvesting periods) in urban and rural areas of China is shown through the high contribution of PMF-resolved BB-related factors. Similar BB OA contribution is found for urban and rural PRD area (24%), and is smaller in urban Beijing (12–19%) and Nanjing (8%) in the autumn period (Zhang et al., 2010a; He et al., 2011a; Huang et al., 2011; Zhang et al., 2015b; Xu et al., 2015). A significant contribution of the BB-related organic aerosol is also found in the winter period (30%) and over the summer months (15%) (Huang et al., 2013a; Zhang et al., 2015a). As it can be seen, there is significant seasonality in BB activities and contribution to PM pollution in China. BB contribution seen through increased $PM_{2.5}$ and its constituents is highly seasonal in magnitude, but present over the whole year. The $PM_{2.5}$ increase in autumn and spring is mainly attributed to BB from crop residues burning. In late September and October harvesting takes place and then contribution of BB is found to be the highest in North China (Duan et al., 2004; Zheng et al., 2005; Yu et al., 2013a; Zhang et al., 2015c), which is different from an early summer maximum in East China (Ding et al., 2013ab). Over the summer months BB contribution from wheat straw burning is significant, while winter PM pollution is mainly driven by coal combustion sources that are predominantly used as heating systems, although BB contribution can be significant (Li et al., 2008; Yu et al., 2013a). Apart from seasonal differences, the portion of aerosol mass influenced by BB varies depending on the region of China. Huang et al. (2014) illustrate the higher BB contribution in Guangzhou and Xi'an (5–9% of $PM_{2.5}$) compared to Beijing and Shanghai (4–7% of $PM_{2.5}$).

The main component of smoke submicron carbonaceous mass is the organic aerosol fraction that can go up to 90% (Bond et al., 2004). Global annual emission of OC and BC emitted in open fire events is estimated to be approximately 70% and 40%, respectively (Bond et al., 2004). Studies on both urban and rural areas of Beijing show that during intense BB pollution episodes, more than a half of OC and EC could be from smoke emissions (Duan et al., 2004; Cheng et al., 2013; Cheng et al., 2014b; Yao et al., 2016a).

4.1.2. Other important particulate components

Levoglucosan-like species (levoglucosan, mannosan, galactosan) are anhydrosaccharides formed in the pyrolysis of cellulose and common organic molecular constituents of BB emissions (Simoneit et al., 1999; Li et al., 2016c). Many studies worldwide including China have used levoglucosan (dominant anhydrosaccharide emitted) as a distinctive BB chemical signature (Simoneit et al., 1999; Simoneit, 2002; Fraser et al., 2003; Jordan et al., 2006; Song et al., 2007; Wang et al., 2007a; Zhang et al., 2008c; Wang et al., 2009a; Zhang et al., 2010a). Levoglucosan concentrations considerably vary depending on season and region (Table 1). For instance, He et al. (2006) investigated organic tracer compounds including particulate levoglucosan during all seasons in Beijing. Levoglucosan average mass concentrations were observed to be 0.12, 0.08 and 0.03 μg/m^3 in autumn, winter and summer, respectively. Considerable higher levoglucosan concentrations are found by Wang et al. (2007a) in autumn (0.1–0.9 μg/m^3). Moreover, there is a wide range of levoglucosan in winter (0.08–3.10 μg/m^3) and summer (0.03–0.31 μg/m^3). Potassium rich particles are observed to be a common fraction of BB emissions in China (Li et al., 2007; Li et al., 2010b). BB contributes to high potassium levels in smoke emissions and it has been used as a BB tracer (Duan et al., 2004; Wang et al., 2007a; Zhang et al., 2010a; He et al., 2011a; Huang et al., 2012d; Cheng et al., 2013; Yu et al., 2013a; Cheng et al., 2014b; Zhang et al., 2015b). Similar average potassium concentrations can be observed according to studies summarized in Table 1. Potassium average value varies from 2.42 to 2.78 in winter, 1.6 to 4.9 in summer and 1.7 to 2.26 μg/m^3 in autumn months, depending on the monitored areas. Yu et al. (2013a) suggest 2.2 μg/m^3 for the annual potassium value, based on continuous measurements for one year in Beijing. In contrast to source-specific levoglucosan, water-soluble potassium can indicate particles of more

Table 1
Source apportionment studies including location (and type), season (and date), average contribution of BB to $PM_{2.5}$, OC (OA), EC and average values for potassium and levoglucosan are given in table; Index next to the reference refers to BB activities a) Open field post-harvest agricultural BB b) softwood and stalks burning for heating.

Location Location type	Season/date	Average BB to $PM_{2.5}$ (%)	Average BB to OC (%)	Average BB to EC (%)	Average K^+ conc. ($\mu g/m^3$)	Average levoglucosan conc. ($\mu g/m^3$) in $PM_{2.5}$/max	Reference
PRD (Guangzhou) urban/suburban	(Autumn) 6–31 Oct 2004	4.0–19.0%/3.0–16.8% urban/suburban			2.26 ± 0.50/1.70 ± 0.79 urban/suburban	0.20–0.66/0.12–0.95 urban/suburban	Wang et al. (2007a) [a]
BTH (Beijing) urban	(Summer, Autumn, Winter) 25 July–5 Aug 2002 27 Oct–3 Nov. 2002 3–10 Jan 2003					0.03, 0.12 and 0.08/0.07, 0.24, 0.15 for summer, autumn and winter	He et al. (2006) [a]
YRD (Shanghai) urban	(Summer) 28 May–3 June 2009				2.84		Huang et al. (2012a, b) [a]
BTH (Beijing) urban	(Summer and winter) 2–31 Aug 2005 16 Aug − 10 Sep 2006 16 Jan–2 Feb 2007	8.4% and 24.9% summer 2006 and winter 2007	11.7%, 9.9% and 26.1% summer 2005, summer 2006 and winter 2007			0.08, 0.17 and 0.68 summer 2005, summer 2006 and winter 2007	Wang et al. (2009b) [a, b]
BTH (Beijing) urban	(All Seasons) Jan, Apr, July and Oct 2000	annual average of 11%					Song et al. (2006) [a]
BTH (Beijing) Urban (6 sites)	(Summer and winter) 11–19 Aug 2004 11–19 Jan 2004	13% and 15% in summer and winter				0.31 and 3.10 in summer and winter	Song et al. (2007) [a, b]
BTH (Beijing) urban	(Summer and winter) 3 June–23 July 2011 1 Dec–30 Jan 2011/12		~50%	~50%	1.74 ± 2.29 and 2.42 ± 5.86 in summer and winter /45.76 5.81 ± 2.75 (for summer BB episode)	0.23 ± 0.37/2.30 and 0.59 ± 0.42/1.94 summer and winter 0.75 ± 0.68 (for summer BB episode) and annual average of 0.43 ± 0.44	Cheng et al. (2013) [a, b]
YRD urban (5 sites)	(Summer) 28 May–6 June 2011	37%	70%	61%	1.6–4.9 (measured at three sites)		Cheng et al. (2014) [a]
BTH (Beijing) urban	(All seasons) 1 Jan–31 Dec 2010	5.8 $\mu g/m^3$; 11.2% 4.1, 5.8 6.1 and 7.1 $\mu g/m^3$ spring, summer, autumn and winter			annual average of 2.22 1.88, 2.09, 2.14 and 2.78 in spring, summer, autumn and winter		Yu et al. (2013) [a]
PRD (Hong Kong) urban	(Autumn) 25 Oct–2 Dec 2009		24.1% (AMS)				He et al. (2011) [a]
PRD (Kaiping) rural	(Autumn) 12 Oct–18 Nov 2008		24.5% (AMS)				Huang et al. (2011) [a]
YRD (Jiaxing) regional	(Summer and Winter) 29 June–15 July 11–23 December		30.1% in winter (AMS)				Huang et al. (2013a) [a]
YRD (Nanjing) urban	(Summer and Autumn) 1–15 June 2013 15–30 Oct 2013		15% and 8% in summer and autumn (AMS)				Zhang et al. (2015b) [a]
BTH (Beijing) urban	(Autumn) 14 Oct–12 Nov 2014		12–19% (AMS)				Xu et al. (2015) [a]

than one origin (Zhang et al., 2010b; Aiken et al., 2010). In the absence of other important sources, such as soil dust, sea salt and meat charbroiling, water soluble potassium can be a satisfactory BB marker (Andreae, 1983; Schauer et al., 1999). Wang et al. (2007a) showed that application of potassium as a reliable smoke tracer has limitations in Guangzhou area during the October BB period due to interferences with meat charbroiling and transportation-related potassium emissions. Fireworks are also found to elevate potassium concentrations (Vecchi et al., 2008; Zhang et al., 2010a). In particular, water soluble potassium has not been considered to be suitable, or at least it should not be used as the only BB tracer during winter in Beijing, which is a season with significant festival fireworks influences (Yu et al., 2013a; Cheng et al., 2013; Cheng et al., 2014a).

Although all results illustrate the significant impact of BB sources on PM pollution over China, until recently, it has been mostly ignored as a significant contributor in pollution inventories (e.g. Zhang et al., 2009a). Zhang and Cao (2015a, b) suggested that regulations on BB emissions should be revised, and it should be scaled down in both urban and rural areas and for open BB as well as in household consumption. It is estimated by Cheng et al. (2014b) that $PM_{2.5}$ level could be reduced by 47% in the YRD region if open post-harvest BB activities were banned, suggesting significant benefits for the environment and human health.

4.2. Physical properties of smoke particles

4.2.1. Size distribution

Studies have confirmed BB as a major source of fine particles in the atmosphere, and size distribution of freshly emitted smoke particles resides mainly within the accumulation mode with geometric median diameter (GMD) at 50– 200 nm. Unimodal and bimodal distributions in volume concentration have both been reported, and the discrepancy of GMD and distribution pattern relates to fuel type, combustion environment, burning conditions, measurement technologies, and also aging extent of smoke plumes (Reid et al., 2005b; Capes et al., 2008; Gunthe et al., 2011; Zhang et al., 2011a; Nie et al., 2015; Li et al., 2015). Rapid growth in size occurs immediately after smoke particle emissions, and tens of nanometers per hour increment in GMD has been observed for smoke particles in ambient atmospheric investigations during transport and in aerosol chamber simulations. It has also been found that coagulation is the dominant mechanism contributing to particle growth, and that humidity facilitates the process (Reid et al., 2005b; Capes et al., 2008; Li et al., 2015). The ultrafine size enables smoke particles to be efficient CCN/IN and also to deposit deeper in the respiratory system, presenting potential climate effect and human health hazards, respectively, while changes in size distribution alter the optical properties, increasing the single scattering albedo (SSA) as smoke particles increase towards sizes where scattering is more efficient (Li et al., 2002; Delfino et al., 2005; Dusek et al., 2006; Pierce and Adams, 2007; Araujo et al., 2008; Gunthe et al., 2011). Atmospheric aging of smoke particles has a direct impact on particle size and chemical composition changes; changes in particle composition and morphology associated with gas-to-particle transformation and internal mixing are also shown to increase the SSA and light extinction coefficient (Abel et al., 2003; Capes et al., 2008).

4.2.2. Hygroscopicity

Hygroscopicity of smoke particles has been characterized using ensemble (e.g., Hygroscopic-Tandem Differential Mobility Analyzers, H-TDMA; scanning mobility CCN counter) and single-particle techniques (e.g., TEM, electrodynamic balance, and optical tweezers) to derive hygroscopic growth factor (GF) and hygroscopicity parameter κ (Semeniuk et al., 2007; Lewis et al., 2009; Rose et al., 2011; Rickards et al., 2013; Li et al., 2016b). κ parameter is commonly used to link hygroscopicity and CCN activity of particles, which presented as a function of particle size and chemical compositions. However, consistency between κ estimated from hygroscopic growth and critical supersaturation measurements is still under investigations (Su et al., 2010; Petters and Kreidenweis, 2013; Rickards et al., 2013). Smoke particles range from weakly hygroscopic (κ ~ 0.02) to strongly hygroscopic (κ ~ 0.80) (Petters et al., 2009; Dusek et al., 2011; Li et al., 2016b), and the values vary with fuel type and burning conditions. Smoldering of biomass produces more hydrophobic organic aerosol, such as tar ball particles with less κ, while particles emitted from flaming phase under higher temperature contain more inorganic salts, of stronger hygroscopicity. Empirical function of $\kappa = f_{inorg} \times \kappa_{inorg} + f_{org} \times \kappa_{org}$ is widely applied in outdoor investigation and aerosol chamber simulation to extrapolate κ_{inorg} and κ_{org} from linear regression of size-resolved bulk κ value and particulate organic and inorganic mass fractions (Dusek et al., 2010; Nowak et al., 2010; Li et al., 2016b). Constant κ_{inorg} (0.6– 0.8) and κ_{org} (~0.1) corresponding to inorganic and organic components for ambient aerosol and fresh/aged smoke aerosol are derived, implying the significant role of alkali species in CCN activity of particles, especially for smoke particles, in which carbonaceous materials dominates. κ_{org} of smoke particles is within the characteristic range for individual organic components, ranging from zero for absolutely insoluble species such as soot, to ~0.5 for more hygroscopic oxalic acid; studies have reported that humic-like substances (mainly carboxylic acids and levoglucose) are the primary hygroscopic materials in smoke particles (Wex et al., 2007; Carrico et al., 2008; Giordano et al., 2013). κ_{inorg} should deposit in the character of $(NH_4)_2SO_4$-NH_4NO_3 mixtures for ambient aerosol and of KCl dominated inorganic mixtures for smoke particles (Rose et al., 2011; Li et al., 2016a, b). Variation of κ responses to chemical composition and physical characteristic changes of aerosol, though photochemical oxidation produces more organic aerosol (OA) and increases the O/C ratio in organic components, the change of hygroscopicity is still in doubt (Jimenez et al., 2009; Dusek et al., 2010; Mcintire et al., 2010; Duplissy et al., 2011; Engelhart et al., 2012; Giordano et al., 2013; Rickards et al., 2013). Engelhart et al. (2012) found that photochemical processing reduces variability of smoke particle CCN activity, and initial discrete κ parameters converge to a value of 0.2 after several hours of oxidation. Tritscher et al. (2011) concluded that the hygroscopicity of SOA will increase from initial formation, and then roughly stays constant for the further ripening and oxidation. Heterogeneous reactions of inorganic salts can also change κ_{inorg} and inorganic mass fraction to alter the bulk κ of smoke particles eventually (Li et al., 2015). Besides, mixing state, morphology, and size changes during aging (e.g., from initial amorphous non-uniformly internal mixing to more homogeneously mixing state, size growth, mixing with ambient aerosol like sea salts, dust, engine emissions, etc.) influence the κ values (Zhang et al., 2008b; Lewis et al., 2009; Rose et al., 2011; Chen et al., 2015a, 2015b).

4.2.3. Density

Effective density bonds the aerodynamic diameter of the particle and its mobility diameter, and it also plays a crucial role in the mass concentration conversion, mass closure calculation and deposition model assessment of aerosol (DeCarlo et al., 2004; Beddows et al., 2010). Smoke particle density as a function of individual compound density and mixing state influences the estimation of bulk hygroscopicity parameter and refractive index of OC and EC content (Petters and Kreidenweis, 2007; Schkolnik et al., 2007; Schmid et al., 2009). Based on different techniques, density can be measured as effective, online size-resolved, using APM (Aerosol Particle Mass Analyzer) combined with an SMPS/TDMA system (Rissler et al., 2014; Yin et al., 2015; Li et al., 2016b), or estimated as bulk density from volume and corresponded mass concentrations of PM (Pitz et al., 2003; Kostenidou et al., 2007). Khlystov et al. (2004) and Schmid et al. (2007) also report an algorithm method to derive particle density via merging coincident aerodynamic and mobility size distributions. Smoke particle densities are reported to vary from 1.0 to 1.9 g/cm^3. Rose et al. (2011) applied density as 1.7 g/cm^3 in ambient biomass smoke plume research; Martins et al. (1996) derived particle density to be 1.5 g/cm^3 for temperate forest fire; Levin et al. (2010) calculated bulk densities of various BB aerosol from chemical

compositions to be 1.2–1.9 g/cm^3; Hennigan et al. (2011) assumed smoke aerosol density to be 1.3 g/cm^3 throughout photo-oxidation process; while Li et al. (2015, 2016a) reported densities for fresh particles from crop residues burning to be 1.1–1.4 g/cm^3, and the densities are size and fuel type dependent, and particle densities scale with inorganic mass fractions, with the aging of smoke aerosol, density increase and size-dependence phase out.

4.2.4. Volatility

Volatility is an important property of the organic materials and it determines SOA formation and partition between gaseous and particulate phases (Seinfeld and Pandis, 2012). Volatility of PM has been commonly applied in thermo-optical method based OC-EC measurement, organic chemical compound analysis with thermal-denuder mass spectrometer, and thermogravimetric analysis (Pratt and Prather, 2009; Seinfeld and Pandis, 2012). Particles' volatility expressed as refractory fraction remaining in term of volume (VFR) and mass (MFR) at a function of temperature are measured using V-TDMA (Volatility-TDMA) system, or combined with APM, MS techniques (e.g., ATOFMS, AMS, CIMS), which can help in gaining insight into the mixing state of particle and also into thermodynamics mechanisms of carbonaceous aerosol formation and aging processes (Pratt and Prather, 2009; Wehner et al., 2009; Tiitta et al., 2010; Tritscher et al., 2011). However, volatility of smoke particles from primary emission to atmospheric evolution remain poorly characterized (Rose et al., 2011; Li et al., 2016b). Li et al. (2016a) combined on-line V-TDMA-APM and off-line OC-EC measurements for various fresh smoke particles, and concluded that VFR-MFR are size and fuel type dependent, with more volatile organic materials having less density and lower OM/OC (organic matter to organic carbon) ratios in the externally mixed smoke particles. In polluted urban air, particles with smaller radius and larger volatile fractions at 300 °C can be regarded as aged and internally mixed soot particles, and the refractory materials are considered to be mostly engine and combustion sourced soot or EC (Sadezky et al., 2005; Cheng et al., 2009; Wehner et al., 2009). Tan et al. (2016) report external and core-shell mixture of BC particles leading to high σ_{sp} and SSA in PRD. Wehner et al. (2009) monitored mixing state of nonvolatile aerosol and the corresponded light absorption during CAREBeijing-2006 campaign. Rose et al. (2011) found externally mixed soot particles from biomass combustion to be less volatile and weak CCN-activated. Photochemical oxidation effect on the volatility changes of organic aerosol depends on specific physiochemical mechanisms. Formation of SOA upon oxidation of semi-volatile vapors from primary emissions to less volatile species, which transfer to organic aerosol, will increase the volatility of preexisting particles. Heterogeneous reaction, such as functionalization and oligomerization, decrease volatility of OA, while fragmentation forms species in various thermostabilities albeit mostly at lower volatilities (Reinhardt et al., 2007; Tritscher et al., 2011).

4.2.5. Optical properties

Smoke particles contain major organic materials (over 70 wt.% on average) and a considerable amount of inorganic salts, which present distinctly different optical properties (Reid et al., 2005a; Seinfeld and Pandis, 2012). Carbonaceous materials such as BC-soot particles are the main light absorbers over the entire visible spectrum. Enrichment of smoke in light absorption components (like humic species, PAHs, and lignin etc.) makes the rest of the smoke organic matter to be brown carbon with light absorbing efficiency next to BC. Most absorption by brown carbon takes place in the UV band and in the short visible wavelength due to the presence of resonant ring structures (Hoffer et al., 2006; Mustard et al., 2008; Lin et al., 2010), while inorganic salts, such as sulfate and nitrate, exhibit specific light scattering character, which can cool the atmosphere by increasing the Earth's reflectivity. Smoke particles, internal mixed or coated inorganic salts, can act as lens to enhance light absorption of BC. The net BB radiative forcing is small (0.0 ± 0.2 W/m^2) (IPCC, 2013) but represent great uncertainty in the climate effect assessment due to the need to resolve the balance between the positive radiative forcing by BC and BrC, and the negative radiative forcing by OC and inorganics. Mass absorption efficiency (MAE) of fresh soot particle is 4–9 m^2/g at 550 nm wavelength, aggregation and encapsulation with organic or inorganic condensates though atmospheric aging might increase its MAE by 30%–50% (Fuller et al., 1999; Bond and Bergstrom, 2006; Mustard et al., 2008; Zhang et al., 2008b; Yang et al., 2009). MAE for the BrC in smoke particles varies from 0.03 to 0.60 m^2/g at 550 nm, depending on different measurement techniques and derived chemical fractions (Kirchstetter et al., 2004; Yang et al., 2009). Mustard et al. (2008) estimated MAE of brown carbon sphere to be 3.6–4.1 m^2/g at 550 nm, and Chakrabarty et al. (2010) measured MAE for tar ball particle to be ~2.5 m^2/g at 530–730 nm. Single scattering albedo (SSA) is the key optical parameter that describes the strength of aerosol's direct radiative forcing, and spectral defined SSA for smoke aerosol mainly depends on burning condition but also on fuel type and oxidation level (Ramanathan et al., 2001; Ramanathan et al., 2001; Liu et al., 2014; Saleh et al., 2014). SSA is inversely related to MCE (modified combustion efficiency): smoldering phase emits more nonopaque carbonaceous materials with higher SSA (~1.0 at MCE < 0.9), smoke particles from flaming fire containing more BC have much lower SSA (Ramanathan et al., 2001; McMeeking et al., 2009; Liu et al., 2014). Sharp increment of aerosol scattering and absorption coefficients was observed during field burning events (Garland et al., 2008; Yu et al., 2013b). Atmospheric aging processes including photochemical oxidation to produce more SOA, increase the SSA (Abel et al., 2003; Yokelson et al., 2009; Liu et al., 2014), humidification to change the mixing state and morphology also decreases light absorption of smoke particles (Adler et al., 2011; Guyon et al., 2003; Haywood et al., 2003; Lewis et al., 2009).

4.3. Morphology and mixing state

Analytical transmission electron microscopy (TEM) is a powerful tool for characterizing individual aerosol particles because it provides simultaneous morphological, compositional, and structural information. Individual aerosol particles in smoke plumes from biomass fires have been studied using analytical TEM in southern Africa and China, which allowed detailed characterization of particle types in smoke. Based on composition, morphology, and microstructure, three distinct types of BB particles are present in the smoke: (1) soot, (2) tar ball particles (carbon-rich, spherical particles), and (3) organic particles with inorganic (K-salt) inclusions. It is well established that the relative number concentrations of organic particles with inorganic inclusions are the largest in young smoke, whereas tar balls are dominant in a slightly aged smoke from a smoldering fire. Flaming fires emit relatively more soot particles than smoldering fires.

Soot. i.e. BC, is common in BB emissions, which is believed to be formed via a vaporization-condensation mechanism during combustion processes (Li et al., 2003; Chen et al., 2005; Chen et al., 2006). Soot is clearly distinguishable from the other particles under the TEM. Soot forms branching aggregates containing from less than ten to thousands of spheres, each of which is 20 to 60 nm in diameter. Typical soot aggregate with fractal-like chain structures can extend to a couple of micrometers or more. HRTEM image of the soot spheres shows onion-like structures of curved, disordered graphitic layers. STEM-EDX mapping shows the soot aggregate mainly contains C and minor O. Typical SAED patterns of soot aggregates exhibit three distinct rings, which are indexed to the crystalline structure of graphite (Viktória et al., 2006). The SAED pattern obtained from soot aggregates shows broad and diffuse 002 and *hk* rings, indicating a microstructure consisting of randomly distributed crystallites that have a fine size and do not possess long range order (Chen et al., 2005). Dark-field imaging has been used to visualize individual microcrystallites. The bright spots in the dark-field image are produced by diffraction from the 002 planes of microcrystallites. These bright spots are distributed unevenly within

the particles. Observation of such patterns could be due to a different density of circumferential 002 lattice planes parallel to the electron beam (Chen et al., 2005; Viktória et al., 2006).

The soot content varied greatly in different smoke samples. Besides the major component of C and O, most of the soot aggregates contained potassium, and some had minor amounts of silicon. The potassium enrichment in soot has been used as a fingerprint of its BB origin. High-spatial-resolution electron energy-loss spectroscopy (EELS) results showed chemical heterogeneity even within one aggregate, with varied potassium contents in different soot spheres. Some of the soot particles showed a modified morphology, which most likely resulted from atmospheric aging (China et al., 2013; Adachi and Buseck, 2013). Once emitted into the air, the irregular geometry and complex microstructure of soot aggregates may provide active sites for deposition of common atmospheric gases such as O_3, NO_2, and SO_2, which could readily oxidize soot surfaces (Decesari et al., 2002). The soot-O_3 reaction is particularly rapid, and prolonged exposure to ozone under laboratory conditions may lead to the collapse of the graphitic structure (Zhang et al., 2008b; Yokelson et al., 2009).

Tar ball. Tar ball particles form an important fraction of the total particle number concentration in some of the smoke plumes. Tar balls are readily recognized in TEM images by their spherical shape, amorphous, and are typically not aggregated with other particle types. Tar balls are produced by a gas-to-particle transformation followed by condensational growth in biomass smoke (Pósfai et al., 2003; Hand et al., 2005). Tar balls range in diameter from 100 to 500 nm, with a few particles larger than 1 μm. HRTEM images of tar balls did not indicate any semiordered graphitic microstructure typical of soot. Their EDX spectra indicated elemental compositions consisting of C and O with trace amounts of S, K, Cl and Si. Electron energy-loss maps show that the distribution of C and O in tar ball is homogeneous, and thickness profiles indicate that most are perfectly spherical. In contrast to other widespread and spherical aerosol particle types, such as sulfate and K-rich particles, tar balls were stable under the TEM and did not change visibly under prolonged exposure to the electron beam, suggesting they were composed of refractory material. It has been reported that the chemical compositions, densities, and carbon functional groups of tar balls were distinctly different from soot and black carbon and more closely resembled high molecular weight polymeric humic-like substances, which could account for their reported optical properties (Li et al., 2003; Pósfai et al., 2004; Hoffer et al., 2006).

Of special interest was to compare tar ball with K-containing organic particles, both of which showed similar elemental compositions, with comparable amounts, amorphous microstructures, overlapping sizes, and strong resistances against electron bombardment. Since Pósfai et al. (2003) proposed that tar balls probably corresponded to an intermediate stage in the aging of organic particles from BB, it was proposed that a fraction of K-containing organic particles could originate from tar balls. When exposed to an electron beam, surface sulfates sublimated. Elemental maps proved that C, O, and Si elements homogeneously distribute within the bulk of the particle. Homogeneous internal distributions of C and O in tar balls were previously reported (Hand et al., 2005). Also such assumption was supported by a few field studies performed in southern Africa and California (Pósfai et al., 2003; Pósfai et al., 2004; Hand et al., 2005). Both tar balls and the organic particles with minor K, Cl, and S contents were characteristic products in aged biomass plumes.

Organic particles with inorganic inclusions. "Organic particles with inorganic inclusions" referring to the crystalline, visible inorganic constituents and the high C contents of particles that belong to this type. Organic particles with inorganic inclusions do not have distinct morphologies under the TEM (Fig. 5). They typically contain crystalline K-salts, primarily either KCl or K_2SO_4, but the presence of KNO_3 was also inferred from composition data. The bulks of the particles contain C and minor O, and are stable in the electron beam. The composition of the inorganic inclusions varied with age of the smoke, and probably the type of biomass burnt. Potassium-salt particles were the most abundant inorganic aerosol constituents in the smoke from BB (Hand et al., 2010). Most had amorphous organic coatings or formed small inclusions in organic particles. These potassium salts were very beam-sensitive. They ranged in diameter from 20 nm to 1.5 μm, with the majority from 100 to 600 nm. Most KCl particles had euhedral morphologies, and some were rounded. Some round particles contained potassium and chlorine, and they were more beam-sensitive than the pure KCl particles. These particles were likely mixtures of KCl and NH_4Cl, which formed through reactions of chlorine and NH_3 species emitted from the biomass fire (Duo et al., 2015). Some of the potassium sulfate and nitrate crystals were rectangular or rounded, but most were irregularly shaped. Selected-area diffraction patterns of KCl and K_2SO_4 particles were obtained to confirm their crystallinity.

Particles with organic coatings. Several TEM studies have shown the biomass particles with organic coating were widespread in urban atmosphere (Adachi and Buseck, 2008; Li et al., 2010b). Most of smoke particles are in the atmosphere are coated with a carbonaceous. Similar particles, with various thickness of organic coating, have been widely observed in a variety of samples, including those from polluted continental environments (Russell et al., 2002; Niemi et al., 2006; Adachi and Buseck, 2008; Li et al., 2010b), especially in the serious fog and haze episodes in China. Organic coating was lost under strong beam bombardment, although it was shown to be less sensitive to the electron beam than sulfates and nitrates, which were different from tar ball and soot. It is believed that organic coating is composed of secondary organic fraction, which commonly forms through condensation of precursor gases on pre-existing particles such as soot (Fan et al., 2006). The high ozone and VOC concentrations in urban Shanghai atmosphere suggested that the formation of SOA from the vapor phase and their subsequent condensation may be a significant pathway in the formation of the organic coating. Previous studies have suggested that ozone, hydroxyl radical, nitrate radical, and other oxidants presented during atmospheric transport played a central role in the formation of SOA in Beijing atmosphere (Li et al., 2010b). In Shanghai, about half of VOCs come from motor vehicles, and 10–35% of VOCs was from industrial activities, indicating the organic coating in these aerosol particles were likely formed by VOCs from fuel combustion, and a lesser extent, from industrial activities (Geng et al., 2009). Laboratory experiments have found that SOA is slightly hygroscopic and exhibits a smooth water uptake with increasing humidity (Varutbangkul et al., 2006; Semeniuk et al., 2007), suggesting the formation of such coating by aqueous-phase processing of the particles during transport in the atmosphere. Organic coatings could modify the particle hygroscopicity, CCN abilities and heterogeneous chemical reactivity, indicating that the ubiquitous presence of this particle type in the atmosphere has important ramifications for the regional climate (Russell et al., 2002; Li et al., 2003; Adachi and Buseck, 2008).

Internally mixed particles. The smoke particles, such as soot or organic particles, are often internally mixed with S-rich particles during aging in the atmosphere. In TEM images, S-rich particles were euhedral or rounded. The sulfates readily decomposed when exposed to an electron beam. When decomposing, they left a similar carbonaceous residue. Laboratory studies showed that sulfate nucleation was often coupled with aromatic acids (Zhang et al., 2004); thus, it was not surprising that organics were present in small sulfate particles. A smaller size of the sulfate grains seemed to be homogeneous and was usually coated with an organic layer, while the larger ones were usually internally mixed with soot and organic matter (or more chemical species). Within the internally mixed particles, most of the organics may be beam-sensitive SOA. This is consistent with the usual findings that SOA was coupled with S-rich particles (Kanakidou et al., 2005). However, some particles also contained beam-resistant dark inclusions without clear morphological characteristics, which may be organic particles, collapsed soot or tar balls. Previous water dialysis experiments of individual particles have demonstrated that the coatings were water

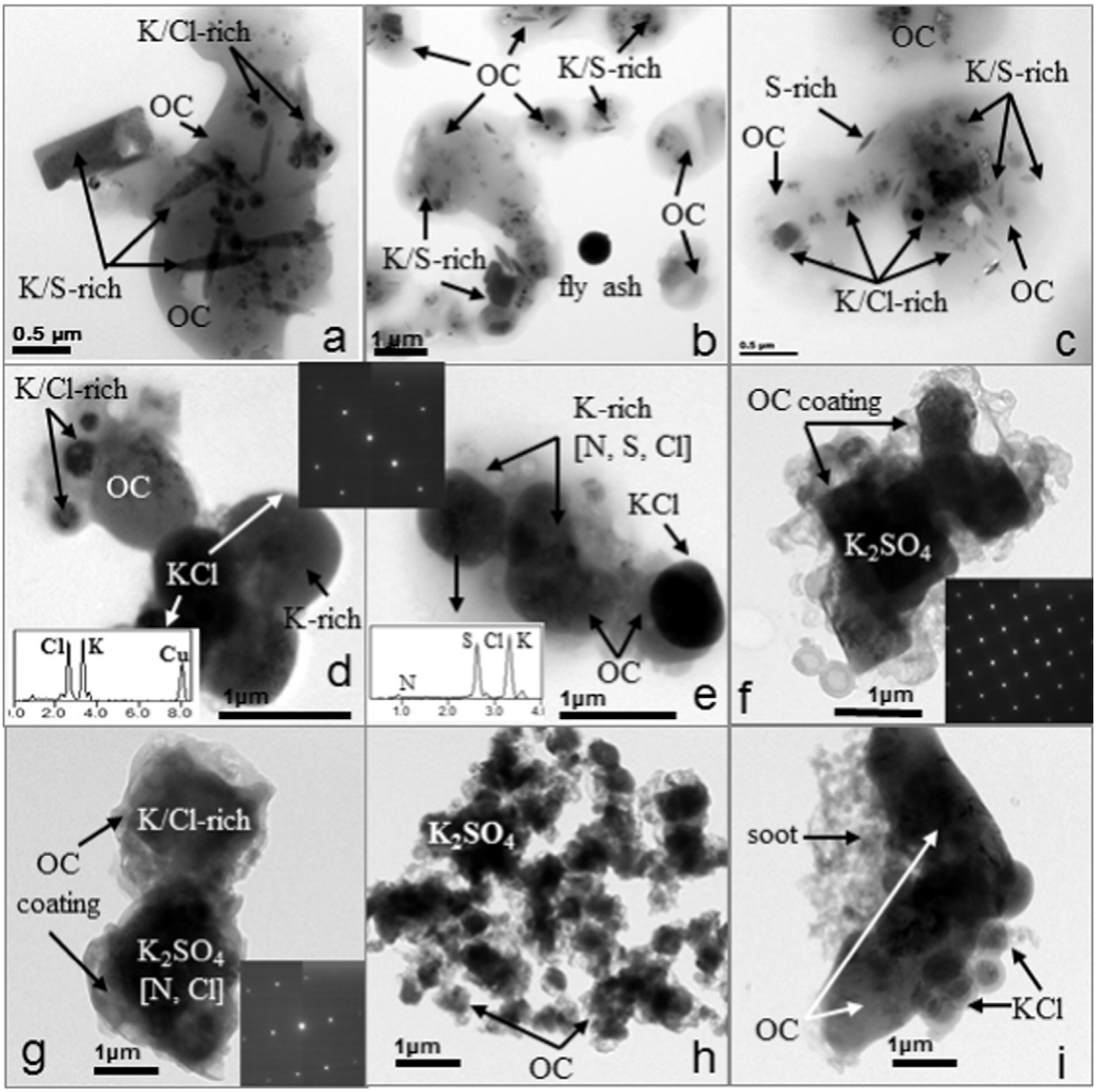

Fig. 5. TEM images of typical organic particles with inorganic inclusions. (a), (b) and (c) organic particle internally mixed with K/Cl-rich, K/S-rich and/or S-rich particles. (d) the rounded crystal KCl mixed with OC and K-rich particle. The inset is the diffraction pattern of potassium chloride. (e) the irregular K-rich particle with OC coating containing minor N, S, and Cl elements, which were likely mixtures of KCl and NH_4Cl. (f) the rectangular potassium sulfate particle with OC coating. The diffraction pattern is indexed into K_2SO_4. (g) the euhedral K_2SO_4 particle and K/Cl-rich particle coated by the OC layer. (h) the aggregated K_2SO_4 particles attached with OC particle. (i) the OC attached with soot and rounded KCl particle.

soluble, while organic inclusions were insoluble (Okada et al., 2001; Li et al., 2010b).

Such internally mixed particles may be preferentially formed in a stagnant aerosol mass, which often occurs during episodes of serious pollution (such as urban haze), when there is insufficient wind velocity to carry pollutants away from the city. During these periods of pollutant retention, aerosols continue to collide and combine with each other, resulting in larger average sizes and complex components (Li et al., 2011b). Larger sizes are commonly associated with the polluted environment and adverse meteorological conditions (Li et al., 2010b). In high pollution areas such as Mexico City, over half of the aerosol particles consist of internally mixed soot, organic matter, and sulfates (Adachi and Buseck, 2008; Moffet et al., 2010). Sulfate coatings can have either negative or positive effects on the radiative forcing of BC. On one hand, the internally mixed sulfates can make organic matter and soot more hydrophilic and eventually make them efficient CCN. While, on the other hand, embedding sulfates act as lenses that focus light on soot and thus amplify absorption of the internal particles (Adachi and Buseck, 2008; Adachi et al., 2010; Healy et al., 2015).

4.4. Gaseous pollutants

BB is an important source of volatile organic compounds (VOCs) and carbon monoxide (CO), which are precursors of ozone (O_3) and secondary organic aerosol (SOA), posing damage to air quality and human health. Guo et al. (2004) identified the contribution of BB to VOCs to be 11% ± 1% at a background site in eastern China (i.e., Lin'an in Zhejiang Province). Comparable contribution to VOCs was identified at a background site in central Pearl River Delta (PRD) (i.e., 11% ± 1%), southern China, and at an urban site in southwestern Hong Kong (i.e., 9% ± 2%) (Guo et al., 2011). With the source-tracer-ratio method, Yuan et al. (2010) identified the average BB contribution of 12.6% to VOCs including the oxygenated VOCs (OVOCs) in PRD. In central China, BB even accounted for 54.8% ± 0.5% of VOCs during the haze

episodes in the autumn harvest season, and it was identified as the main cause of the haze pollution in warm seasons in that region (Lyu et al., 2016). Through the bottom-up approach, the contribution of BB to VOCs was also estimated based on the emission inventories. However, they varied within a large range. For example, the contributions increased from 1.82–3.17% not necessarily the lowest (Zhang et al., 2013), to 7.6% (Bo et al., 2008), up to 13.9% not necessarily the highest (Yan et al., 2006) in Guangdong province. The uncertainties in emission factors and activity levels were the main causes of these discrepancies. In addition to these factors, the differences between the results from the top-down (e.g., source apportionment) and bottom-up methods were also due to the fact that the contributions of BB beyond the study area might be included in the results, as determined by the receptor-oriented source apportionment model, due to the long lifetimes of some BB related VOCs (i.e., ethane, ethyne and benzene). On the other hand, CO was also largely emitted from BB. Wang et al. (2002) found that CO increased considerably during the autumn season and correlated well with methyl chloride (CH_3Cl), a common tracer of BB, at a rural site in eastern China, indicating the contribution of BB to CO. This contribution was further quantified as 18 ± 3% by Guo et al. (2004). Based on the emission inventory, the CO emissions from BB reached 0.5 Tg/yr in PRD (He et al., 2011b) and even summed up to 16.5 Tg/yr in whole China in the early 2000s (Yan et al., 2006).

The source profiles of VOCs for the BB were determined from the laboratory and field tests. Although the physical and chemical characteristics of the combustion materials and combustion modes (i.e., fire burning and smoldering) influenced the VOCs emissions, many similarities were found. Zhang et al. (2013) collected the rice straw and sugarcane leaves in PRD and tested the emission factors of VOCs in the laboratory. The results indicated that the top 10 non-methane VOCs (NMVOCs) in the emissions were ethene, ethane, propene, toluene, ethyne, propane, benzene, isoprene, 1-butene and *m*/*p*-xylene, among which the C_2 species accounted for >50% by volume. However, ethane, ethene, propane, ethyne, *n*-butane, propene, *i*-pentane, *n*-pentane, toluene and *i*-butane were the most abundant VOCs in the combustion of sugarcane leaves. Liu et al. (2008) collected the biofuel burning samples in a farmer's house in PRD, and analyzed the source profiles for the combustion of wheat, corn and wood, according to which CH_3Cl, ethene, ethane, ethyne, propene, 1,3-butadiene and BTEX (benzene, toluene, ethylbenzene and xylenes) were suggested as the tracers of BB. In Hong Kong, the outdoor barbecue was a typical type of BB. Two samples were collected near a barbecue stove. Table 2 lists the top 10 NMVOCs in the two samples. It was found that the C_2-C_4 hydrocarbons, benzene and toluene were the main VOCs emitted from barbecues.

Based on the known source profiles of BB, the species-specific loadings of VOCs could be determined with the source apportionment techniques. $CHCl_3$ and acetonitrile (CH_3CN) were often treated as the tracers of BB. It was found that the mixing ratios of CH_3Cl increased significantly in summer and autumn at Lin'an site ($p < 0.05$), when the field and domestic combustion of crop residues increased (Guo et al., 2004). In addition, Lyu et al. (2016) found that CH_3Cl and CH_3CN were both higher on the BB induced haze days than those on the non-haze days in Wuhan, central China. Apart from the typical tracers, BB gave off a large amount of VOCs, such as ethane, ethene and ethyne, representative of incomplete combustion, and the aromatics including benzene, toluene and xylene isomers. It was found that C_2-C_3 alkene, ethyne and benzene were the predominant VOCs in the emissions of BB, which was responsible for 16% ± 3% and 11% ± 2% of ethyne and benzene, respectively, based on the source profiles determined in eastern China (Guo et al., 2004). Similarly, the C_2 hydrocarbons (i.e., ethane, ethene and ethyne) dominated in the emissions of BB in Hong Kong and PRD (southern China), which comprised ~45% and ~80% of ethene in Hong Kong and PRD, respectively (Guo et al., 2011). During the autumn haze episodes in Wuhan (central China), BB emissions contributed 60.8% ± 0.3%, 71.3% ± 0.5%, 65.0% ± 0.4% and 85.2% ± 0.7% to ethane, ethene, ethyne and benzene, respectively (Lyu et al., 2016). OVOCs were also a significant group in BB emissions. It was reported that acetone and acetaldehyde were the most abundant two OVOCs in the emissions of straw burning (Zhang et al., 2013). With CH_3CN as the tracer, Yuan et al. (2010) found that an autumn BB contributed 17.7% and 12.3% to acetaldehyde and acetone, respectively. Apart from these two species, formaldehyde, propanal, methylglyoxal, methanol and isoprene and its oxidation products were also detected in BB emissions.

The ratios between VOCs species were often employed to help identify the sources of VOCs. For example, the ratio of ethyne/ethane (0.49–1.02) in the source of BB identified by Guo et al. (2011) was comparable to that (0.57) in the plume of a fresh BB (Blake et al., 1994). A comparable ratio of ethyne/ethane (0.67) was also observed in a sample collected near a barbecue stove in Hong Kong. However, it was much lower in another barbecue sample (0.12) and those (0.30 and 0.21 for the combustion of rice straw and sugarcane leaves, respectively) determined by laboratory experiments in PRD (Zhang et al., 2013). Similarly, the dry grass combustion samples collected in central PRD had high ratios of ethyne/propane (8.3) and benzene/propane (1.6) (Wang et al., 2005a). However, the ratios were much lower in the combustion emissions of rice straw and sugarcane (Zhang et al., 2013), and barbecue samples. Noticeably, the ratios of VOCs varied within a large range in different studies, which might relate to the materials and modes of the combustions. Therefore, it was not reliable to identify BB with the only signature of VOC ratios. Future analyses should be based on the variations of the tracer concentrations and/or the source apportionments.

Table 2
Top 10 NMVOCs in the two samples collected near a barbecue stove in Hong Kong.

Sample 1		Sample 2	
Species	Mixing ratio/ppbv	Species	Mixing ratio/ppbv
Ethene	458.7	Ethane	2049.5
Ethane	275.4	Ethene	936.7
Ethyne	184.8	Propene	289.9
Propene	94.5	Propane	265.6
Benzene	50.7	Ethyne	253.4
Propane	41.5	Benzene	143.0
1,3-Butadiene	21.2	Toluene	82.0
i-Butane	19.7	*n*-Hexane	33.7
Toluene	18.7	*n*-Butane	32.3
n-Hexane	12.7	1-Butene	28.2

4.5. PAHs

PAHs are a class of hazardous air pollutants, which are predominantly produced from the incomplete combustion of organic materials, e.g. coal, wood and other biomasses. Because PAHs are classified as carcinogenic (IARC, 2010), the US EPA has issued a list of 16 priority PAHs to be monitored in risk assessment exercises. For example, a large scale study by Zhang et al. (2009b) has estimated that the inhalation of airborne PAHs led to the overall population annual excess of the lung cancer incidence rate of 0.65×10^{-5} in China. Meanwhile, BB is an important source of PAHs, especially because most BB provided a favorable condition for PAH formations and consequently has high emission factors for PAHs (Ravindra et al., 2008).

In China, recent studies by Li et al. (2016d) and Tao et al. (2011) have estimated the contribution of BB to the total PAH emission. The combination of firewood and straw burning accounted for the largest proportion of PAH emission in China. But the overall contribution of BB to total emission of PAHs decreased from about 55% in 2003 (Zhang et al., 2008e) to about 40% (Li et al., 2016d). Zhang et al. (2008e) also estimated the PAH emission from open straw burning during the harvest season at 2.4% of the total PAH emission in China in 2003. Although there are differences in the calculation between the two studies in term of PAH emission factors from different sources, the reduction of PAH emission from BB can partly be explained by the reduction in biomass consumption (NBSC, National Bureau of Statistic of China, 2004–2014).

The emissions of PAHs to the atmosphere were dominated by the light weight PAHs such as Naphthalene, Phenanthrene, Pyrene, Fluorene, Acenaphthylene, Anthracene, and Acenaphlene, while the emissions of the heavier PAHs such as Benzo[*a*]pyrene (BaP), Benzo[*b*]fluoranthene, Benzo[*k*]fluoranthene, Benzo[*ghi*]perylene, Dibenz(*ah*)anthracene, and Indeno(1,2,3-*cd*)pyrene were minimal (Li et al., 2016d).

As the extent of BB varies across China, the level of PAH emission from BB also varies from region to region. It was estimated that the Northern China Plain and the Sichuan Basin and southern China region are heavy emitters of biofuel PAHs while the Northeast region of China is the main emitter of PAHs from wildfire burnings (Zhang et al., 2008e). It is because the Northern China Plain and the Sichuan Basin produce the bulk of wheat straw from its crop, which has significantly higher emission factors of PAHs compared with other kinds of crop residues. The southern China region also burns a large quantity of rice straw, but the emission of PAHs is lower thanks to the much lower emission factor of rice straw (Zhang et al., 2008e). A more recent research by Lin et al. (2015b) also confirmed that the high level of PAHs in the North China region was due to biomass/coal combustion using a diagnostic ratio of different PAHs, although there was no method to clearly distinguish between emissions from biomass and coal burnings (Shen et al., 2013).

The seasonal variation of PAH emissions across China was first evaluated by Zhang and Tao (2008) for two types of BBs including biofuel burning from the residential sector and open burning of agricultural wastes and wildfires where the authors used a regression model for energy consumption in all provinces of China. Overall, PAH emissions from BB (a combination of biofuel combustion and open fires) were higher in the cold season (from November to March) due to burning for the purpose heating, and were lower in warm season, except a small emission peak in July and August due to the occurrence of wildfires; however, the profiles differed greatly among the six geographical zones of China (Northeast, North, Northwest, South, Southwest and Tibetan plateau). For example, while North China had the largest variation of PAH emission between winter and summer and was also impacted by open fires in the summer, South and Southwest China had smaller variation thanks to weaker heating demand in winter and were not affected by open fires as they are far away from the burning areas (Zhang et al., 2008e).

In order to better understand the profiles and inventories of PAH emissions from BB, it is important to obtain the reliable emission factors (EFs). However, EFs of PAHs are usually the main source of uncertainties in recently developed emission inventories (Shen et al., 2013). There are multiple causes for this situation. First, there are a limited number of studies reporting EFs of PAHs from BB in the literature including in China. Second, the results of emission measurement varied remarkably depending on fuel types and the design of burning facilities. For example, EFs of $\sum$15PAHs for wheat straw was reported at as high as 234 mg/kg by Zhang et al. (2008a), but was reported only at 1.1 mg/kg in a different study reported later (Zhang et al., 2011a). Therefore, it is necessary to conduct more measurements and to agree on a common measurement protocol, so that the experimental outcomes are comparable and could be utilized in different contexts. It is also noted that PAHs emitted from BB are in both gaseous and particulate phases and their emissions were reported to be closely related to the emissions of particulate matters (PM) of different sizes (Shen et al., 2013). Therefore, the types of biomass fuels that have high EFs for PM would likely to have high EFs for PAHs, posing an increased risk for the exposed population.

Emissions of PAHs from BB, particularly from the residential sector, are important contributors to the total emissions of PAHs in China. More importantly, indoor BB generates a range of air pollutants including PAHs that threaten the healthy living of the inhabitants. Controlling the residential emissions of PAHs will not only reduce the total emissions of PAHs but also lower the health risk of the population with lower economic status. The most effective approach may be to encourage the use of clean stoves or alternative fuels. While BB will continue to be an important energy source in the rural areas because of easy access and very low cost, the introduction of new clean stoves will improve fuel efficiency and reduce indoor air pollution (Chen et al., 2016). At the same time, traditional biomass fuels should be replaced with biogas or pelletized biomass. Those alternative fuels can be produced locally and are not likely to add significant cost to the household energy budget. Such programs could also be promoted by the government through economic incentives and technical assistance to achieve better population health outcome.

4.6. Emissions, trends and control

Studies have estimated short- and long-term BB emissions of carbonaceous aerosol (e.g., BC, OC, $PM_{2.5}$) and pollutants like PAHs, CO_2, VOCs etc. in China. The spatiotemporal distributions and dynamic trends for the emissions have also been characterized based on inventory calculation, atmospheric chemical transportation simulation, and national economic-official data assessments (Saikawa et al., 2009; Zhao et al., 2011; Qin and Xie, 2012; Li et al., 2014b; Zhang et al., 2015a). Domestic fuel use of biomass has declined dramatically in rural areas due to the more widespread supply of clean and cheap energy like electricity, LPG (liquid petroleum gases), and methane, in the process of new countryside construction and urbanization (Zeng et al., 2007; Zhang, 2011). In contrast, field burnings, especially agricultural fire emissions increased sharply over the past decades (He et al., 2011b; Lu et al., 2011; Qin and Xie, 2011, 2012). Crop straw productions and percentage of straw field burnt are the two key parameters to assess agricultural open burning emissions, and they are also what make BB a major source of anthropogenic pollution (Reid et al., 2005a; Cao et al., 2006; Zhao et al., 2012). Annual crop straw productions are of the magnitude of 10^2 million tons in China. A significant yearly exponential growth of 3.4% has been observed since 1949 when crop production was only ~0.8×10^{14} g, to reach over 7.4×10^{14} g in 2014. National field burning rate of the crop residues is commonly believed to be 15.2%–27.2% (Cao et al., 2006; Wang and Zhang, 2008; Zhang et al., 2011a), which means over 100 million tons crop straws is being burnt annually in the field. Vast uncertainties in provincial or regional burning rates are reported in different publications, e.g., the variable rate is 0 in Beijing in the work of Cao et al. (2006, 2011), but 17% reported by Wang and Zhang (2008). He et al. (2011a, 2011b) estimated field burning rate for Pearl River Delta to be 31.9%, however, according to a government report in 2013 (National Development and Reform Commission report, [2014] No. 516, data available at *http://www.sdpc.gov.cn/*, in Chinese), the corresponding figure is 28.4%. Zhao et al. (2012) have assumed that 100% of crop straws are field combusted in Huabei region, while official reported data are 22.3%. Besides, regional field burning rates are proposed and proved to be proportional to the peasants' income level, i.e., ignoring government policy-profit orientation and awaken of public environmental protection awareness, more agricultural residues will be discarded to be burnt with the development of rural economies (Chen, 2001; Cao et al., 2006; Qin and Xie, 2011). Qin and Xie (2011, 2012) deduced year-specific regional open burning rates from 1980 to 2009 based on parameters of the fixed year, over a tenfold increment of the burning rates were found within the past decades. Furthermore, multi-year anthropogenic BC emission figures were derived using the dynamic emission factors and burning activity rates. The results showed a rapid increase, with annual fluctuation of national BC emissions, from ~0.87 Tg in 1980 to ~1.88 Tg in 2009. Residential biofuel consumption contributed ~40% of this increase with 15%–20% from crop residues burning and 15%–30% from firewood combustion, while agricultural waste open burnings made up <6%. Temporal emission characters of BC show a diminishing trend of residential contribution since 1996 but a rapid and steady increase trend of biomass open burning production (Qin and Xie, 2011, 2012). Moreover, specific spatial distribution of BB emissions was identified, with the emissions occurring mainly in the North Plain, the Northeast and the Pan-Pearl River Delta regions,

echoing the distributions of fire sites and the crop planting or forestry regions, especially Shandong, Hebei, Henan, Anhui and Heilongjiang where contributed over 65% of the total emissions, leading the top five provinces of BB emissions (Cao et al., 2006; Wang and Zhang, 2008; Yuan et al., 2010; Zha, 2013; Zhao et al., 2012). The seasonal pattern of open burning in China that favors to occur predominantly in the autumn and winter, and agricultural field fires are commonly observed during post-harvest period that concentrated in June to November (Wang and Zhang, 2008; Zha, 2013). Extensive emissions from biomass open burnings facilitate formation of haze over the entire China, and particularly in the North and East areas, leading to serious health and climate effects (Ge, 2008; Cheng et al., 2014a; Gao et al., 2015; He et al., 2015; Hua et al., 2015; Yang et al., 2015).

Streets et al. (2003) concluded that open burning is much more serious in China and contributed 25% of the total biomass burnt in Asia, producing 0.11 Tg BC and 0.73 Tg OC annually. Ohara et al. (2007) postulated that domestic combustion is the primary source of BC (~1.08 Tg/yr) and OC (~2.56 Tg/yr) emissions in China, and that residential biofuel burning contributed 43% BC and 82% OC emissions, which are comparable to that of coal use. Study by Lu et al. (2011) and Streets et al. (2008) also identified historical trends of carbonaceous aerosol emissions in China for the period from 1980 to 2010, a slight decrease of OC and BC emissions during 1995–2000 over the entire increasing trends was observed, which was attributed to the less use of biofuel and coal, while the contribution of biofuel burning presented the inverted figure towards the trends of OC and BC emissions. Forecasting of BB emissions for the nearest future in China has been conducted by many studies. Zhou et al. (2003) developed three emission scenarios for 2010 and 2030 based on long-term energy-economic structures and energy-emission control technology development, and on the basis of emission scenarios and emissions for 2000. The results showed that biofuel burning emissions and their atmospheric contributions decreased under all three scenarios for 2010 and 2030. Ohara et al. (2007) applied the projection from Zhou et al. (2003) to assess emissions in China for 2010–2020, and they found that BC emissions in 2020 would decrease by ~28.7% on average, compared with that in 1995, and that this would mainly result from a reduction in emissions from biofuel and coal. Driven by IPCC scenarios, Streets et al. (2001) predicted the same BC emission changes with 8% decrement for 2020 in China (open burning emissions were excluded), because of decreased use of biofuel and coal. Later, Streets et al. (2004) forecasted the future worldwide emissions of primary carbonaceous aerosol for 2030 and 2050 on the basis of 1996 emission figures, considering the only sources of energy generation and open BB. The authors projected the decline of both OC and EC emissions for 2030 and 2050 in the East Asia, as China moves away from residential use of coal and also biomass open burning. Based on emission inventories for BC, OC, sulfate and SO_2 in China for 2000 (BB emissions dominated), Saikawa et al. (2009) analyzed future emissions for 2030 upon the hypothesis of governmental policy implementation and enforcement, and they found that aggressive emission control will lead to 50% reduction in premature deaths, while high emission scenario would present the inverse effect, and the radiative forcing effect changes would also depend on the emission scenarios.

However, the predictions of BB emissions in China driven by environmental and economic prospects or historical trends are all moderate and conservative, the government policy enforcement can be more severe and effective, it may not be economically efficient, but harsh enough to achieve the emission control goals, like the fire-forbidding policy implementations during Beijing Olympic Games 2008, Shanghai World EXPO 2010, Beijing APEC 2015, and the nearest Hangzhou G20 Forum 2016, etc., primary emissions over wide-scale regions are surely decreased to realize the short-term control policy and meet the "blue sky" standard (e.g., APEC blue) (Wang et al., 2010; Xin et al., 2010; Huang et al., 2012b; Guo et al., 2013; Huang et al., 2013a; Chen et al., 2015a, 2015b; Yang et al., 2016). Normalization of BB or agricultural field burning forbidden will be forecastable, the reduction of primary anthropogenic pollutants emissions will also be divinable, and then we may meet more complicated environmental problems, such as the transformation from atmospheric pollutions leading by fine particles to ozone pollution, and marginal effect in pollutants control to meet the WHO (World Health Organization) standard (Hope, 2008; Shindell et al., 2012; Huang et al., 2014; Doherty, 2015; Wang et al., 2016a).

5. Biomass burning plume

5.1. Transport

Smoke from BB and desert dust are two of the main atmospheric constituents that affect the air quality and climate due to their massive plumes that can travel thousands of kilometers downwind. The monitoring of these plumes is only possible through the satellite measurements (Kahn et al., 2007). The OMI is a nadir viewing imaging spectrometer onboard NASA's Aura satellite, which was especially designed to replace the Total Ozone Mapping Spectrometer (TOMS) in measurements of ozone and UV-absorbing aerosols, such as smoke and desert dust (Torres et al., 2007; Torres et al., 2013) via the UV aerosol index (AI)/absorbing aerosol index (AAI). Therefore, smoke plumes have a clear signal in AI values (Kaskaoutis et al., 2011, 2014) allowing us to monitor their transport pathways. However, a similar sensitivity of AI is for the desert dust and there is no way to discriminate between these aerosol types using only OMI-AI retrievals. Thus, the discrimination between smoke plumes and desert dust is possible with the combined use of other satellite retrievals, such as AIRS or MOPITT CO measurements, since CO is a product of BB (Ding et al., 2015). Furthermore, another disadvantage in considering AI as a measure of the BB aerosols is its great sensitivity to the height of the aerosol plume. Therefore, smoke plumes at elevated heights result in larger AI values, even if they are not as thick as the plumes near the ground. This fact limits the utilization of AI for monitoring of the BB aerosols. Furthermore, the OMI measures several air pollutants, including NO_2, SO_2 with global daily coverage (*http://aura.gsfc.nasa.gov/instruments/omi.html*), which are products of any kind of burning, including biofuel and fossil-fuel combustion. Thus, in combination with FC from MODIS, NO_2, and SO_2 concentrations may be examined over areas far away from urban and industrialized centers in order to assess the contribution of BB (Chubarova et al., 2012; Kaskaoutis et al., 2014).

5.2. Atmospheric aging

Emissions released directly from sources are referred to as primary, or fresh emissions including gaseous organic and particle-phase organic (primary organic aerosol, POA) species. In contrast, processed emissions are the result of atmospheric photochemical processing (aging) of primary species. The aging can be referred to a variety of gas-to-particle conversions and particle changes within the atmosphere. Probably the most important aging pathway is chemical oxidation of primary gaseous compounds (volatile organic species, VOCs), emitted directly from an emission source, to form saturated low-vapor-pressure organic species that often condense onto the pre-existing particles and form secondary organic aerosol (SOA) (Kroll and Seinfeld, 2008; Seinfeld and Pankow, 2003). Gaseous species in smoke emissions can partition onto the particle phase by gas-phase oxidation and form SOA. Therefore, BB aerosols are found to be strongly related to SOA formation (DeCarlo et al., 2010; Cheng et al., 2013). SOA has been recognized as an important contributor to PM pollution, having considerable effects on climate (changing radiation balance by scattering insolation and acting as a CCN) and adverse impacts on human health (Pope and Dockery, 2006; Hallquist et al., 2009). It has been assessed that 40 to 70% of the total VOCs in the atmosphere are transformed through photochemical oxidation process to form SOA (Goldstein and Galbally, 2007). The most common photochemical oxidizers in the atmosphere are hydroxyl radicals (OH) (during daytime), nitrate radical (NO_3) (during nighttime) and

ozone (O_3) (during night and daytime hours) (Jacobson et al., 2000; Rollins et al., 2012; Lambe et al., 2015). In most of the environments, including China, photochemical reactions with OH are the dominant anthropogenic VOCs scavengers (Warneke et al., 2004; Yuan et al., 2013). Some studies suggested the fast formation of SOA species even within a half of a day (Kleinman et al., 2008; DeCarlo et al., 2008; Dzepina et al., 2009). BB aerosol lifespan is estimated to be 3.8 ± 0.8 days, which likely provides enough time for significant atmospheric transformations (Edwards et al., 2006). SOA generation potential from VOC, using an emission inventory, was estimated throughout China. Cities characterized with the highest values were found to be Hong Kong, Beijing and Shanghai respectively (Yuan et al., 2013). According to this study aromatic VOC species can contribute most to SOA yields in China. However, large uncertainties related to this data emphasize the need of characterizing the SOA portions that cannot be estimated by known VOC emission inventories. Under ambient conditions, most of the POA are sufficiently volatile to release their content into the gaseous phase and will not remain for a long period of time in the aerosol phase (Donahue et al., 2009). Therefore another important part of aging process is oxidation of gaseous species that are transferred from primary particle-phase organics. Moreover it is observed that large portion of ambient organic fraction can be present in both, particle and gas phase due to its semivolatile nature and can shift from one phase to another (Shrivastava et al., 2006; Robinson et al., 2007). The semivolatile nature of BB aerosol has been suggested (Robinson et al., 2007; Grieshop et al., 2009). Therefore, atmospheric aging of BB plumes can be considered a complex and a very dynamic process.

So far the main approaches used in China to investigate aging of BB emissions are transmission electron microscopy coupled with energy-dispersive X-ray spectroscopy and aerosol mass spectrometry (AMS). More details about studies performed and results obtained related to these approaches are given in the following paragraphs.

5.2.1. TEM coupled with energy-dispersive X-ray spectroscopy (EDX) approach

Changes in morphology, composition and mixing state of individual BB-related particles during the aging was extensively investigated in China using the TEM coupled with EDX spectroscopy. A similar approach has been used in other parts of the world (Pósfai et al., 2003; Semeniuk et al., 2007). Some important features of BB-related particles transformed during the aging are presented here. Soot (EC), organic fraction, potassium nitrate (KNO_3) and potassium sulfate (K_2SO_4) are the dominant species found in BB plumes emitted during the agricultural burning activities (Li et al., 2010a), the major sources of BB aerosol in China. Potassium species are predominantly composed of KNO_3 and K_2SO_4 that are formed in heterogeneous reactions of nitric and sulfuric acids with potassium chloride (KCl), an important fraction of fresh plume emissions (Li et al., 2003; Engling et al., 2009; Li et al., 2015). It was observed that during the aging of BB smoke potassium rich particles form inclusions/aggregations with organic matter, and that organic species found in these forms are mostly of hydrophobic nature. Potassium rich species in aging studies, observed in China, are also often covered by a layer of organics, which are found to be predominantly water soluble species (Li et al., 2010a). Organic coatings are associated with SOA formation, more precisely they are formed in the partitioning of low volatility species that are products of VOC oxidation (Li et al., 2010b; Fu et al., 2012; Yao et al., 2016b). Li and Shao (2009) suggested that organic coatings can be an explanation for the increased cooling effect observed in China during periods of high brown haze and relative humidity. Soot particles in BB emissions can be found in a form of aggregates or inclusions mostly with potassium and sulfur rich compounds and/or organic species (Johnson et al., 2005; Li and Shao, 2010; Li et al., 2010b). Therefore processing of soot aerosol with plume age often alters its inert and hydrophobic structure. Spherical species similar to tar balls, which are suggested to be a fraction of aged plumes (Pósfai et al., 2003), were also found in BB emissions in China (Fu et al., 2012). According to these studies, organics can significantly change the morphology, composition, mixing state, size and hygroscopicity of inorganic and soot particles and can further drive the atmospheric fate of these species (e.g. CCN potential and physicochemical reactivity).

5.2.2. Aerosol mass spectrometry approach

In general, the main aim of monitoring aging of smoke plumes was directed to organic species as they are mostly non-inert atmospheric fractions with comprehensive structure and therefore complex atmospheric fate. The chemical aging of OA portion in BB plumes has been extensively investigated using the AMS technique (Capes et al., 2008; Yokelson et al., 2009; DeCarlo et al., 2010; Cubison et al., 2011). The AMS method provides a real time size-resolved chemical characterization of submicron (PM_1) non-refractory species (Jimenez et al., 2003; Drewnick et al., 2009).

Using the AMS approach fresh and aged BB emissions can be distinguished by different organic mass signatures in the AMS mass spectra (Alfarra et al., 2007; Cubison et al., 2011). The evolution of BB emissions in the ambient and simulated atmosphere often results in enhanced portion of oxygenated organic fraction (OOA) and degradation of species that are indicators of BB origin (DeCarlo et al., 2008; Capes et al., 2008; Cubison et al., 2011). The parameter f44, the ratio of the integrated signal at m/z 44 (fragment CO_2^+) to the total signal intensity originated from organic component of mass spectrum, measured by the AMS, has been found to be the main marker for OOA fraction (Volkamer et al., 2006; Jimenez et al., 2009; Ortega et al., 2013). In addition, the AMS parameter f60 is widely used as BB emission signature. Signal intensity for m/z 60 (fragment $C_2H_4O_2^+$) is directly correlated to the concentration of levoglucosan-like species, previously identified as a substantial fraction and tracer of BB emissions (Simoneit et al., 1999; Alfarra et al., 2007; Aiken et al., 2009). It has been estimated that aerosols characterized by an f60 value higher than 0.3 ± 0.06% are influenced by plume emissions (Cubison et al., 2011).

A graphical approach introduced by Cubison et al. (2011) has been widely applied in characterization and evolution estimation of BB plumes. Fresh BB aerosols can be easily distinguished from aged, highly oxidized species by estimating f44 and f60 from the plot (f44 vs f60). Most of the studies have demonstrated the same trend of f44 increase and f60 decrease with aging (Alfarra et al., 2007; May et al., 2015). This approach has limited use in studies performed in China due to difficulties to separate the BB plume emissions from a number of other pollutants abundant in China (Zhang et al., 2015b; Xu et al., 2015). In the Xu et al. (2015) study, that employed the AMS during intense BB periods in China, decreasing trend of f60 and increasing trend of f44 with aging was observed.

Aging of smoke plumes as they move from the source can also be illustrated by the change in the mass spectrum of different factors extracted by a PMF. The PMF evaluation tool (Paatero and Tapper, 1994) has been extensively used in the source apportionment of the AMS OA data (Lanz et al., 2007; Ulbrich et al., 2009; Crippa et al., 2014). PMF apportions the OA spectrum into factors that can be related to specific sources. Some studies have reported different PMF factors that correspond to smoke plumes of different degree of processing, fresh-like and aged-like BB organic aerosol (BBOA) factors (Capes et al., 2008; Bougiatioti et al., 2014; Brito et al., 2014). BBOA factors have distinctive m/z 60. However, fragments related to fresh hydrocarbon-like organic fraction m/z 27, 29, 41, 43, 55, and 57 are prominent in "fresh" BBOA spectra while enhanced OOA-related m/z 28 and 44 are signatures of "aged" BBOA mass spectra. The oxygen-to-carbon (OC) ratio indicates the oxidation state of organic species and it strongly correlated with f44 intensity (Aiken et al., 2008). The OC ratio of BBOA factor thus reflects processing level of BB emission.

Fresh BBOA factor was extracted during the autumn season in urban and rural areas of Pearl River Delta (PRD) with OC ratio of 0.32 and 0.27, respectively (Huang et al., 2011; He et al., 2011a). Detected BB aerosol was associated with crop burning emissions. BBOA profile with the

same OC ratio (0.26) was seen in winter for Yangtze River Delta (YRD) region, possibly due to open burning in the farmlands (Huang et al., 2013b). Low OC ratio in these studies indicates presence of primary emissions. BBOA profiles with similar OC contribution were extracted in many laboratory and ambient studies (DeCarlo et al., 2008; Aiken et al., 2009; Grieshop et al., 2009; He et al., 2010; Chirico et al., 2010; Crippa et al., 2014). PMF resolved aged BBOA profile was also extracted in China. During an autumn period in Beijing (Xu et al., 2015) BBOA factor with OC ratio of 0.5 was extracted, similarly to the profile observed in YRD during the same season period (Zhang et al., 2015b). These oxygenated BB profiles are comparable to studies outside of China (DeCarlo et al., 2010; Brito et al., 2014) and can be related to aged plumes probably transported from the surrounding regions. Aged BB aerosol can lose its BB signature during the atmospheric transformations and transit to a highly oxygenated aerosol fraction, which corresponds to the PMF resolved low volatility OOA (LVOOA) factor (Jimenez et al., 2009). Zhang et al. (2015b) observed a decreasing trend of BBOA factors with aging suggesting the fast evolution of smoke organic fraction into OOA-like species.

Aerosol processing has been investigated in Beijing during winter (Sun et al., 2013) and summer (Sun et al., 2012) periods, using an aerosol chemical speciation monitor for chemical composition measurements. The portion of organic fraction was found to be higher in winter time (52%) compared to summer time (40%). This trend was attributed to increased POA fraction (mainly coal emissions but also includes BB and traffic plumes) that contributes to 70% of OC, while SOA contribution was shown to be similar in both seasons. In addition, it is suggested that contrary to the summer period, when photochemical processing is dominant due to increased temperature and solar radiation, winter time is instead characterized by aqueous reactions of primary emissions that are emitted and accumulated over the night, when partitioning of gaseous species due to low temperature and high relative humidity take place.

5.2.3. Ozone formation in biomass burning emissions

It has been observed that aging of BB plumes can induce production of tropospheric ozone (Real et al., 2007). Excess of main ozone precursors, VOCs, nitrogen oxides and carbon monoxide (CO), generated by fire emissions promote additional atmospheric pathways for ozone production (Real et al., 2007; Ding et al., 2008; Parrington et al., 2013; Ding et al., 2013b; Ding et al., 2015). Ozone enrichments that have been associated with BB have been observed mainly in Eastern China. The highest ozone concentration over the PRD region was showed to be in the spring season with concentrations up to 138 ppbv (Liu et al., 1999). Increased ozone pollution in this region has frequently been observed by number of studies and attributed to transport of photochemically produced ozone initiated by the BB plumes from fires in the South-East Asia (Indo Burma region) (Chan et al., 2000; Chan et al., 2003; Deng et al., 2008; Zhou et al., 2013). Increased ozone concentrations related to BB activities (dominantly from post-harvest crop burning) during the summer period have also been observed in YRD (Cheung and Wang, 2001) and in urban and rural parts of Northern China (Ding et al., 2008; Meng et al., 2009). These authors also suggested a significant impact of transported aged smoke masses that carry photochemically formed ozone.

As ozone is a secondary pollutant that reflects the photochemical potential of the atmosphere, ozone enhancement in BB emissions has been used as a proxy for air mass photochemical activity (Hobbs et al., 2003; Real et al., 2007; Yokelson et al., 2009; Jaffe et al., 2012). According to studies in China, high photochemical activity illustrated by ozone enrichments can indicate an environment conducive to secondary aerosol formation. The ratio of ozone relative to CO ($\Delta O_3/\Delta CO$) increases with the aging of BB aerosols (Yokelson et al., 2009; Jaffe et al., 2013; Wigder et al., 2013). According to Mauzerall et al. (1998) and Honrath et al. (2004), $\Delta O_3/\Delta CO$ values for aged BB aerosols range between 0.1 and 0.7 (Jaffe et al., 2012). To the best of our knowledge studies like this have not been published so far in China. This again emphasizes the need to perform smoke tracking experiments in China especially in the highly polluted Eastern part, in order to estimate the potential for SOA formation and the role of ozone in this process in highly polluted areas.

Overall, numerous AMS measurements in regards to BB aging have been performed worldwide. Field studies included ground-based measurements and aircraft measurements, where more details can be obtained by tracking the plume (Capes et al., 2008; Yokelson et al., 2009; DeCarlo et al., 2010). Tracking smoke plumes provides insights into the real time atmospheric transformation processes (dilution, nucleation, condensation, repartitioning, oxidation, fragmentation etc.). There are also many laboratory-based measurements on this subject (Hennigan et al., 2011; Heringa et al., 2011; Ortega et al., 2013). Many studies have investigated the evolution of smoke plume emissions and there is no demonstrated consistency in the OA production in BB emission with aging. While some studies have shown increased OA mass with plume age (Lee et al., 2008; Yokelson et al., 2009; DeCarlo et al., 2010; Heringa et al., 2011), others have found no-significant change in the OA fraction (Capes et al., 2008; Cubison et al., 2011; Akagi et al., 2012; Brito et al., 2014; May et al., 2015).

The evolution and processing of smoke emissions and their influence on air quality in China is still poorly understood (Zhang et al., 2015b). It is a challenge to isolate the plume emissions and monitor them in highly polluted environments with a number of different sources. It has been observed that BB emissions which are in the process of aging can be promptly transformed into the OOA fraction. Therefore BB emissions can significantly influence the SOA budget in China. Ozone enrichments in BB plumes also suggest intensive photochemistry in the atmosphere across China (Ding et al., 2008, 2013b; Zhou et al., 2015). It is also important to characterize the mixing of plumes with other regional pollutants in the atmosphere during the aging process (Cubison et al., 2011), as China has many other important pollution sources. According to the reviewed studies, better regulation of BB activities is still needed in order to provide a less polluted environment. Huang et al. (2014) suggested regulating BB activities in China, especially in Guangzhou and Xi'an where higher non-fossil carbon fractions of SOA (up to 85% of SOA mass) than in Shanghai and Beijing was attributed to the enhanced BB contribution.

6. Impacts resulting from biomass burning

6.1. Severe haze episodes

According to Du et al.'s classification, haze episode is defined as the visibility below 10 km and accompanied by relative humidity <90% (RH < 90%) for a period lasting longer than 4 h (Du et al., 2011). As the low visibility is mainly because of high $PM_{2.5}$ mass concentration during haze episodes, here, we simply define severe haze episodes as $PM_{2.5}$ mass concentration higher than 200 μg/m^3, accompanied by RH < 90% and longer than 4 h. Many severe haze episodes associated with BB were promptly reported by news, TV and media in China. Scientific papers reporting haze events usually appear more than one year after the actual events. During 9–11 June 2012, a thick yellow haze blanketed Nanjing and adjacent cities in the west Yangtze River delta region (Ding et al., 2013a). In late afternoon of 9 June 2012, the $PM_{2.5}$ concentration at the SORPES station in Nanjing experienced a sharp increase in a 5 min maximum, up to 468 μg/m^3 at 20:00 LT, followed by prolonged high concentration of $PM_{2.5}$ mass with an average value in excess of 200 μg/m^3 that lasted for about 36 h. Higher KCl /$PM_{2.5}$ ratios and lower $SO_4^{2-}/PM_{2.5}$ and $CO/PM_{2.5}$ ratios were evident during the episode days, suggesting emissions from and chemical characteristics of BB and fossil fuel combustion plumes (Ding et al., 2013a). However, 2–3 days after this event, when the BB plumes recirculated from the South of the YRD region, severe ozone pollution was recorded at the same site (Ding et al., 2013b).

Sun et al. (2015) reported aerosol chemical species from a summer campaign at Xianghe, a suburban site located between the megacities of Beijing and Tianjin during 1–30 June 2013. The mass concentration of organics in PM_1 rapidly increased from <20 μg/m^3 to 247 μg/m^3 on 23 June due to the impact of agricultural burning. They found that the contribution of BBOA (BB organic aerosol) was increased to 21% during the BB period in late June, indicating a large impact of agricultural burning on air pollution in summer 2013. BB also exerted a significant impact on aerosol optical properties, and it was estimated that ~60% enhancement of absorption at the ultraviolet spectral region was caused by the organic compounds from BB (Sun et al., 2015).

Wang et al. (2016b) investigated the mixing state of individual carbonaceous particles during the severe haze episode by a single-particle aerosol mass spectrometer (SPAMS) in Nanjing in January 2013. On clear days, the top ranked carbonaceous particle types were biomass (48.2%), EC-biomass (15.7%), OC/EC (11.1%), and sodium (9.6%), while on hazy days they were biomass (37.3%), EC-biomass (17.6%), EC-secondary (16.6%), and sodium (12.7%) (Wang et al., 2016b). In the average mass spectra for EC-biomass particles, large peaks of dual polarity EC cluster ions ($12[C]^{+/-}$, $24[C2]^{+/-}$, $36[C3]^{+/-}$,…$[Cn]^{+/-}$) suggested that biomass particles may be mixed with EC or aggregated with EC particles during the aging process of EC. The fractions of EC-biomass particles were 15.7% and 17.6% on clear and hazy days, respectively (Wang et al., 2016b).

There have been reported many cases of haze episodes by BB with seized-resolved source apportionment and water-soluble potassium (K^+) increased properties (Wang et al., 2014; Tian et al., 2016; Liu et al., 2016). It is obvious that BB is one of the most significant reasons to drive rapidly server haze episodes (Wang et al., 2005b).

6.2. Air quality impact

BB is a global phenomenon that releases large quantities of gaseous and particulate pollutants into the atmosphere, including CO_2, CO, VOCs, PM_{10}, $PM_{2.5}$, BC, OC, EC and other compounds (Streets et al., 2003; Li et al., 2007; Yamaji et al., 2009; Shi and Yamaguchi, 2014; Zhang et al., 2015a; Ding et al., 2016b). In China, it has been estimated that the total annual emissions due to crop residue burning were 120 Tg CO_2, 4.6 Tg CO, 0.88 Tg $PM_{2.5}$, 0.39 Tg OC and 0.02 Tg EC in the year 2008 (Ni et al., 2015). The tremendous annual amounts of combustion products from BB into the atmosphere pose a threat to China's air quality. Literature indicated that BB has adverse environmental effects both locally and at large distances downwind. It is necessary to prohibit the open burning of crop residues in order to protect public health and the environment (Zhang and Cao, 2015b; Gustafsson et al., 2009).

6.2.1. Annual and seasonal characteristics

The annual and seasonal contributions of the biomass-burning source to ambient $PM_{2.5}$ have been reported for Beijing, Dongying and Chengdu (Zhang et al., 2013; Tao et al., 2014; Yao et al., 2016a), three cities located in North, Central East, and Southwest China, respectively. Combining PMF receptor model and BB markers (levoglucosan and K^+), it was possible to show that BB had higher contributions during intense farming (spring and autumn) and cold (winter) seasons, than in the hot season (summer) (Fig. 6), consistent with the timings of open burning of crop residues for elimination of agricultural waste and domestic combustion of biomass fuels for heating and cooking. On annual average basis, BB contributed 12%, 15.8%, and 11% of $PM_{2.5}$ mass in Beijing, Dongying, and Chengdu, respectively.

Besides using receptor statistical models for source apportionment, satellite remote sensing sensors such as MODIS are also frequently used to detect agricultural fires on the ground (Zhang et al., 2010a; Sang et al., 2011; Huang et al., 2012a, b; Chen and Xie, 2014; Hua et al., 2015; Wang et al., 2015b). According to Zha (2013), the numbers of total agricultural fire sites in China were 5514 in 2009 and 4225 in 2010, among which >80% were scattered across the heartland of agricultural regions such as Anhui, Jiangsu, Shandong, Henan and Hebei provinces. Moreover, the agricultural fires had a seasonal pattern, with two distinct peaks in summer (late spring/early summer) and autumn harvest periods, especially in June (61–86%) and October (5–14%) (Zha et al., 2013). This seasonal pattern was also supported by Zhang et al. (2016b) since their results revealed that the monthly $PM_{2.5}$ emission ratios of straw burning to other anthropogenic sources during June, the harvest period for many regions, were several times larger than the annual ratios at national, regional, and province levels.

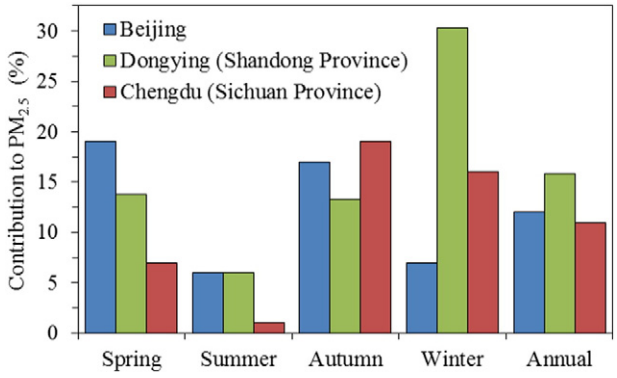

Fig. 6. Annual and seasonal contributions of biomass burning to $PM_{2.5}$ mass using PMF model in Beijing (Zhang et al., 2013), Dongying (Yao et al., 2016) and Chengdu (Tao et al., 2014).

6.2.2. Impact assessment of BB episodes

Field burning of crop residues is common both in rural agricultural regions and peri-urban areas in China which are used to control weeds and clear agricultural combustible waste inexpensively. Although the emissions are not spread evenly throughout the year, open burning of biomass (e.g. rice straw, wheat straw, corn stalk, etc.) results in intensive emissions of air pollutants into the environment in a short period, which rapidly degrades the local air quality and eventually causes regional air pollution. Assessments of air quality impact due to BB events with respect to particulate matter and gaseous pollutants have been studied over many regions of China, focusing on North, East, South, and Southwest China. The locations of some of the above mentioned provinces and cities can be seen in the map in Fig. 7.

a. ***North China.*** Based on MODIS images, large-scale flow field charts and environmental monitoring data, Li et al. (2008) found that winter wheat area of the North China Plain was the main source of straw burning pollution in Beijing in June, and that the transport paths for this type of pollution were mainly southerly.

Due to BB activities, the AOD from the Giovanni map showed that the monthly average value for 550 nm wavelength in northern China had its maximum of 0.7 in June 2007 (Li et al., 2010b). Yu et al. (2013b) characterized the aerosol optical properties during different pollution episodes in Beijing and found both total AOD and single scattering albedo (SSA) increased during BB days, from 0.24 and 0.865 for AOD and SSA on clean days to corresponding 0.64 and 0.922 on BB days.

Impacts on specific species of air pollutants from BB have been reported in North China. Based on radiocarbon (^{14}C) measurements at a regional background site in Bohai Rim in June 2013, Zong et al. (2015) found that 74% of water-insoluble OC and 59% of EC in $PM_{2.5}$ were derived from BB and biogenic sources when the air masses were from the south region, and 63% and 48% for the air masses from the north, respectively. In Beijing, high $PM_{2.5}$ levoglucosan concentrations (0.23 ± 0.37 μg/m^3 in summer and 0.59 ± 0.42 μg/m^3 in winter) were reported by Cheng et al. (2013) and their PMF model analysis showed that about 50% of the OC and EC in $PM_{2.5}$ in Beijing were associated with BB

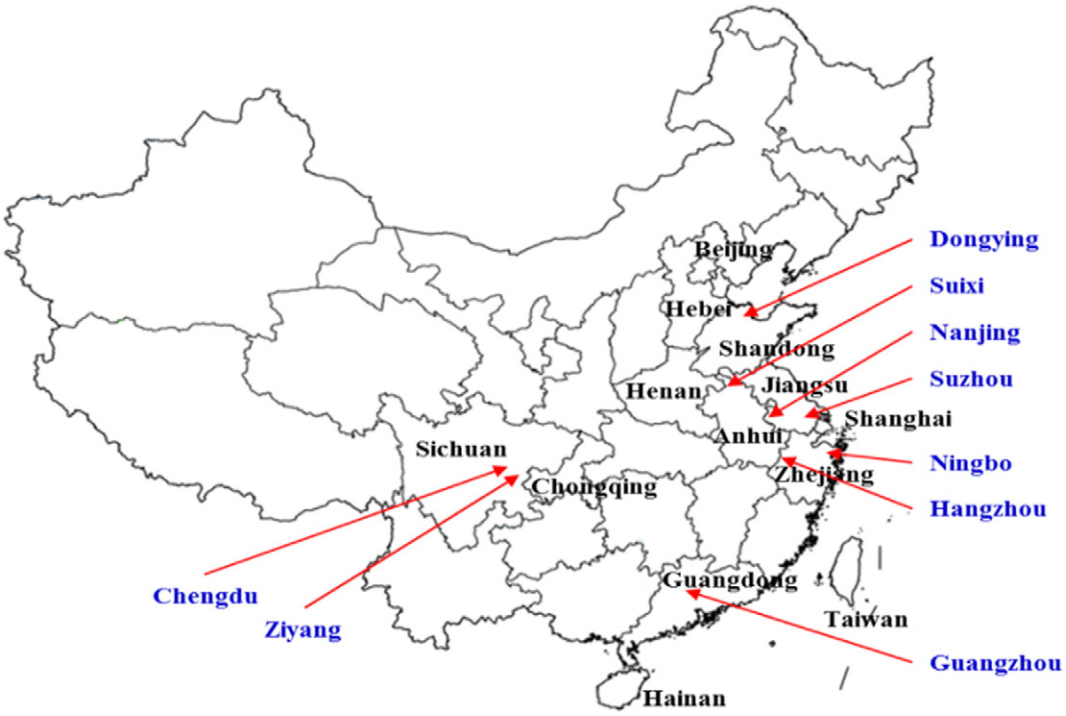

Fig. 7. Locations of some mentioned provinces and cities in China.

processes. They also suggested that combustion of crop residuals was the major source of BB aerosol in Beijing (Cheng et al., 2013). Recently, the VOCs measurements were carried out at a rural site in North China during summer of 2013, and the results indicated that extensive transport of BB emissions from Shandong and Hebei provinces had an important effect on the local VOCs pollution levels, and that during the BB period VOCs had higher ozone formation potential values, especially the aromatics and alkynes (Zhu et al., 2016b).

Transported BB emissions not only increased the atmospheric loading but also changed the chemical and physical properties of aerosol particles in the downwind areas. During June 2013 at a suburban site in the North China, Sun et al. (2016b) found that the contribution of BB OA (organic aerosol) to PM_1 OA was significantly elevated from 11% to 21% during the period influenced by agricultural burning, and about 60% enhancement of absorption coefficient at ultraviolet spectral region for submicron aerosols was caused by BB emissions. Using transmission electron microscopy for individual-particle analysis, Li and Shao (2010) found that copious organic matter, soot particles, and gases emitted by agricultural BB enhanced the formation of secondary particles and coagulation of pre-existing inorganic particles during a haze period in urban Beijing in June 2007.

b. ***East China***. East China is a major agricultural zone with a dense population and suffers from severe air pollution during June, the agricultural harvest season. MODIS remote sensing fire map revealed that about 80% agricultural fires occurred in the agriculture areas of Anhui, Jiangsu, Shandong, and Henan provinces (Li et al., 2010a; Huang et al., 2012a, b; Ding et al., 2013a, b), and that these fires had significant contributions to worsening the regional air quality of East China during the harvest season. Integrating field investigations, satellite observations and model calculations, Cheng et al. (2014b) and Li et al. (2014a) analyzed the causes of pollution episodes that took place in the harvest season (May–June), and quantified the contributions of BB to particulate pollution. In both of the studies, the pollution episodes were divided into three phases: pre-pollution, pollution, and post- pollution periods. The sharp increases in PM, fine particulate OC, EC and K^+ observed during pollution periods are summarized in Table 3, confirming the notable contribution of BB to elevated PM concentrations. The contributions of BB to $PM_{2.5}$, OC, and EC during pollution periods were estimated to be 23–51%, 48–86%, and 38–78%, respectively (Cheng et al., 2014b; Li et al., 2014a). Cheng et al. (2014b) suggested that, in absence of open BB, the average $PM_{2.5}$ concentration would be reduced by 51% for the Yangtze River Delta region, and the exposure level would decrease by 47% during the post-harvest season.

Changes in the optical and physical properties of aerosols in Shanghai due to the transport of biomass-burning plumes in May 2009 were reported by He et al. (2015). They found that the BB plume led to a 37% increase in the average AOD at 500 nm (from 0.73 to 1.00), to a remarkable decrease in SSA at 670 nm, and to a significant increase of the volume concentration of fine-mode aerosols (He et al., 2015). Wang et al. (2009b) investigated a haze event in June 2007 in urban Nanjing and found concentrations of levoglucosan, high molecular weight (HMW) n-alkanes, and HMW fatty acids in aerosols elevated by 3–40 times on hazy days, mainly due to the emissions from field burning of wheat straw. The work of Liu et al. (2013) indicated that BB was one of the major contributors to water-insoluble OC in $PM_{2.5}$ in Ningbo, whereas the work of Fu et al. (2014) highlighted that BB could be an important source of soluble iron in $PM_{2.5}$ in Shanghai in summer.

c. ***South China.*** Combining the back trajectory analysis, fire count maps and field observations, Zhang et al. (2010a) found that regional open BB in the Indo-Myanmar region of Asia was probably one of the major potential sources of carbonaceous aerosols in South China region. In summer 2006, the intensive measurements conducted by Zhang et al. (2010c) in Guangzhou revealed that the relative contributions of smoke particles to OC in PM_{10} were on average 7.0 and 14% at daytime and nighttime, respectively, with maxima of 9.7 and 32% during the episodic transport events, indicating the significant impact from the biomass and biofuel burning activities in the rural parts of the Pearl River Delta and neighboring regions. Moreover, Zhang et al. (2014c) found that during the periods with

Table 3
Concentrations and biomass burning contributions of PM_{10}, $PM_{2.5}$ and fine particulate OC, EC and K^+ during pollution episodes in harvest season (May–June) in East China.

Phase	Unit	Shanghai[a]					Suzhou (Jiangsu)[a]					Hangzhou (Zhejiang)[a]			
		PM_{10}	$PM_{2.5}$	OC	EC	K^+	PM_{10}	$PM_{2.5}$	OC	EC	K^+	PM_{10}	$PM_{2.5}$	OC	EC
Pre-pollution	$\mu g/m^3$	60	37	8	2	0.3	109	55	15	4	1.5	115	64	—[c]	—
Pollution	$\mu g/m^3$	160	128	28	6	4.5	220	139	27	4	5.3	225	157	—	—
Post-pollution	$\mu g/m^3$	28	25	6	2	0.6	73	40	10	3	1.7	58	41	—	—
Contribution	%	—	26[d]/35[f]	48[d]/69[f]	44[d]/68[f]	—	—	30[d]/43[f]	60[d]/86[f]	56[d]/78[f]	—	—	23[f]	56[f]	38[f]

Phase	Unit	Nanjing (Jiangsu)[a]					Suixi (Anhui)[b]					Ningbo (Zhejiang)[a]			
		PM_{10}	$PM_{2.5}$	OC	EC	K^+	PM_{10}	$PM_{2.5}$	OC	EC	K^+	PM_{10}	$PM_{2.5}$	OC	EC
Pre-pollution	$\mu g/m^3$	114	60	2	5	3.2	—	81	14	4	2	91	51	—	—
Pollution	$\mu g/m^3$	240	180	5	10	14	—	164	37	12	11	176	125	—	—
Post-pollution	$\mu g/m^3$	99	64	2	4	3.5	—	70	12	4	4	41	32	—	—
Contribution	%	—	47[d]/48[f]	71[d]/83[f]	70[d]/61[f]	—	—	51[e]	76[e]	75[e]	90[e]	—	41[f]	86[f]	71[f]

[a] According to Cheng et al. (2014a, 2014b).
[b] According to Li et al. (2014a).
[c] Not available.
[d] Calculated by CMB (Chemical Mass Balance) model.
[e] Calculated by PMF (Positive Matrix Factorization) model.
[f] Calculated by WRF/CMAQ (Weather Research and Forecasting/Community Multiscale Air Quality) model.

enhanced open biomass-burning activities in Southeast Asia or Southeast China, the EC and OC in $PM_{2.5}$ contributed by non-fossil combustion have increased by 5–10% in Hainan Island, the southernmost province of China.

The impact of BB on $PM_{2.5}$ in Guangzhou has been estimated during BB seasons by using acetonitrile and levoglucosan as tracers (Wang et al., 2007a). According to Wang et al. (2007a), the frequencies of $PM_{2.5}$ pollution episodes significantly influenced by BB were 100% for Xinken (a suburban site in Guangzhou) and 58% for downtown Guangzhou in October 2004; and during that period BB contributed 3.0–16.8% and 4.0–19.0% of $PM_{2.5}$ concentrations in Xinken and Guangzhou downtown, respectively. The study showed that the impact of BB on $PM_{2.5}$ was ubiquitous in both suburban and urban Guangzhou.

The earliest works reporting impacts of Southeast Asia BB to atmospheric components in South China started appearing from 1990s and were based on ozonesonde measurements: Chan et al. (1998) and then by Chan et al. (2000 and 2003). These studies found that the forest fires in South Asia caused a substantial enhancement of O_3 at altitude around 3-km in spring, especially in March. The NASA Global Troposphere Experiment, Transport and Chemical Evolution over the Pacific (TRACE-P), organized aircraft measurement campaign and successfully captured the BB plumes over Hong Kong and the South China Sea (Jacob et al., 2003). Based on 11 years (2000 − 2010) ozonesonde data in Hong Kong and Lagrangian dispersion modeling of CO, Zhou et al. (2013) studied the impact of South Asia BB to O_3 interannual variation in South China.

An investigation of CO characteristic during BB period was carried out by Yu et al. (2010) at the summit of Mountain Lulin in central Taiwan. The results showed that the average difference of CO levels between the two air parcel categories (one which passed over the fire regions and the other which did not) was approximately 79 ppb, suggesting that Asian BB played an important role in CO levels at this remote site during springtime (Yu et al., 2010). In another study at Mei-Feng mountain site in central Taiwan, they also reported that a net influence of Southeast Asian BB on both tropospheric O_3 and CO was approximately 23% in March (Lin et al., 2013). Yuan et al. (2010) measured ambient VOCs at a rural site (Jiangmen) in the Pearl River Delta during autumn 2008 and found that BB contributed 9.5–17.7% to the mixing ratios of the nine measured VOCs, using two different tracer methods. Particularly, Shih et al. (2008) selected two areas in southern Taiwan to measure polychlorinated dibenzo-*p*-dioxins and dibenzofurans (PCDD/Fs) concentrations in the ambient air, and their results revealed that during the BB season, the total PCDD/F I-TEQ (international-toxic equivalent quantity) concentrations in the ambient air were approximately 4 and 17 times higher than those without biomass open burning, respectively.

d. ***Southwest China***. Compared with the three regions mentioned above, the studies focusing on BB impacts were relatively limited in the Southwest China. However, a recent study showed that BB activities in late spring and early summer seemed to be a very important factor affecting $PM_{2.5}$ mass concentration and its chemical composition in megacity of Chengdu (Tao et al., 2013). During BB episodes, $PM_{2.5}$-bound levoglucosan, OC and K^+ concentrations in Chengdu increased by a factor of 2–7 (Tao et al., 2013). Using a synergy of on-line measurement, manual sampling, and remote sensing, Chen and Xie (2014) studied the heaviest and most long-lasting pollution event in the historical record of Chengdu during 18–21 May 2012. Their results showed that this pollution event in Chengdu was mainly caused by a combination of increased PM emissions from BB and unfavorable meteorological conditions (Chen and Xie, 2014).

BB had a significant influence on ambient VOCs in Chengdu–Chongqing Region, as concluded by Li et al. (2014b). They intensively measured VOCs at Ziyang (a suburban site of Chengdu-Chongqing Region) and found that BB contributed 9.4–36.8% to the mixing ratios of selected VOC species, and that it contributed most (above 30% each) to aromatics, formaldehyde, and acetaldehyde (Li et al., 2014b). Yang et al. (2012) examined the variability of fungal abundance in $PM_{2.5}$ during a BB season (spring 2009) in Chengdu. They found that in the case of influence by pollution plumes from BB regions, the concentrations of fungal tracers (arabitol and mannitol) reached very high values, and statistically significant correlations were found between fungal and BB tracers, suggesting that elevated fungal material in $PM_{2.5}$ was mainly associated with BB activities (Yang et al., 2012).

6.3. Health impacts

As a renewable energy source, biomass materials include wood, animal waste, crops, and seaweed. From the very early stage of the civilization, people have been using biomass energy for surviving. Biomass-based energy was the most popular energy before the industrial revolution (Fernandes et al., 2007). The use of biomass energy is getting popular in the current century (Field et al., 2008). According to the annual

global energy consumption Gtoe, 2010, the total biomass energy usage all over the world accounts for approximately 8–14% (fossil fuels 10.45, oil 4.03, coal 3.56, natural gas 2.86, renewables 0.94, hydro 0.78, wind, commercial biomass 0.16, estimated biomass 1–2) (Berndes et al., 2003; Parikka, 2004; Hoogwijk et al., 2005; Agarwal, 2007; Bioenergy, 2007; Demirbas, 2007; Wit and Faaij, 2009; Williams et al., 2012). Ethanol and biodiesel fuel, wood and agricultural products, gas and biogas, and solid waste are the most popular biomass in the current century. Thermal, chemical, electrochemical, and biochemical conversion process are commonly used to convert the biomass into other forms of energy. During the conversion process, biomass emits carbon dioxide, carbon monoxide, voltage organic compounds, nitrogen oxides, and other pollutants including particles (Andreae and Merlet, 2001; Baxter, 2005; Zhang et al., 2007). The open burning of biomass emits PAHs, which is a group of more than 100 different chemicals (Jenkins et al., 1996). PAHs are usually formed during the incomplete burning of the biomass and contribute to production of particulate matter. The common source of PAHs is cigarette smoke, asphalt road, coal exhaust, vehicle engine exhaust, wood burning for cooking, agricultural burning, hazardous waste management, and bushfire (Mumtaz and George, 1995; Finlayson-Pitts and Pitts, 1997). The air contains a significant amount of suspended particles, liquids as well as solids, organic and inorganic substances, viruses, and bacteria (Seaton et al., 1995; Seinfeld et al., 2008; Tena and Clarà, 2012). PAHs can be in the form of volatile, semi-volatile and particulate phase (Allen et al., 1996; Finlayson-Pitts and Pitts, 1997; Thrane and Mikalsen, 1981). The PAHs mainly attached to the dust particle in air and thus particle-bound PAHs are treated as threats to human health (WHO, 2010). The PAHs have a significant impact on health, especially on the respiratory system and cancer incidence (Leiter et al., 1942; Kim et al., 2013). During inhalation, the particle attached-PAHs can enter into the human respiratory system.

Fig. 8(a) shows a schematic of the human lung upper and lower respiratory system. Throughout the inhalation and exhalation process, depending on the particle size, shape, and flow rate, particles deposit in the different regions of the respiratory track (Islam et al., 2015).

Depending on the inhaled particle size distribution, the smaller particle can reach the alveolar region of the respiratory system. The fine particles penetrate into the alveolar region and might be absorbed into the bloodstream of the human body. The fine particles enter the alveolar sacs and cross the alveolar epithelial wall (Fig. 8b). After that particles enter into the interstitial space and penetrate into the blood stream of the lung capillary. Generally, after deposition, particles are cleared from the lung wall by mucociliary clearance. The health effects will depend mainly on the extent of exposure (e.g., length of time), the concentration of toxicants during exposure, the toxicity, the route of exposure (e.g., via inhalation, ingestion, or skin contact), pre-existing health conditions and age. The inhalation of particles would lead to various respiratory diseases like asthma and respiratory allergies, chronic obstructive pulmonary diseases (COPD) chronic bronchitis, cystic fibrosis, lung cancer occurs. According to WHO, 235 million people are affected by asthma and more than 3 million people die each year from COPD, which is 6% of all deaths all over the world (*http://www.who.int/respiratory/en/*). WHO assessed that 8.2 million people died of cancer in 2012 and among them 1.59 million died of lung cancer which is the most common cause of cancer death (*http://www.who.int/mediacentre/factsheets/fs297/en/*). The rates of asthma, COPD, and lung cancer are increasing especially in developing countries in the past few decades, and air pollution is postulated to be the primary reason for these increments. Biomass is the only fuel for cooking or heating for >2.4 billion households around the world, and more than 90% of the rural people (in low- and middle-income countries) use solid biomass (wood, crop waste, charcoal, and coal) energy in their daily life (Smith et al., 2004). Incomplete burning of biomass produces highly toxic, and health-damaging pollutant particles. The emitted PAHs and particles penetrate into the alveolar region and enter the human bloodstream. Women, children and elders have particularly high exposure to the household biomass pollutant emission. According to WHO, 4.3 million people died prematurely from illnesses related to household air pollution in 2012, and 22% of them are suffering from COPD, and 6% from lung cancer (*http://www.who.int/mediacentre/factsheets/fs292/en/*). Women are highly affected by COPD compared to men because of higher inhalation of household smoke and more vulnerable airway. Men, who are more frequently addicted by tobacco, have a strong possibility of COPD and lung cancer. Pneumonia is a life-threating disease for children less than 5 years old.

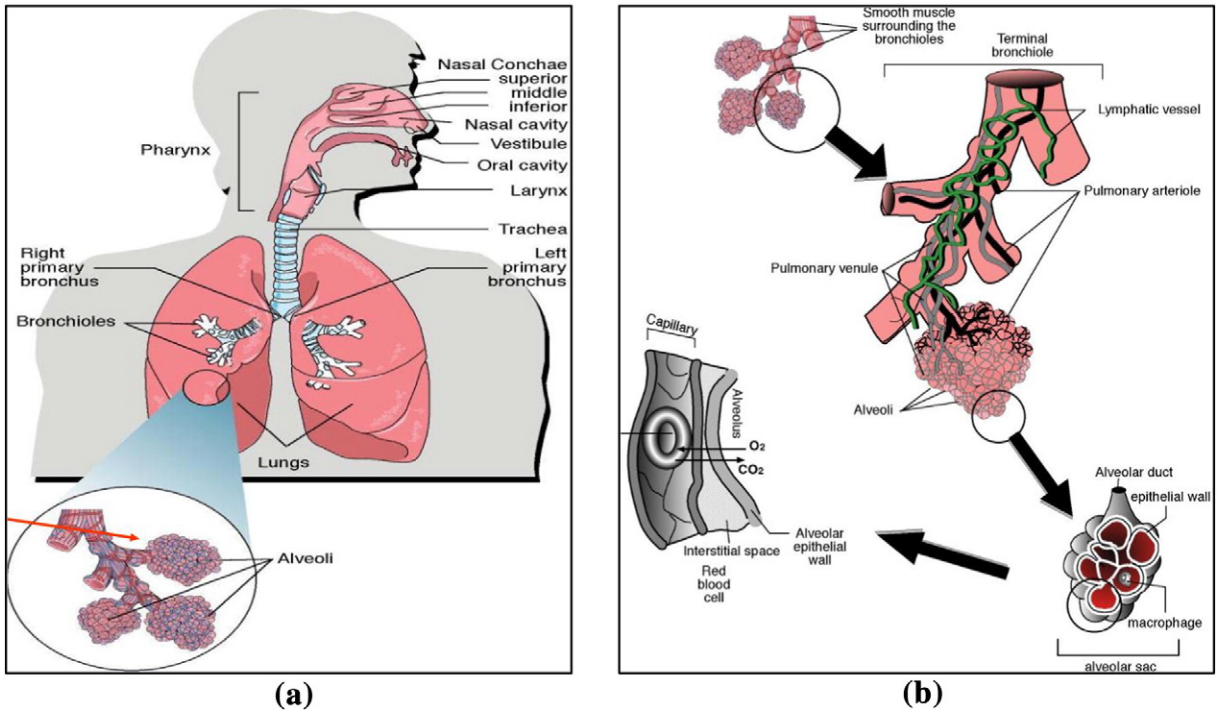

Fig. 8. (a) Schematic representation of human lung upper airway, and alveoli, and (b) alveolar sacs, and alveolar capillary for blood transport (http://www.who.int/indoorair/interventions/antiguamod21.pdf).

In 2012, among 4.3 million premature deaths due to air pollution around the world, 12% are attributable to children pneumonia. A meta-analysis of 24 studies found that the exposure to PAHs emitted from biomass s increase the risk of pneumonia by 2-fold (Ciencewicki and Jaspers, 2008). The exposure to pollutants from household biomass burning also causes stroke (34% of deaths in 2012) and ischemic heart diseases (26% of deaths in 2012) (*http://www.who.int/mediacentre/factsheets/fs292/en/*). Besides, ultrafine particles from biomass burning may impair the respiratory tract, damage the immune system and influence the blood supply. There is other evidence showing a link between indoor air pollution and low birth weight, tuberculosis, and laryngeal cancer (*http://www.who.int/mediacentre/factsheets/fs292/en/*) (Bruce et al., 2000). There is evidence that the lung function growth of the children in the high-polluted area is significantly lower than those who live in the less-polluted (Eisner et al., 2010). The findings also suggest that the movement from the high-polluted area to the less-polluted area could improve the lung growth of the children. The highly toxic particle-bounded PAHs produce inflammation in the respiratory epithelium characterized by inflammable cell employment and vascular endothelial adhesion molecules (Laumbach and Kipen, 2012). The damaged epithelium eventually decreases the mucociliary clearance in the respiratory system, consequently leading to severe lung diseases (Diat-Sanchez, 1997).

The BB also produces BC, a dark and light-absorbing component of atmospheric aerosols containing EC. BC is usually produced during the combustion reaction when burning biomass. The size of BC ranges from 20 to 150 nm. BC is also a subcategory of $PM_{2.5}$. Indoor sources, such as cooking and environmental tobacco smoke, also contribute to the significant amount of BC, which may lead to peaks in exposure (Lanki et al., 2007; Raaschou-Nielsen et al., 2011). In general, BC can reach at the very deep portion of respiratory tract due to its small size. Small-sized BC can penetrate at the alveoli sacs and finally enter into the blood stream. It is well acknowledged that there is no threshold below which particle exposure has no hazardous effects. There is a conceptual disagreement about the toxicity of BC, which can serve as a transporter for different toxic substances, like PAH and heavy metals. As one of the main toxic components of $PM_{2.5}$, BC appear causally associated with all-cause, cardiovascular, and lung cancer mortality, and perhaps with adverse birth outcomes and central nervous system effects (Grahame et al., 2014). Multiple short-term and long-term epidemiological studies have suggested that BC was a valuable additional air quality indicator to evaluate the cardiopulmonary morbidity and mortality in association with air quality dominated by primary combustion particles (Ostro et al., 2010; Janssen et al., 2011; Levy et al., 2012).

6.4. Climate and weather impact

BB has long been considered as an important source influencing global and regional climate change. Fires of plants and agricultural straw influence chemical composition in the atmosphere hence play important role in climate change and water cycle by influencing surface energy fluxes and radiative forcing (Robock, 1991; Penner et al., 1992; Andreae and Merlet, 2001; Bond and Keeley, 2005; Randerson et al., 2006).

From a global perspective, BB play an important role in global warming because 1/5 of the emission of CO_2 and other greenhouse gases (GHGs) can be traced back to BB, including wildfires, slash-and-burn agriculture and the burning of wood waste (Langenfelds et al., 2002; Jacobson, 2014). Unlike the long-lived and well-mixed GHGs, carbonaceous aerosols (BC and BrC) emitted directly or formed as secondary products during BB are distributed much less uniformly, posing impacts on climate mostly on a regional scale and in a much more complex way. IPCC (2013) in the Fifth Assessment Report (AR5) gave an estimation of the radiative forcing due to BB particles as 0.0 (-0.2 to $+0.2$) W/m^2 at the top of the atmosphere (TOA). However, a near-zero global forcing at TOA, BB-induced climate forcing differ vertically. Smoke plumes consisting of light-absorbing components generally absorb solar radiation and thus heat the middle and lower atmosphere, but decrease net radiation at the surface (Hobbs et al., 1997; Randerson et al., 2006; Ramanathan and Carmichael, 2008). In addition to this, through perturbations on solar radiation and acting as the CCN, smoke particles cool the surface, stabilize the atmosphere, reduce the evaporation, and change the dynamic and microphysical evolution of cloud, plausibly induce feedbacks on cloudiness, precipitation, the hydrological cycle and even large scale circulations (Hansen et al., 1997; Ackerman et al., 2000; Ramanathan et al., 2001; Andreae et al., 2004; Koren et al., 2004; Sakaeda et al., 2011; Tosca et al., 2013; Lee et al., 2014a, 2014b).

In China and other Asian monsoon regions, the impact of BB on regional climate and weather has been mainly studied with a focus on springtime forest burning in the South Asia and agricultural burning in East China in early summer. With an important contribution from BB, the carbonaceous aerosol layer in Southeast Asia, also known as Atmospheric Brown Clouds (ABC), has been found to be partly responsible for surface cooling, reduced evaporation, a latitudinal asymmetry in sea surface temperature, a delaying of the start of the Asian monsoon and regional drought (Ramanathan et al., 2005). Based on GEOS-5/AGCM model, Lee et al. (2014a, 2014b) investigated the impact of BB emission in Southeast Asia on precipitation in South China in the pre-monsoon period (February–May). They found that BB aerosols could stabilize the atmosphere by reducing surface latent heat fluxes and cooling land surface temperature, but at the same time could increase cloud droplet number concentrations and decrease droplet effective radii. However, the indirect effect of absorption aerosols was less important when the plumes experienced a short transport time. Based on ground based measurements in Guangzhou, South China, Nowak et al. (2010) also found that aerosol particles from open burning of agricultural waste were generally less CCN active, especially for the freshly emitted smoke with more organic aerosols.

The impact of BB to regional air quality or climate in the Central east China is more complicated because of an overlap of straw burning area with fossil fuel combustion sources (Huang et al., 2012b, c; Ding et al., 2013a; Huang et al., 2016). Based on MODIS data and WRF-Chem simulations, Guo et al. (2014) reported a case of mixed BB and anthropogenic pollution on the convective precipitation on 4 July 2008, and found that precipitation amount was increased by up to 17% and the maximum rainfall rate was enhanced during the whole cloud lifetime under the influence of air pollution. However, based on the measurements at the "flagship" type station SORPES in YRD region and modeling simulations, Ding et al. (2013a) reported a unique episode with two-fold influence from mixed BB and anthropogenic sources. During the daytime, a local convective precipitation was "burned off" by BB aerosols due to its direct effect in reducing the surface flux and changing the boundary layer dynamics (see the conceptual model given in Fig. 9); while at nighttime the downwind rainfall was enhanced because of its indirect effect on change in microphysics of cloud and change of circulation due to dynamic forcing (Ding et al., 2013a; Huang et al., 2016). These results are also consistent with that reported in a study for Amazon by Vendrasco et al. (2009).

The impact of BB to climate and weather will further cause feedback to air pollution dispersion and atmospheric chemistry. As an important source of absorption aerosols, like BC and BrC, BB plume could cause significant impact to the boundary layer dynamics through the "Dome effect" (Ding et al., 2016a), and further enhance the air pollution in megacities and in the downwind region of the BB emissions. The mixture of BB pollutants with anthropogenic sources could also enhance heterogeneous reactions and contribute to the formation of reactive trace gases, like HONO, and secondary aerosols, such as sulfate, especially after an enhancement of relative humidity trough aerosol-PBL-weather interactions (Xie et al., 2015; Nie et al., 2015). The complex physical and chemical interactions/feedbacks create great challenges

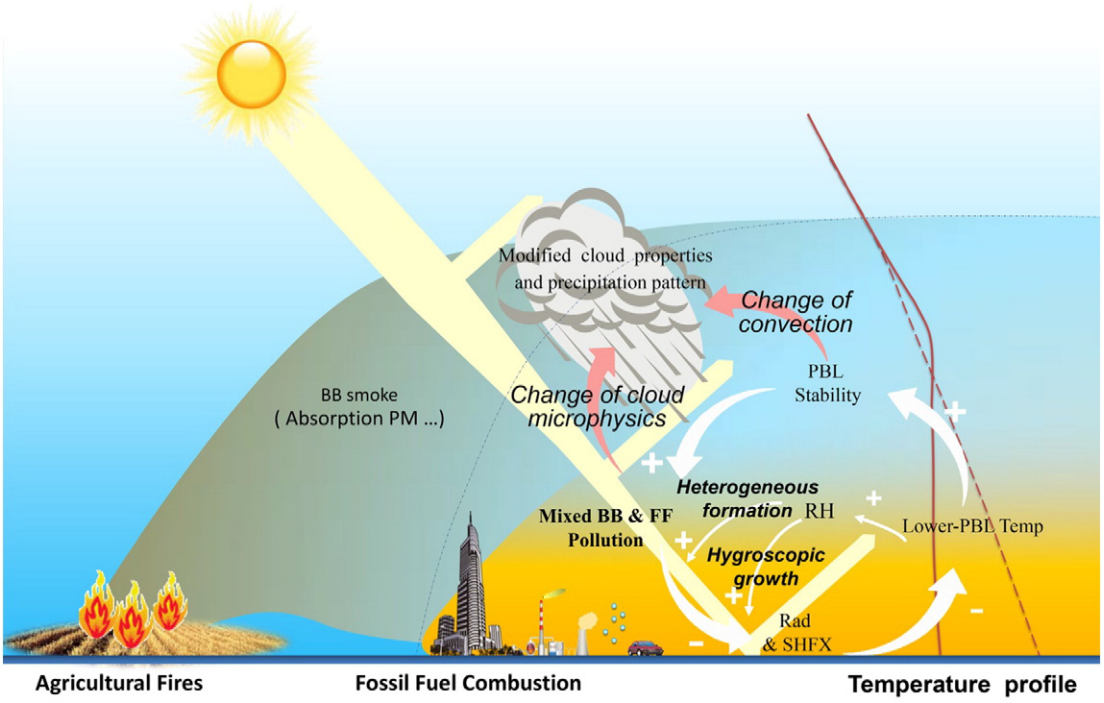

Fig. 9. A schematic figure for interactions of air pollution-boundary layer-weather under a condition of mixed agricultural burning and fossil fuel combustion plumes (Modified from Ding et al., 2013a).

in understanding the climate system (Menon et al., 2002) and also for weather forecasting in East Asia (Fan et al., 2015; Ding et al., 2013a).

7. Research priorities and insights

This review focuses on literature findings concerning BB emissions, the impacts on air quality, health and climate in China, including the relationship to atmospheric dynamics and chemical processes. The following are the conclusions and recommendations from the review:

7.1. Field campaigns

BB was the main focus of many campaigns which have been conducted in China, such as CAREBeijing in 2013 and 2014. The research region covered 65,000 km^2 (Yao et al., 2016a). The new findings encompassed topics of atmospheric PAHs: spatial distribution, OH reactivity, and air pollutants distribution in the North China Plain (Zhu et al., 2016c; Fuchs et al., 2016; Yao et al., 2016a).

The crop residue is so far the most bulk biomass open-burned in China. As BB plume disperses according to the meteorological factors and weather condition, it is strongly suggested that BB campaigns should be comprehensively designed to be conducted in harvest seasons and in winter across large regions, with the application of available technologies to quantify the emission factors, aging, transport, and chemical processes. It is necessary to carry out BB campaigns in different regions since emissions of OC/EC, PAHs and particle size distribution and composition from different types of crop are quite different between South and North China with (Zhang et al., 2011a; Li et al., 2015; Zhang et al., 2016c).

7.2. Aging

Primary emissions from BB contribute to varying atmospheric concentrations of inorganic inclusions such as KCl, sulfate and nitrite, which has been demonstrated in dark chamber simulations (Li et al., 2015; Li et al., 2016a, b; Popovicheva et al., 2016). The organic coatings observed on sulfur-rich and potassium-rich particles indicated the formation of SOA from the oxidation of precursor VOCs during the aging of smoke released from BB (Yao et al., 2016b). Water-soluble organics in atmospheric aerosols are particularly important as they are main parts of aqSOA (Kawamura and Bikkina, 2016).

We recommend that optical properties of smoke particles and their components during aging are investigated (Chen et al., 2015; Peng et al., 2016), as well as morphology, mixing state with urban pollutants and toxicological organics. Such data are essential for modeling of BB on health and climate effects.

7.3. Health and climate

The BB smoke particles serve as a major source of BC and BrC, which have adverse health and climate effects. Indoor smoke particles emitted for cooking and heating are of particular significance in China. Therefore, it would be interesting and urgent to compare the biological effect of indoor fresh and aged smoke particles that carry various carcinogenic substances, as ambient fine BB particles are found to contain an amount of PAHs and also their nitrated, hydroxylated, and oxygenated derivatives (Lin et al., 2015b). Given that a significant fraction of the Earth's BB originating in China, studies probing the climate effects of BC and BrC should be given high priority by the international research community.

Acknowledgments

This work is supported by National Natural Science Foundation of China (21190053, 21177025,41275122, 41422504), Cyrus Tang Foundation (No. CTF-FD2014001), Ministry of Science and Technology of the People's Republic of China (2016YFC0202700, 2014BAC22B01), Research Grants Council of the Hong Kong Special Administrative Region (PolyU152052/14E), Australian Research Council Discovery grant (DP120100126, DP150100828, LP150100737), Environment and Conservation Fund (ECF 16/2015), City University of Hong Kong (7004470), Ministry of Environmental Protection of China (201509002), State Key Joint Laboratory of Environment Simulation and Pollution Control (15K08ESPCT), State Key Laboratory of Environmental Criteria and Risk

Assessment (SKLECRA201641), and Australia-China Centre for Air Quality Science and Management for organizing this special issue on air pollution in China. Phong Thai is funded by a QUT VC Research Fellowship. We are grateful to the GIOVANNI (*http://giovanni.gsfc.nasa.gov/giovanni*) NASA teams for providing data through their websites. MODIS fire product MCD14ML used in this study is downloaded from an ftp server at University of Maryland (*http//:fuoco.geog.umd.edu*).

References

Abel, S.J., Haywood, J.M., Highwood, E.J., Li, J., Buseck, P.R., 2003. Evolution of biomass burning aerosol properties from an agricultural fire in southern Africa. Geophys. Res. Lett. 30 (15). http://dx.doi.org/10.1029/2003GL017342.

Ackerman, A.S., Toon, O.B., Stevens, D.E., Heymsfield, A.J., Ramanathan, V., Welton, E.J., 2000. Reduction of tropical cloudiness by soot. Science 288 (5468), 1042–1047.

Adachi, K., Buseck, P.R., 2008. Internally mixed soot, sulfates, and organic matter in aerosol particles from Mexico City. Atmos. Chem. Phys. 8 (21), 6469–6481.

Adachi, K., Buseck, P.R., 2013. Changes of ns-soot mixing states and shapes in an urban area during CalNex. J. Geophys. Res. Atmos. 9:3723–3730. http://dx.doi.org/10.1002/jgrd.50321.

Adachi, K., Chung, S.H., Buseck, P.R., 2010. Shapes of soot aerosol particles and implications for their effects on climate. J. Geophys. Res. Atmos. 115 (D15). http://dx.doi.org/10.1029/2009JD012868.

Adler, G., Flores, J.M., Abo Riziq, A., Borrmann, S., Rudich, Y., 2011. Chemical, physical, and optical evolution of biomass burning aerosols: a case study. Atmos. Chem. Phys. 11 (4), 1491–1503.

Agarwal, A.K., 2007. Biofuels (alcohols and biodiesel) applications as fuels for internal combustion engines. Prog. Energy Combust. Sci. 33 (3), 233–271.

Agus, E.L., Lingard, J.J.N., Tomlin, A.S., 2008. Suppression of nucleation mode particles by biomass burning in an urban environment: a case study. J. Environ. Monit. 10 (8), 979.

Aiken, A.C., Decarlo, P.F., Kroll, J.H., Worsnop, D.R., Huffman, J.A., Docherty, K.S., Ulbrich, I.M., et al., 2008. O/C and OM/OC ratios of primary, secondary, and ambient organic aerosols with high-resolution time-of-flight aerosol mass spectrometry. Environ. Sci. Technol. 42 (12), 4478–4485.

Aiken, A.C., Salcedo, D., Cubison, M.J., Huffman, J.A., DeCarlo, P.F., Ulbrich, I.M., Docherty, K.S., et al., 2009. Mexico City aerosol analysis during MILAGRO using high resolution aerosol mass spectrometry at the urban supersite (T0)–part 1: fine particle composition and organic source apportionment. Atmos. Chem. Phys. 9 (17), 6633–6653.

Aiken, A.C., Foy, B.D., Wiedinmyer, C., DeCarlo, P.F., Ulbrich, I.M., Wehrli, M.N., Szidat, S., et al., 2010. Mexico city aerosol analysis during MILAGRO using high resolution aerosol mass spectrometry at the urban supersite (T0)–part 2: analysis of the biomass burning contribution and the non-fossil carbon fraction. Atmos. Chem. Phys. 10 (12), 5315–5341.

Akagi, S.K., Craven, J.S., Taylor, J.W., McMeeking, G.R., Yokelson, R.J., Burling, I.R., Urbanski, S.P., et al., 2012. Evolution of trace gases and particles emitted by a chaparral fire in California. Atmos. Chem. Phys. 12 (3), 1397–1421.

Alfarra, M.R., Prevot, A.S., Szidat, S., Sandradewi, J., Weimer, S., Lanz, V.A., Schreiber, D., et al., 2007. Identification of the mass spectral signature of organic aerosols from wood burning emissions. Environ. Sci. Technol. 41 (16), 5770–5777.

Allen, J.O., Dookeran, N.M., And, K.A.S., Sarofim, A.F., And, K.T., Lafleur, A.L., 1996. Measurement of polycyclic aromatic hydrocarbons associated with size-segregated atmospheric aerosols in Massachusetts. Environ. Sci. Technol. 30 (3), 1023–1031.

Andreae, M.O., 1983. Soot carbon and excess fine potassium: long-range transport of combustion-derived aerosols. Science 220 (4602), 1148–1151.

Andreae, M.O., Merlet, P., 2001. Emission of trace gases and aerosols from biomass burning. Glob. Biogeochem. Cycles 15 (4), 955–966.

Andreae, M.O., Rosenfeld, D., Artaxo, P., Costa, A.A., Frank, G.P., Longo, K.M., Silva-Dias, M., 2004. Smoking rain clouds over the Amazon. Science 303 (5662), 1337–1342.

Andreae, M.O., Schmid, O., Yang, H., Chand, D., Yu, J.Z., Zeng, L., Zhang, Y., 2008. Optical properties and chemical composition of the atmospheric aerosol in urban Guangzhou, China. Atmos. Environ. 42 (25), 6335–6350.

Araujo, J.A., Barajas, B., Kleinman, M., Wang, X., Bennett, B.J., Gong, K.W., Navab, M., et al., 2008. Ambient particulate pollutants in the ultrafine range promote early atherosclerosis and systemic oxidative stress. Circ. Res. 102 (5), 589–596.

Arola, A., Lindfors, A., Natunen, A., Lehtinen, K., 2007. A case study on biomass burning aerosols: effects on aerosol optical properties and surface radiation levels. Atmos. Chem. Phys. 7 (16), 4257–4266.

Aurell, J., Gullett, B.K., Tabor, D., 2015. Emissions from southeastern U.S. Grasslands and pine savannas: comparison of aerial and ground field measurements with laboratory burns. Atmos. Environ. 111, 170–178.

Badarinath, K., Kharol, S.K., Sharma, A.R., 2009. Long-range transport of aerosols from agriculture crop residue burning in Indo-Gangetic Plains-a study using LIDAR, ground measurements and satellite data. J. Atmos. Sol. Terr. Phys. 71 (1), 112–120.

Barnaba, F., Angelini, F., Curci, G., Gobbi, G.P., 2011. An important fingerprint of wildfires on the European aerosol load. Atmos. Chem. Phys. 11 (20), 10487–10501.

Baxter, L., 2005. Biomass-coal co-combustion: opportunity for affordable renewable energy. Fuel 84 (10), 1295–1302.

Beddows, D.C.S., Dall'Osto, M., Harrison, R.M., 2010. An enhanced procedure for the merging of atmospheric particle size distribution data measured using electrical mobility and time-of-flight analysers. Aerosol Sci. Technol. 44 (11), 930–938.

Berndes, G., Hoogwijk, M., Broek, R.V.D., 2003. The contribution of biomass in the future global energy supply: a review of 17 studies. Biomass Bioenergy 25 (1), 1–28.

Bi, Y.Y., Wang, Y.J., Gao, C.Y., 2010. Straw resource quantity and its regional distribution in China. J. Agric. Mechanizat. Res. 3, 1–7.

Bioenergy, I., 2007. Potential Contribution of Bioenergy to the World's Future Energy Demand.

Blake, D.R., Smith, T.W., Chen, T.Y., Whipple, W.J., Rowland, F.S., 1994. Effects of biomass burning on summertime nonmethane hydrocarbon concentrations in the Canadian wetlands. J. Geophys. Res. Atmos. 99 (D1):1699–1719. http://dx.doi.org/10.1029/93JD02598.

Bo, Y., Cai, H., Xie, S.D., 2008. Spatial and temporal variation of historical anthropogenic NMVOCs emission inventories in China. Atmos. Chem. Phys. 8 (23), 7297–7316.

Bølling, A.K., Pagels, J., Yttri, K.E., Barregard, L., Sallsten, G., Schwarze, P.E., Boman, C., 2009. Health effects of residential wood smoke particles: the importance of combustion conditions and physicochemical particle properties. Part. Fibre Toxicol. 6 (29), 20.

Bond, T.C., Bergstrom, R.W., 2006. Light absorption by carbonaceous particles: an investigative review. Aerosol Sci. Technol. 40 (1), 27–67.

Bond, W.J., Keeley, J.E., 2005. Fire as a global "herbivore": the ecology and evolution of flammable ecosystems. Trends Ecol. Evol. 20 (7), 387–394.

Bond, T.C., Streets, D.G., Yarber, K.F., Nelson, S.M., Woo, J.H., Klimont, Z., 2004. A technology-based global inventory of black and organic carbon emissions from combustion. J. Geophys. Res. Atmos. 109 (D14). http://dx.doi.org/10.1029/2003JD003697.

Bougiatioti, A., Stavroulas, I., Kostenidou, E., Zarmpas, P., Theodosi, C., Kouvarakis, G., Canonaco, F., et al., 2014. Processing of biomass-burning aerosol in the eastern Mediterranean during summertime. Atmos. Chem. Phys. 14 (9), 4793–4807.

Bougiatioti, A., Bezantakos, S., Stavroulas, I., Kalivitis, N., Kokkalis, P., Biskos, G., Mihalopoulos, N., et al., 2016. Biomass-burning impact on CCN number, hygroscopicity and cloud formation during summertime in the eastern Mediterranean. Atmos. Chem. Phys. 16 (11), 7389–7409.

Brito, J., Rizzo, L.V., Morgan, W.T., Coe, H., Johnson, B., Haywood, J., Longo, K., et al., 2014. Ground-based aerosol characterization during the South American Biomass Burning Analysis (SAMBBA) field experiment. Atmos. Chem. Phys. 14 (22), 12069–12083.

Bruce, N., Perez-Padilla, R., Albalak, R., 2000. Indoor air pollution in developing countries: a major environmental and public health challenge. World Health Organ. 78 (9), 1078–1092.

Cahoon Jr., D.R., Stocks, B.J., Levine, J.S., Cofer III, W.R., Pierson, J.M., 1994. Satellite analysis of the severe 1987 forest fires in northern China and southeastern Siberia. J. Geophys. Res. 99 (D9):18627–18638. http://dx.doi.org/10.1029/94JD01024.

Calfapietra, C., Morani, A., Sgrigna, G., Di Giovanni, S., Muzzini, V., Pallozzi, E., Guidolotti, G., et al., 2016. Removal of ozone by urban and peri-urban forests: evidence from laboratory, field, and modeling approaches. J. Environ. Qual. 45 (1), 224–233.

Calvo, A.I., Martins, V., Nunes, T., Duarte, M., Hillamo, R., Teinilä, K., Pont, V., et al., 2015. Residential wood combustion in two domestic devices: relationship of different parameters throughout the combustion cycle. Atmos. Environ. 116, 72–82.

Cao, G., Zhang, X., Zheng, F., 2006. Inventory of black carbon and organic carbon emissions from China. Atmos. Environ. 40 (34), 6516–6527.

Cao, J.J., Lee, S.C., Chow, J.C., Watson, J.G., Ho, K.F., Zhang, R.J., Jin, Z.D., et al., 2007. Spatial and seasonal distributions of carbonaceous aerosols over China. J. Geophys. Res. Atmos. 112 (D22). http://dx.doi.org/10.1029/2006JD008205.

Cao, G., Zhang, X., Gong, S., An, X., Wang, Y., 2011. Emission inventories of primary particles and pollutant gases for China. Chin. Sci. Bull. 56 (8), 781–788.

Cape, J.N., Cornell, S.E., Jickells, T.D., Nemitz, E., 2011. Organic nitrogen in the atmosphere-where does it come from? A review of sources and methods. Atmos. Res. 102 (1–2), 30–48.

Capes, G., Johnson, B., McFiggans, G., Williams, P.I., Haywood, J., Coe, H., 2008. Aging of biomass burning aerosols over West Africa: Aircraft measurements of chemical composition, microphysical properties, and emission ratios. J. Geophys. Res. Atmos. 113 (D23). http://dx.doi.org/10.1029/2008JD009845.

Carrico, C.M., Petters, M.D., Kreidenweis, S.M., Collett, J.L., Engling, G., Malm, W.C., 2008. Aerosol hygroscopicity and cloud droplet activation of extracts of filters from biomass burning experiments. J. Geophys. Res. Atmos. 113 (D8). http://dx.doi.org/10.1029/2007JD009274.

Carrico, C.M., Prenni, A.J., Kreidenweis, S.M., Levin, E.J., McCluskey, C.S., DeMott, P.J., McMeeking, G.R., et al., 2016. Rapidly evolving ultrafine and fine mode biomass smoke physical properties: comparing laboratory and field results. J. Geophys. Res. Atmos. 121 (10). http://dx.doi.org/10.1002/2015JD024389.

Chakrabarty, R.K., Moosmüller, H., Chen, L.W.A., Lewis, K., Arnott, W.P., Mazzoleni, C., Dubey, M.K., et al., 2010. Brown carbon in tar balls from smoldering biomass combustion. Atmos. Chem. Phys. 10 (13), 6363–6370.

Chakrabarty, R.K., Gyawali, M., Yatavelli, R.L., Pandey, A., Watts, A.C., Knue, J., Chen, L.A., et al., 2016. Brown carbon aerosols from burning of boreal peatlands: microphysical properties, emission factors, and implications for direct radiative forcing. Atmos. Chem. Phys. 16 (5), 3033–3040.

Chan, C.K., Yao, X., 2008. Air pollution in mega cities in China. Atmos. Environ. 42 (1), 1–42.

Chan, L.Y., Liu, H.Y., Lam, K.S., Wang, T., 1998. Analysis of the seasonal behavior of tropospheric ozone at Hong Kong. Atmos. Environ. 32 (2), 159–168.

Chan, L.Y., Chan, C.Y., Liu, H.Y., Christopher, S., Oltmans, S.J., Harris, J.M., 2000. A case study on the biomass burning in Southeast Asia and enhancement of tropospheric ozone over Hong Kong. Geophys. Res. Lett. 27 (10):1479–1482. http://dx.doi.org/10.1029/1999GL010855.

Chan, C.Y., Chan, L.Y., Harris, J.M., Oltmans, S.J., Blake, D.R., Qin, Y., Zheng, Y.G., et al., 2003. Characteristics of biomass burning emission sources, transport, and chemical speciation in enhanced springtime tropospheric ozone profile over Hong Kong. J. Geophys. Res. Atmos. 108 (D1). http://dx.doi.org/10.1029/2001JD001555.

Chen, X.F., 2001. Economics analysis on pollution from straw burning and managing in rural China. China Rural Economy, pp. 47–52 (in Chinese).

Chen, Y., Xie, S.D., 2014. Characteristics and formation mechanism of a heavy air pollution episode caused by biomass burning in Chengdu, Southwest China. Sci. Total Environ. 473–474 (3), 507–517.

Chen, Y., Shah, N., Braun, A., Huggins, F.E., Huffman, G.P., 2005. Electron microscopy investigation of carbonaceous particulate matter generated by combustion of fossil fuels. Energy Fuel 19 (4), 1644–1651.
Chen, Y., Shah, N., Huggins, F.E., Huffman, G.P., 2006. Microanalysis of ambient particles from Lexington, KY, by electron microscopy. Atmos. Environ. 40 (4), 651–663.
Chen, L., Xing, L., Han, L., 2009. Renewable energy from agro-residues in China: solid biofuels and biomass briquetting technology. Renew. Sust. Energ. Rev. 13 (9), 2689–2695.
Chen, H., Hu, D., Wang, L., Mellouki, A., Chen, J., 2015a. Modification in light absorption cross section of laboratory-generated black carbon-brown carbon particles upon surface reaction and hydration. Atmos. Environ. 116, 253–261.
Chen, C., Sun, Y.L., Xu, W.Q., Du, W., Zhou, L.B., Han, T.T., Wang, Q.Q., et al., 2015b. Characteristics and sources of submicron aerosols above the urban canopy (260 m) in Beijing, China, during the 2014 APEC summit. Atmos. Chem. Phys. 15 (22), 812–879 (895).
Chen, Y., Shen, G., Huang, Y., Zhang, Y., Han, Y., Wang, R., Shen, H., et al., 2016. Household air pollution and personal exposure risk of polycyclic aromatic hydrocarbons among rural residents in Shanxi, China. Indoor Air 26 (2), 246–258.
Cheng, Y.F., Berghof, M., Garland, R.M., Wiedensohler, A., Wehner, B., Müller, T., Su, H., et al., 2009. Influence of soot mixing state on aerosol light absorption and single scattering albedo during air mass aging at a polluted regional site in northeastern China. J. Geophys. Res. Atmos. 114 (D2). http://dx.doi.org/10.1029/2008JD010883.
Cheng, Y., Engling, G., He, K., Duan, F., Ma, Y., Du, Z., Liu, J., et al., 2013. Biomass burning contribution to Beijing aerosol. Atmos. Chem. Phys. 13 (15), 7765–7781.
Cheng, Z., Wang, S., Fu, X., Watson, J.G., Jiang, J., Fu, Q., Chen, C., et al., 2014a. Impact of biomass burning on haze pollution in the Yangtze River delta, China: a case study in summer 2011. Atmos. Chem. Phys. 14 (9), 4573–4585.
Cheng, Y., Engling, G., He, K., Duan, F., Du, Z., Ma, Y., Liang, L., et al., 2014b. The characteristics of Beijing aerosol during two distinct episodes: impacts of biomass burning and fireworks. Environ. Pollut. 185, 149–157.
Cheung, V.T., Wang, T., 2001. Observational study of ozone pollution at a rural site in the Yangtze Delta of China. Atmos. Environ. 35 (29), 4947–4958.
China, S., Mazzoleni, C., Gorkowski, K., Aiken, A.C., Dubey, M.K., 2013. Morphology and mixing state of individual freshly emitted wildfire carbonaceous particles. Nat. Commun.:2122 http://dx.doi.org/10.1038/ncomms3122.
Chirico, R., DeCarlo, P.F., Heringa, M.F., Tritscher, T., Richter, R., Prévôt, A., Dommen, J., et al., 2010. Impact of aftertreatment devices on primary emissions and secondary organic aerosol formation potential from in-use diesel vehicles: results from smog chamber experiments. Atmos. Chem. Phys. 10 (23), 11545–11563.
Chubarova, N., Nezval, Y., Sviridenkov, I., Smirnov, A., Slutsker, I., 2012. Smoke aerosol and its radiative effects during extreme fire event over Central Russia in summer 2010. Atmos. Meas. Tech. 5 (3), 557–568.
Ciencewicki, J., Jaspers, I., 2008. Air pollution and respiratory viral infection. Inhal. Toxicol. 19 (19), 1135–1146.
Costanza, R., D'Arge, R., De Groot, R., Faber, S., Grasso, M., Hannon, B., Limburg, K., et al., 1997. The Value of the World's Ecosystem Services and Natural Capital.
Crippa, M., Canonaco, F., Lanz, V.A., Äijälä, M., Allan, J.D., Carbone, S., Capes, G., et al., 2014. Organic aerosol components derived from 25 AMS data sets across Europe using a consistent ME-2 based source apportionment approach. Atmos. Chem. Phys. 14 (12), 6159–6176.
Crutzen, P.J., Andreae, M.O., 1990. Biomass burning in the tropics: impact on atmospheric chemistry and biogeochemical cycles. Science 250, 1669–1678.
Cubison, M.J., Ortega, A.M., Hayes, P.L., Farmer, D.K., Day, D., Lechner, M.J., Brune, W.H., et al., 2011. Effects of aging on organic aerosol from open biomass burning smoke in aircraft and laboratory studies. Atmos. Chem. Phys. 11 (23), 12049–12064.
Da Rocha, G.O., Allen, A.G., Cardoso, A.A., 2005. Influence of agricultural biomass burning on aerosol size distribution and dry deposition in Southeastern Brazil. Environ. Sci. Technol. 39 (14), 5293–5301.
DeCarlo, P.F., Slowik, J.G., Worsnop, D.R., Davidovits, P., Jimenez, J.L., 2004. Particle morphology and density characterization by combined mobility and aerodynamic diameter measurements. Part 1: theory. Aerosol Sci. Technol. 38 (12), 1185–1205.
DeCarlo, P.F., Dunlea, E.J., Kimmel, J.R., Aiken, A.C., Sueper, D., Crounse, J., Wennberg, P.O., et al., 2008. Fast airborne aerosol size and chemistry measurements above Mexico City and Central Mexico during the MILAGRO campaign. Atmos. Chem. Phys. 8 (14), 4027–4048.
DeCarlo, P.F., Ulbrich, I.M., Crounse, J., Foy, B.D., Dunlea, E.J., Aiken, A.C., Knapp, D., et al., 2010. Investigation of the sources and processing of organic aerosol over the Central Mexican Plateau from aircraft measurements during MILAGRO. Atmos. Chem. Phys. 10 (12), 5257–5280.
Decesari, S., Facchini, M.C., Matta, E., Mircea, M., Fuzzi, S., Chughtai, A.R., Smith, D.M., 2002. Water soluble organic compounds formed by oxidation of soot. Atmos. Environ. 36 (11), 1827–1832.
Delfino, R.J., Sioutas, C., Malik, S., 2005. Potential role of ultrafine particles in associations between airborne particle mass and cardiovascular health. Environ. Health Perspect. 113 (8), 934–946.
Demirbas, A., 2007. Progress and recent trends in biofuels. Prog. Energy Combust. Sci. 33 (1), 1–18.
Deng, X., Tie, X., Zhou, X., Wu, D., Zhong, L., Tan, H., Li, F., et al., 2008. Effects of Southeast Asia biomass burning on aerosols and ozone concentrations over the Pearl River Delta (PRD) region. Atmos. Environ. 42 (36), 8493–8501.
Dhammapala, R., Claiborn, C., Simpson, C., Jimenez, J., 2007. Emission factors from wheat and Kentucky bluegrass stubble burning: comparison of field and simulated burn experiments. Atmos. Environ. 41 (7), 1512–1520.
Diat-Sanchez, D., 1997. The role of diesel exhaust particles and their associated polyaromatic hydrocarbons in the induction of allergic airway disease. Allergy 52 (38), 57–58.
Ding, A.J., Wang, T., Thouret, V., Cammas, J., Nédélec, P., 2008. Tropospheric ozone climatology over Beijing: analysis of aircraft data from the MOZAIC program. Atmos. Chem. Phys. 4 (7), 9795–9827.
Ding, A.J., Fu, C.B., Yang, X.Q., Sun, J.N., Petäjä, T., Kerminen, V., Wang, T., et al., 2013a. Intense atmospheric pollution modifies weather: a case of mixed biomass burning with fossil fuel combustion pollution in eastern China. Atmos. Chem. Phys. 13 (20), 10545–10554.
Ding, A.J., Fu, C.B., Yang, X.Q., Sun, J.N., Zheng, L.F., Xie, Y.N., Herrmann, E., Nie, W., Petaja, T., Kerminen, V.-M., Kulmala, M., 2013b. Ozone and fine particle in the western Yangtze River Delta: an overview of 1 yr data at the SORPES station. Atmos. Chem. Phys. 13 (11), 5813–5830.
Ding, K., Liu, J., Ding, A., Liu, Q., Zhao, T.L., Shi, J., Han, Y., Wang, H., Jiang, F., 2015. Uplifting of carbon monoxide from biomass burning and anthropogenic sources to the free troposphere in East Asia. Atmos. Chem. Phys. 15 (5), 2843–2866.
Ding, A.J., Huang, X., Nie, W., Sun, J.N., Kerminen, V.-M., Petaja, T., Su, H., Cheng, Y.F., Yang, X.Q., Wang, M.H., Chi, X.G., Wang, J.P., Virkkula, A., Guo, W.D., Yuan, J., Wang, S.Y., Zhang, R.J., Wu, Y.F., Song, Y., Zhu, T., Zilitinkevich, S., Kulmala, M., Fu, C.B., 2016a. Enhanced haze pollution by black carbon in megacities in China. Geophys. Res. Lett. 43: 2873–2879. http://dx.doi.org/10.1002/2016GL067745.
Ding, X., He, Q.F., Shen, R.Q., Yu, Q.Q., Zhang, Y.Q., Xin, J.Y., Wen, T.X., et al., 2016b. Spatial and seasonal variations of isoprene secondary organic aerosol in China: Significant impact of biomass burning during winter. Sci. Rep.-Uk http://dx.doi.org/10.1038/srep20411.
Doherty, R.M., 2015. Atmospheric chemistry: ozone pollution from near and far. Nat. Geosci. 8 (9), 664–665.
Donahue, N.M., Robinson, A.L., Pandis, S.N., 2009. Atmospheric organic particulate matter: from smoke to secondary organic aerosol. Atmos. Environ. 43 (1), 94–106.
Dozier, J., 1981. A method for satellite identification of surface temperature fields of subpixel resolution. Remote Sens. Environ. 11, 221–229.
Drewnick, F., Hings, S.S., Alfarra, M.R., Prevot, A., Borrmann, S., 2009. Aerosol quantification with the aerodyne aerosol mass spectrometer: detection limits and ionizer background effects. Atmos. Meas. Tech. 2 (1), 33–46.
Du, H., Kong, L., Cheng, T., Chen, J., Du, J., Li, L., Xia, X., et al., 2011. Insights into summertime haze pollution events over shanghai based on online water-soluble ionic composition of aerosols. Atmos. Environ. 45 (29), 5131–5137.
Duan, F., Liu, X., Yu, T., Cachier, H., 2004. Identification and estimate of biomass burning contribution to the urban aerosol organic carbon concentrations in Beijing. Atmos. Environ. 38 (9), 1275–1282.
Duo, B., Zhang, Y., Kong, L., Fu, H., Hu, Y., Chen, J., Li, L., et al., 2015. Individual particle analysis of aerosols collected at Lhasa City in the Tibetan plateau. J. Environ. Sci. 29, 165–177.
Duplissy, J., DeCarlo, P.F., Dommen, J., Alfarra, M.R., Metzger, A., Barmpadimos, I., Prevot, A.S., et al., 2011. Relating hygroscopicity and composition of organic aerosol particulate matter. Atmos. Chem. Phys. 11 (3), 1155–1165.
Dusek, U., Frank, G.P., Hildebrandt, L., Curtius, J., Schneider, J., Walter, S., Chand, D., et al., 2006. Size matters more than chemistry for cloud-nucleating ability of aerosol particles. Science 312 (5778), 1375–1378.
Dusek, U., Frank, G.P., Curtius, J., Drewnick, F., Schneider, J., Kürten, A., Rose, D., et al., 2010. Enhanced organic mass fraction and decreased hygroscopicity of cloud condensation nuclei (CCN) during new particle formation events. Geophys. Res. Lett. 37 (3). http://dx.doi.org/10.1029/2009GL040930.
Dusek, U., Frank, G.P., Massling, A., Zeromskiene, K., Iinuma, Y., Schmid, O., Helas, G., et al., 2011. Water uptake by biomass burning aerosol at sub- and supersaturated conditions: closure studies and implications for the role of organics. Atmos. Chem. Phys. 11 (18), 9519–9532.
Dzepina, K., Volkamer, R.M., Madronich, S., Tulet, P., Ulbrich, I.M., Zhang, Q., Cappa, C.D., et al., 2009. Evaluation of recently-proposed secondary organic aerosol models for a case study in Mexico City. Atmos. Chem. Phys. 9 (15), 5681–5709.
Edwards, D.P., Emmons, L.K., Gille, J.C., Chu, A., Attié, J.L., Giglio, L., Wood, S.W., et al., 2006. Satellite-observed pollution from Southern Hemisphere biomass burning. J. Geophys. Res. Atmos. 111 (D14). http://dx.doi.org/10.1029/2005JD006655.
Eisner, M.D., Anthonisen, N., Coultas, D., Kuenzli, N., Perez-Padilla, R., Postma, D., Romieu, I., et al., 2010. An official American Thoracic Society public policy statement: novel risk factors and the global burden of chronic obstructive pulmonary disease. Am. J. Respir. Crit. Care Med. 5 (182), 52–56.
Engelhart, G.J., Hennigan, C.J., Miracolo, M.A., Robinson, A.L., Pandis, S.N., 2012. Cloud condensation nuclei activity of fresh primary and aged biomass burning aerosol. Atmos. Chem. Phys. 12 (15), 7285–7293.
Engling, G., Lee, J.J., Tsai, Y., Lung, S.C., Chou, C.C., Chan, C., 2009. Size-resolved anhydrosugar composition in smoke aerosol from controlled field burning of rice straw. Aerosol Sci. Technol. 7, 662–672.
Fan, J., Zhang, R., Collins, D., Li, G., 2006. Contribution of secondary condensable organics to new particle formation: a case study in Houston, Texas. Geophys. Res. Lett. 33 (15). http://dx.doi.org/10.1029/2006GL026295.
Fan, J., Rosenfeld, D., Yang, Y., Zhao, C., Leung, L.R., Li, Z., 2015. Substantial contribution of anthropogenic air pollution to catastrophic floods in Southwest China. Geophys. Res. Lett. 42 (14):6066–6075. http://dx.doi.org/10.1002/2015GL06447.
Fang, M., Chan, C.K., Yao, X., 2009. Managing air quality in a rapidly developing nation: China. Atmos. Environ. 43 (1), 79–86.
Ferge, T., Maguhn, J., Hafner, K., Mühlberger, F., Davidovic, M., Warnecke, R., Zimmermann, R., 2005. On-line analysis of gas-phase composition in the combustion chamber and particle emission characteristics during combustion of wood and waste in a small batch reactor. Environ. Sci. Technol. 39 (6), 1393–1402.
Fernandes, S. D., Trautmann, N. M., Streets, D. G., Roden, C. A. and Bond, T. C. Global biofuel use, 1850–2000, Glob. Biogeochem. Cycles 2007; 2:241–253.
Field, C.B., Campbell, J.E., Lobell, D.B., 2008. Biomass energy: the scale of the potential resource. Trends Ecol. Evol. 2 (23), 65–72.

Fine, P.M., Cass, G.R., Simoneit, B.R., 2002. Chemical characterization of fine particle emissions from the fireplace combustion of woods grown in the southern United States. Environ. Sci. Technol. 36 (7), 1442–1451.

Finlayson-Pitts, B.J., Pitts, J.N., 1997. Tropospheric air pollution: ozone, airborne toxics, polycyclic aromatic hydrocarbons, and particles. Science 276 (5315), 1045–1052.

Formenti, P., Elbert, W., Maenhaut, W., Haywood, J., Osborne, S., Andreae, M.O., 2003. Inorganic and carbonaceous aerosols during the Southern African Regional Science Initiative (SAFARI 2000) experiment: chemical characteristics, physical properties, and emission data for smoke from African biomass burning. J. Geophys. Res. Atmos. 108 (D13). http://dx.doi.org/10.1029/2002JD002408.

Fraser, M.P., Yue, Z.W., Buzcu, B., 2003. Source apportionment of fine particulate matter in Houston, TX, using organic molecular markers. Atmos. Environ. 37 (15), 2117–2123.

Fu, H., Zhang, M., Li, W., Chen, J., Wang, L., Quan, X., Wang, W., 2012. Morphology, composition and mixing state of individual carbonaceous aerosol in urban Shanghai. Atmos. Chem. Phys. 481 (2), 693–707.

Fu, H.B., Shang, G.F., Lin, J., Hu, Y.J., Hu, Q.Q., Guo, L., Zhang, Y.C., et al., 2014. Fractional iron solubility of aerosol particles enhanced by biomass burning and ship emission in Shanghai, East China. Sci. Total Environ. 2, 377–391.

Fuchs, H., Tan, Z., Lu, K., Bohn, B., Broch, S., Brown, S.S., Dong, H., et al., 2016. OH reactivity at a rural site (Wangdu) in the North China Plain: Contributions from OH reactants and experimental OH budget. Atmos. Chem. Phys. Discuss. http://dx.doi.org/10.5194/acp-2016-716.

Fuller, K.A., Malm, W.C., Kreidenweis, S.M., 1999. Effects of mixing on extinction by carbonaceous particles. J. Geophys. Res. 15:941–954. http://dx.doi.org/10.1029/1998JD100069.

Fullerton, D.G., Bruce, N., Gordon, S.B., 2008. Indoor air pollution from biomass fuel smoke is a major health concern in the developing world. T. Roy Soc. Trop. Med.e H 102 (9), 843–851.

Galanter, M., Levy, H., Carmichael, G.R., 2000. Impacts of biomass burning on tropospheric CO, NOx, and O_3. J. Geophys. Res. Atmos. 105 (D5), 6633–6653.

Gao, M., Guttikunda, S.K., Carmichael, G.R., Wang, Y., Liu, Z., Stanier, C.O., Saide, P.E., et al., 2015. Health impacts and economic losses assessment of the 2013 severe haze event in Beijing area. Sci. Total Environ. 511, 553–561.

Garland, R.M., Yang, H., Schmid, O., Rose, D., Nowak, A., Achtert, P., Wiedensohler, A., et al., 2008. Aerosol optical properties in a rural environment near the mega-city Guangzhou, China: implications for regional air pollution, radiative forcing and remote sensing. Atmos. Chem. Phys. 8 (17), 5161–5186.

Gautam, R., Hsu, N.C., Eck, T.F., Holben, B.N., Janjai, S., Jantarach, T., Tsay, S., et al., 2013. Characterization of aerosols over the Indochina peninsula from satellite-surface observations during biomass burning pre-monsoon season. Atmos. Environ. 78, 51–59.

Ge, G., 2008. The climatic characteristics and change of haze days over China during 1961–2005. Acta Geograph. Sin. 7(13) (in Chinese).

Geng, F., Zhang, Q., Tie, X., Huang, M., Ma, X., Deng, Z., Yu, Q., et al., 2009. Aircraft measurements of O_3, NOx, CO, VOCs, and SO_2 in the Yangtze River Delta region. Atmos. Environ. 43 (3), 584–593.

George, M., Suhail, S., Chandran, S., Chen, J., Lu, K., Ruth, A., Venables, D., et al., 2016. Open-path in situ measurement of the nitrate radical concentrations during the CAREBeijing-NCP 2014 summer campaign. EGU General Assembly Conference Abstracts. 12189.

Giglio, L., 2010. MODIS Collection 5 Active Fire Product User's Guide Version 2.4. Science Systems and Applications, Inc.

Giglio, L., Descloitres, J., Justice, C.O., Kaufman, Y.J., 2003. An enhanced contextual fire detection algorithm for MODIS. Remote Sens. Environ. 87 (2), 273–282.

Giglio, L., Randerson, J.T., Werf, G.R., 2013. Analysis of daily, monthly, and annual burned area using the fourth-generation global fire emissions database (GFED4). J. Geophys. Res. Biogeosci. 118 (1):317–328. http://dx.doi.org/10.1002/jgrg.20042.

Giordano, M.R., Short, D.Z., Hosseini, S., Lichtenberg, W., Asa-Awuku, A.A., 2013. Changes in droplet surface tension affect the observed hygroscopicity of photochemically aged biomass burning aerosol. Environ. Sci. Technol. 47 (19), 10980–10986.

Goldstein, A.H., Galbally, I.E., 2007. Known and unexplored organic constituents in the earth's atmosphere. Environ. Sci. Technol. 41 (5), 1514–1521.

Grahame, T.J., Klemm, R., Schlesinger, R.B., 2014. Public health and components of particulate matter: the changing assessment of black carbon. J. Air Waste Manage. Assoc. 64 (6), 620–660.

Grieshop, A.P., Donahue, N.M., Robinson, A.L., 2009. Laboratory investigation of photochemical oxidation of organic aerosol from wood fires 2: analysis of aerosol mass spectrometer data. Atmos. Chem. Phys. 9 (4), 2227–2240.

Guan, H., Esswein, R., Lopez, J., Bergstrom, R., Warnock, A., Follette-Cook, M., Fromm, M., et al., 2010. A multi-decadal history of biomass burning plume heights identified using aerosol index measurements. Atmos. Chem. Phys. 10 (14), 6461–6469.

Gunthe, S.S., Rose, D., Su, H., Garland, R.M., Achtert, P., Nowak, A., Wiedensohler, A., et al., 2011. Cloud condensation nuclei (CCN) from fresh and aged air pollution in the megacity region of Beijing. Atmos. Chem. Phys. 11 (21), 11023–11039.

Guo, H., Wang, T., Simpson, I.J., Blake, D.R., Yu, X.M., Kwok, Y.H., Li, Y.S., 2004. Source contributions to ambient VOCs and CO at a rural site in eastern China. Atmos. Environ. 38 (27), 4551–4560.

Guo, H., Cheng, H.R., Ling, Z.H., Louie, P., Ayoko, G.A., 2011. Which emission sources are responsible for the volatile organic compounds in the atmosphere of Pearl River Delta? J. Hazard. Mater. 188 (1), 116–124.

Guo, S., Hu, M., Guo, Q., Zhang, X., Schauer, J.J., Zhang, R., 2013. Quantitative evaluation of emission controls on primary and secondary organic aerosol sources during Beijing 2008 Olympics. Atmos. Chem. Phys. 13 (16), 8303–8314.

Guo, X., Fu, D., Guo, X., Zhang, C., 2014. A case study of aerosol impacts on summer convective clouds and precipitation over northern China. Atmos. Res. 142, 142–157.

Gustafsson, Ö., Kruså, M., Zencak, Z., Sheesley, R.J., Granat, L., Engström, E., Praveen, P.S., et al., 2009. Brown clouds over South Asia: biomass or fossil fuel combustion? Science 323 (5913), 495–498.

Guyon, P., Boucher, O., Graham, B., Beck, J., Mayol-Bracero, O.L., Roberts, G.C., Maenhaut, W., et al., 2003. Refractive index of aerosol particles over the Amazon tropical forest during LBA-EUSTACH 1999. J. Aerosol Sci. 34 (7), 883–907.

Hallett, J., Hudson, J.G., Rogers, C.F., 1989. Characterization of combustion aerosols for haze and cloud formation. Aerosol Sci. Technol. 10 (1), 70–83.

Hallquist, M., Wenger, J.C., Baltensperger, U., Rudich, Y., Simpson, D., Claeys, M., Dommen, J., et al., 2009. The formation, properties and impact of secondary organic aerosol: current and emerging issues. Atmos. Chem. Phys. 9 (14), 5155–5236.

Han, Y.M., Lee, S.C., Cao, J.J., Ho, K.F., An, Z.S., 2009. Spatial distribution and seasonal variation of char-EC and soot-EC in the atmosphere over China. Atmos. Environ. 43 (38), 6066–6073.

Hand, J.L., Malm, W.C., Laskin, A., Day, D., Lee, T., Wang, C., Carrico, C., et al., 2005. Optical, physical, and chemical properties of tar balls observed during the Yosemite Aerosol Characterization Study. J. Geophys. Res. Atmos. 110 (D21). http://dx.doi.org/10.1029/2004JD005728.

Hand, J.L., Day, D.E., McMeeking, G.M., Levin, E., Carrico, C.M., Kreidenweis, S.M., Malm, W.C., et al., 2010. Measured and modeled humidification factors of fresh smoke particles from biomass burning: role of inorganic constituents. Atmos. Chem. Phys. 10 (13), 6179–6194.

Hansen, J., Sato, M., Ruedy, R., 1997. Radiative forcing and climate response. J. Geophys. Res. Atmos. 102 (D6):6831–6864. http://dx.doi.org/10.1029/96JD03436.

Hays, M.D., Geron, C.D., Linna, K.J., Smith, N.D., Schauer, J.J., 2002. Speciation of gas-phase and fine particle emissions from burning of foliar fuels. Environ. Sci. Technol. 36 (11), 2281–2295.

Hays, M.D., Fine, P.M., Geron, C.D., Kleeman, M.J., Gullett, B.K., 2005. Open burning of agricultural biomass: physical and chemical properties of particle-phase emissions. Atmos. Environ. 39 (36), 6747–6764.

Haywood, J., Boucher, O., 2000. Estimates of the direct and indirect radiative forcing due to tropospheric aerosols: a review. Rev. Geophys. 38 (4), 513–543.

Haywood, J.M., Osborne, S.R., Francis, P.N., Keil, A., Formenti, P., Andreae, M.O., Kaye, P.H., 2003. The mean physical and optical properties of regional haze dominated by biomass burning aerosol measured from the C-130 aircraft during SAFARI 2000. J. Geophys. Res. Atmos. 108 (D13). http://dx.doi.org/10.1029/2002JD002226.

He, G., Ying, B., Liu, J., Gao, S., Shen, S., Balakrishnan, K., Jin, Y., et al., 2005. Patterns of household concentrations of multiple indoor air pollutants in China. Environ. Sci. Technol. 39 (4), 991–998.

He, L., Hu, M., Huang, X., Zhang, Y., Tang, X., 2006. Seasonal pollution characteristics of organic compounds in atmospheric fine particles in Beijing. Sci. Total Environ. 359 (1), 167–176.

He, L., Lin, Y., Huang, X., Guo, S., Xue, L., Su, Q., Hu, M., et al., 2010. Characterization of high-resolution aerosol mass spectra of primary organic aerosol emissions from Chinese cooking and biomass burning. Atmos. Chem. Phys. 10 (23), 11535–11543.

He, L.Y., Huang, X.F., Xue, L., Hu, M., Lin, Y., Zheng, J., Zhang, R., et al., 2011a. Submicron aerosol analysis and organic source apportionment in an urban atmosphere in Pearl River Delta of China using high-resolution aerosol mass spectrometry. J. Geophys. Res. Atmos. 116 (D12). http://dx.doi.org/10.1029/2010JD014566.

He, M., Zheng, J., Yin, S., Zhang, Y., 2011b. Trends, temporal and spatial characteristics, and uncertainties in biomass burning emissions in the Pearl River Delta, China. Atmos. Environ. 45 (24), 4051–4059.

He, Q., Zhao, X., Lu, J., Zhou, G., Yang, H., Gao, W., Yu, W., et al., 2015. Impacts of biomass-burning on aerosol properties of a severe haze event over Shanghai. Particuology 20 (3), 52–60.

Healy, R.M., Wang, J.M., Jeong, C.H., Lee, A., Willis, M.D., Jaroudi, E., Zimmerman, N., et al., 2015. Light-absorbing properties of ambient black carbon and brown carbon from fossil fuel and biomass burning sources. J. Geophys. Res. Atmos. 120 (13): 6619–6633. http://dx.doi.org/10.1002/2015JD023382.

Hedberg, E., Kristensson, A., Ohlsson, M., Johansson, C., Johansson, P., Swietlicki, E., Vesely, V., et al., 2002. Chemical and physical characterization of emissions from birch wood combustion in a wood stove. Atmos. Environ. 36 (30), 4823–4837.

Hennigan, C.J., Miracolo, M.A., Engelhart, G.J., May, A.A., Presto, A.A., Lee, T., Sullivan, A.P., et al., 2011. Chemical and physical transformations of organic aerosol from the photooxidation of open biomass burning emissions in an environmental chamber. Atmos. Chem. Phys. 11 (15), 7669–7686.

Heringa, M.F., DeCarlo, P.F., Chirico, R., Tritscher, T., Dommen, J., Weingartner, E., Richter, R., et al., 2011. Investigations of primary and secondary particulate matter of different wood combustion appliances with a high-resolution time-of-flight aerosol mass spectrometer. Atmos. Chem. Phys. 11 (12), 5945–5957.

Hinds, W.C., 2012. Aerosol Technology: Properties, Behavior, and Measurement of Airborne Particles. John Wiley & Sons.

Ho, K.F., Lee, S.C., Ho, S.S.H., Kawamura, K., Tachibana, E., Cheng, Y., Zhu, T., 2010. Dicarboxylic acids, ketocarboxylic acids, α-dicarbonyls, fatty acids, and benzoic acid in urban aerosols collected during the 2006 Campaign of Air Quality Research in Beijing (CAREBeijing-2006). J. Geophys. Res. Atmos. 115 (D19). http://dx.doi.org/10.1029/2009JD013304.

Hobbs, P.V., Reid, J.S., Kotchenruther, R.A., Ferek, R.J., Weiss, R., 1997. Direct radiative forcing by smoke from biomass burning. Science 275 (5307), 1777–1778.

Hobbs, P.V., Sinha, P., Yokelson, R.J., Christian, T.J., Blake, D.R., Gao, S., Kirchstetter, T.W., et al., 2003. Evolution of gases and particles from a savanna fire in South Africa. J. Geophys. Res. Atmos. 108 (D13). http://dx.doi.org/10.1029/2002JD002352.

Hodnebrog, Ø., Solberg, S., Stordal, F., Svendby, T.M., Simpson, D., Gauss, M., Hilboll, A., et al., 2012. Impact of forest fires, biogenic emissions and high temperatures on the elevated Eastern Mediterranean ozone levels during the hot summer of 2007. Atmos. Chem. Phys. 12 (18), 8727–8750.

Hoffer, A., Gelencsér, A., Guyon, P., Kiss, G., Schmid, O., Frank, G.P.A., 2006. Optical properties of humic-like substances (HULIS) in biomass-burning aerosols. Atmos. Chem. Phys. 6 (11), 3563–3570.

Honrath, R.E., Owen, R.C., Val Martin, M., Reid, J.S., Lapina, K., Fialho, P., Dziobak, M.P., et al., 2004. Regional and hemispheric impacts of anthropogenic and biomass burning emissions on summertime CO and O_3 in the North Atlantic lower free troposphere. J. Geophys. Res. Atmos. 109 (D24). http://dx.doi.org/10.1029/2004JD005147.
Hoogwijk, M., Faaij, A., Eickhout, B., Vries, B.D., Turkenburg, W., 2005. Potential of biomass energy out to 2100, for four IPCC SRES land-use scenarios. Biomass Bioenergy 29 (4), 225–257.
Hope, C., 2008. Discount rates, equity weights and the social cost of carbon. Energy Econ. 30 (3), 1011–1019.
Hu, W., Hu, M., Hu, W., Niu, H., Zheng, J., Wu, Y., Chen, W., et al., 2016. Characterization of submicron aerosols influenced by biomass burning at a site in the Sichuan Basin, southwestern China. Atmos. Chem. Phys.:1–39 http://dx.doi.org/10.5194/acp-2016-114.
Hua, Y., Cheng, Z., Wang, S., Jiang, J., Chen, D., Cai, S., Fu, X., et al., 2015. Characteristics and source apportionment of $PM_{2.5}$ during a fall heavy haze episode in the Yangtze River Delta of China. Atmos. Environ. 123, 380–391.
Huang, X., He, L., Hu, M., Canagaratna, M.R., Kroll, J.H., Ng, N.L., Zhang, Y., et al., 2011. Characterization of submicron aerosols at a rural site in Pearl River Delta of China using an aerodyne high-resolution aerosol mass spectrometer. Atmos. Chem. Phys. 11 (5), 1865–1877.
Huang, K., Zhuang, G., Lin, Y., Fu, J.S., Wang, Q., Liu, T., Zhang, R., et al., 2012a. Typical types and formation mechanisms of haze in an Eastern Asia megacity, Shanghai. Atmos. Chem. Phys. 12 (1), 105–124.
Huang, X., He, L., Xue, L., Sun, T., Zeng, L., Gong, Z., Hu, M., et al., 2012b. Highly time-resolved chemical characterization of atmospheric fine particles during 2010 Shanghai World Expo. Atmos. Chem. Phys. 12 (11), 4897–4907.
Huang, X., Song, Y., Li, M., Zhu, T., 2012c. Harvest season, high polluted season in East China. Environ. Res. Lett. 7 (4), 044033.
Huang, X., Li, M., Li, J., Song, Y., 2012d. A high-resolution emission inventory of crop burning in fields in China based on MODIS Thermal Anomalies/Fire products. Atmos. Environ. 50, 9–15.
Huang, K., Zhuang, G., Lin, Y., Wang, Q., Fu, J.S., Fu, Q., Liu, T., et al., 2013a. How to improve the air quality over megacities in China: pollution characterization and source analysis in Shanghai before, during, and after the 2010 World Expo. Atmos. Chem. Phys. 13 (12), 5927–5942.
Huang, X., Xue, L., Tian, X., Shao, W., Sun, T., Gong, Z., Ju, W., et al., 2013b. Highly time-resolved carbonaceous aerosol characterization in Yangtze River Delta of China: composition, mixing state and secondary formation. Atmos. Environ. 64, 200–207.
Huang, R., Zhang, Y., Bozzetti, C., Ho, K., Cao, J., Han, Y., Daellenbach, K.R., et al., 2014. High secondary aerosol contribution to particulate pollution during haze events in China. Nature 7521, 218–222.
Huang, X., Ding, A., Liu, L., Liu, Q., Ding, K., Niu, X., Nie, W., Xu, Z., Chi, X., Wang, M., Sun, J., Guo, W., Fu, C., 2016. Effects of aerosol–radiation interaction on precipitation during biomass-burning season in East China. Atmos. Chem. Phys. 16, 10063–10082.
Huo, J., Lu, X., Wang, X., Chen, H., Ye, X., Gao, S., Gross, D.S., et al., 2016. Online single particle analysis of chemical composition and mixing state of crop straw burning particles: from laboratory study to field measurement. Front. Environ. Sci. Eng. 10 (2), 244–252.
IARC, 2010. IARC monographs on the evaluation of carcinogenic risks to humans. Volume 92. Some non-heterocyclic polycyclic aromatic hydrocarbons and some related exposures. Lyon: International Agency for Research on Cancer.
IPCC, 2013. Anthropogenic and Natural Radiative Forcing, in Climate Change 2013: The Physical Science Basis. Cambridge Univ. Press, New York, USA.
Islam, S., Saha, S.C., Sauret, E., Gu, Y.T., Ristovski, Z.D., 2015. Numerical investigation of aerosol particle transport and deposition in realistic lung airway. 6th International Conference on Computational Methods, pp. 56–68.
Jacob, D.J., Crawford, J.H., Kleb, M.M., Connors, V.S., Bendura, R.J., Raper, J.L., Sachse, G.W., Gille, J.C., Emmons, L., Heald, C.L., 2003. Transport and chemical evolution over the Pacific(TRACE-P) aircraft mission: design, execution and first results. J. Geophys. Res. 108:D20. http://dx.doi.org/10.1029/2002JD003276.
Jacobson, M.Z., 2014. Effects of biomass burning on climate, accounting for heat and moisture fluxes, black and brown carbon, and cloud absorption effects. J. Geophys. Res. Atmos. 119 (14):8980–9002. http://dx.doi.org/10.1002/2014JD021861.
Jacobson, M.C., Hansson, H.C., Noone, K.J., Charlson, R.J., 2000. Organic atmospheric aerosols: review and state of the science. Rev. Geophys. 38 (2), 267–294.
Jaffe, D.A., Wigder, N.L., 2012. Ozone production from wildfires: a critical review. Atmos. Environ. 51, 1–10.
Jaffe, D.A., Wigder, N., Downey, N., Pfister, G., Boynard, A., Reid, S.B., 2013. Impact of wildfires on ozone exceptional events in the western US. Environ. Sci. Technol. 47 (19), 11065–11072.
Janssen, N.A.H., Hoek, G., Simic-Lawson, M., Fischer, P., van Bree, L., Ten Brink, H., Keuken, M., Atkinson, R.W., Anderson, H.R., Brunekreef, B., Cassee, F.R., 2011. Black carbon as an additional indicator of the adverse health effects of airborne particles compared with PM_{10} and $PM_{2.5}$. Environ. Health Perspect. 119 (12), 1691–1699.
Jenkins, B.M., Jones, A.D., Turn, S.Q., Williams, R.B., 1996. Particle concentrations, gas-particle partitioning, and species intercorrelations for polycyclic aromatic hydrocarbons (PAH) emitted during biomass burning. Atmos. Environ. 30 (22), 3825–3835.
Jiménez, S., Ballester, J., 2005. Effect of co-firing on the properties of submicron aerosols from biomass combustion. P. Combust. Inst. 30 (2), 2965–2972.
Jimenez, J.L., Jayne, J.T., Shi, Q., Kolb, C.E., Worsnop, D.R., Yourshaw, I., Seinfeld, J.H., et al., 2003. Ambient aerosol sampling using the aerodyne aerosol mass spectrometer. J. Geophys. Res. Atmos. (D7) http://dx.doi.org/10.1029/2001JD001213.
Jimenez, J.L., Canagaratna, M.R., Donahue, N.M., Prevot, A., Zhang, Q., Kroll, J.H., DeCarlo, P.F., et al., 2009. Evolution of organic aerosols in the atmosphere. Science 326 (5959), 1525–1529.
Jin, Y., Zhou, Z., He, G., Wei, H., Liu, J., Liu, F., Tang, N., et al., 2005. Geographical, spatial, and temporal distributions of multiple indoor air pollutants in four Chinese provinces. Environ. Sci. Technol. 39 (24), 9431–9439.
Johnson, K.S., Zuberi, B., Molina, L.T., Molina, M.J., Iedema, M.J., Cowin, J.P., Gaspar, D.J., et al., 2005. Processing of soot in an urban environment: case study from the Mexico City metropolitan area. Atmos. Chem. Phys. 5 (11), 3033–3043.
Johnston, F.H., Henderson, S.B., Chen, Y., Randerson, J.T., Marlier, M., DeFries, R.S., Kinney, P., et al., 2015. Estimated Global Mortality Attributable to Smoke from Landscape Fires. University of British Columbia.
Jolleys, M.D., Coe, H., McFiggans, G., Capes, G., Allan, J.D., Crosier, J., Williams, P.I., et al., 2012. Characterizing the aging of biomass burning organic aerosol by use of mixing ratios: a meta-analysis of four regions. Environ. Sci. Technol. 46 (24), 13093–13102.
Jordan, T.B., Seen, A.J., Jacobsen, G.E., 2006. Levoglucosan as an atmospheric tracer for woodsmoke. Atmos. Environ. 40 (27), 5316–5321.
Justice, C.O., Giglio, L., Korontzi, S., Owens, J., Morisette, J.T., Roy, D., Descloitres, J., et al., 2002. The MODIS fire products. Remote Sens. Environ. 83 (1), 244–262.
Justice, C., Giglio, L., Boschetti, L., Roy, D., Csiszar, I., Morisette, J., Kaufman, Y., 2006. MODIS Fire Products Algorithm Technical Background Document. MODIS Science Team.
Kahn, R.A., Li, W.H., Moroney, C., Diner, D.J., Martonchik, J.V., Fishbein, E., 2007. Aerosol source plume physical characteristics from space-based multiangle imaging. J. Geophys. Res. Atmos. (D11) http://dx.doi.org/10.1029/2006JD007647.
Kanakidou, M., Seinfeld, J.H., Pandis, S.N., Barnes, I., Dentener, F.J., Facchini, M.C., Dingenen, R.V., et al., 2005. Organic aerosol and global climate modelling: a review. Atmos. Chem. Phys. 5 (4), 1053–1123.
Kaskaoutis, D.G., Kharol, S.K., Sifakis, N., Nastos, P.T., Sharma, A.R., Badarinath, K., Kambezidis, H.D., 2011. Satellite monitoring of the biomass-burning aerosols during the wildfires of August 2007 in Greece: climate implications. Atmos. Environ. 45 (3), 716–726.
Kaskaoutis, D.G., Gautam, R., Singh, R.P., Houssos, E.E., Goto, D., Singh, S., Bartzokas, A., et al., 2012. Influence of anomalous dry conditions on aerosols over India: transport, distribution and properties. J. Geophys. Res. Atmos. (D9) http://dx.doi.org/10.1029/2011JD017314.
Kaskaoutis, D.G., Kumar, S., Sharma, D., Singh, R.P., Kharol, S.K., Sharma, M., Singh, A.K., et al., 2014. Effects of crop residue burning on aerosol properties, plume characteristics, and long-range transport over northern India. J. Geophys. Res. Atmos. 9:5424–5444. http://dx.doi.org/10.1034/j.1600-0560.2003.00064.x.
Kaul, D.S., Gupta, T., Tripathi, S.N., Tare, V., Collett Jr., J.L., 2011. Secondary organic aerosol: a comparison between foggy and nonfoggy days. Environ. Sci. Technol. 45 (17), 7307–7313.
Kawamura, K., Bikkina, S., 2016. A review of dicarboxylic acids and related compounds in atmospheric aerosols: molecular distributions, sources and transformation. Atmos. Res. 170, 140–160.
Khlystov, A., Stanier, C., Pandis, S.N., 2004. An algorithm for combining electrical mobility and aerodynamic size distributions data when measuring ambient aerosol special issue of aerosol science and technology on findings from the fine particulate matter supersites program. Aerosol Sci. Technol. 38 (1), 229–238.
Kim, K., Jahan, S.A., Kabir, E., Brown, R.J., 2013. A review of airborne polycyclic aromatic hydrocarbons (PAHs) and their human health effects. Environ. Int. 60, 71–80.
Kirchstetter, T.W., Novakov, T., Hobbs, P.V., 2004. Evidence that the spectral dependence of light absorption by aerosols is affected by organic carbon. J. Geophys. Res. Atmos. (D21) http://dx.doi.org/10.1029/2004JD004999.
Kleinman, L.I., Springston, S.R., Daum, P.H., Lee, Y., Nunnermacker, L.J., Senum, G.I., Wang, J., et al., 2008. The time evolution of aerosol composition over the Mexico City plateau. Atmos. Chem. Phys. 8 (6), 1559–1575.
Kong, F.H., Li, X.Z., Zhao, S.L., Yin, H.W., 2003. Research advance in forest restoration on the burned blanks. J. Forest Res. 180–184 (in Chinese).
Koppejan, J., Van Loo, S., 2012. The Handbook of Biomass Combustion and Co-firing. Routledge.
Koren, I., Kaufman, Y.J., Remer, L.A., Martins, J.V., 2004. Measurement of the effect of Amazon smoke on inhibition of cloud formation. Science 303 (5662), 1342–1345.
Kostenidou, E., Pathak, R.K., Pandis, S.N., 2007. An algorithm for the calculation of secondary organic aerosol density combining AMS and SMPS data. Aerosol Sci. Technol. 41 (11), 1002–1010.
Kroll, J.H., Seinfeld, J.H., 2008. Chemistry of secondary organic aerosol: formation and evolution of low-volatility organics in the atmosphere. Atmos. Environ. 42 (16), 3593–3624.
Kumar, R., Naja, M., Satheesh, S.K., Ojha, N., Joshi, H., Sarangi, T., Pant, P., et al., 2011. Influences of the springtime northern Indian biomass burning over the central Himalayas. J. Geophys. Res. Atmos. (D19) http://dx.doi.org/10.1029/2010JD015509.
Kumar, R., Naja, M., Pfister, G.G., Barth, M.C., Brasseur, G.P., 2013. Source attribution of carbon monoxide in India and surrounding regions during wintertime. J. Geophys. Res. Atmos. 118 (4):1981–1995. http://dx.doi.org/10.1002/jgrd.50134.
Kumar, K.R., Yin, Y., Sivakumar, V., Kang, N., Yu, X., Diao, Y., Adesina, A.J., et al., 2015. Aerosol climatology and discrimination of aerosol types retrieved from MODIS, MISR and OMI over Durban (29.88°S, 31.02°E), South Africa. Atmos. Environ. 117 (117), 9–18.
Lack, D.A., Langridge, J.M., Bahreini, R., Cappa, C.D., Middlebrook, A.M., Schwarz, J.P., 2012. Brown carbon and internal mixing in biomass burning particles. Proc. Natl. Acad. Sci. 109 (37), 14802–14807.
Lai, L.Y., Sequeira, 2001. Visibility degradation across Hong Kong: its components and their relative contributions. Atmos. Environ. 35 (34), 5861–5872.
Lambe, A.T., Chhabra, P.S., Onasch, T.B., Brune, W.H., Hunter, J.F., Kroll, J.H., Cummings, M.J., et al., 2015. Effect of oxidant concentration, exposure time, and seed particles on secondary organic aerosol chemical composition and yield. Atmos. Chem. Phys. 15 (6), 3063–3075.
Langenfelds, R.L., Francey, R.J., Pak, B.C., Steele, L.P., Lloyd, J., Trudinger, C.M., Allison, C.E., 2002. Interannual growth rate variations of atmospheric CO_2 and its δ13C, H_2, CH_4,

and CO between 1992 and 1999 linked to biomass burning. Glob. Biogeochem. Cycles 16(3).
Lanki, T., Ahokas, A., Alm, S., Janssen, N.A.H., Hoek, G., Hartog, J.J.D., Brunekreef, B., et al., 2007. Determinants of personal and indoor $PM_{2.5}$ and absorbance among elderly subjects with coronary heart disease. J. Expo. Sci. Environ. Epidemiol. 17(2).
Lanz, V.A., Alfarra, M.R., Baltensperger, U., Buchmann, B., Hueglin, C., Prévôt, A., 2007. Source apportionment of submicron organic aerosols at an urban site by factor analytical modelling of aerosol mass spectra. Atmos. Chem. Phys. 7 (6), 1503–1522.
Laumbach, R.J., Kipen, H.M., 2012. Respiratory health effects of air pollution: update on biomass smoke and traffic pollution. J. Allergy Clin. Immunol. 129 (1), 3–11.
Lawrence, M.G., Lelieveld, J., 2010. Atmospheric pollutant outflow from southern Asia: a review. Atmos. Chem. Phys. 10 (22), 11017–11096.
Lee, S., Kim, H.K., Yan, B., Cobb, C.E., Hennigan, C., Nichols, S., Chamber, M., et al., 2008. Diagnosis of aged prescribed burning plumes impacting an urban area. Environ. Sci. Technol. 42 (5), 1438–1444.
Lee, S.S., Feingold, G., McComiskey, A., Yamaguchi, T., Koren, I., Vanderlei Martins, J., Yu, H., 2014a. Effect of gradients in biomass burning aerosol on shallow cumulus convective circulations. J. Geophys. Res. Atmos. 16:9948–9964. http://dx.doi.org/10.1002/2014JD021819.
Lee, D., Sud, Y.C., Oreopoulos, L., Kim, K., Lau, W.K., Kang, I., 2014b. Modeling the influences of aerosols on pre-monsoon circulation and rainfall over Southeast Asia. Atmos. Chem. Phys. 14 (13), 6853–6866.
Leiter, J., Shimkin, M., Shear, M., 1942. Production of subcutaneous sarcomas in mice with tars extracted from atmospheric dusts. J. Natl. Cancer Inst. 3 (2), 155–165.
Levin, E.J.T., McMeeking, G.R., Carrico, C.M., Mack, L.E., Kreidenweis, S.M., Wold, C.E., Moosmüller, H., et al., 2010. Biomass burning smoke aerosol properties measured during Fire Laboratory at Missoula Experiments (FLAME). J. Geophys. Res. 115 (D18). http://dx.doi.org/10.1029/2009JD013601.
Levy, J.I., Diez, D., Dou, Y., Barr, C.D., Dominici, F., 2012. A meta-analysis and multisite time-series analysis of the differential toxicity of major fine particulate matter constituents. Am. J. Epidemiol. 175 (11), 1091–1099.
Levy, R.C., Mattoo, S., Munchak, L.A., Remer, L.A., Sayer, A.M., Patadia, F., Hsu, N.C., 2013. The collection 6 MODIS aerosol products over land and ocean. Atmos. Meas. Tech. 6 (11), 2989–3034.
Lewis, K.A., Arnott, W.P., Moosmuller, H., Chakrabarty, R.K., Carrico, C.M., Kreidenweis, S.M., Day, D.E., et al., 2009. Reduction in biomass burning aerosol light absorption upon humidification: roles of inorganically-induced hygroscopicity, particle collapse, and photoacoustic heat and mass transfer. Atmos. Chem. Phys. 9, 8949–8966.
Li, W., Shao, L., 2009. Transmission electron microscopy study of aerosol particles from the brown hazes in northern China. J. Geophys. Res. Atmos. 114 (D9). http://dx.doi.org/10.1029/2008JD011285.
Li, W., Shao, L., 2010. Mixing and water-soluble characteristics of particulate organic compounds in individual urban aerosol particles. J. Geophys. Res. Atmos. 115 (D2). http://dx.doi.org/10.1029/2009JD012575.
Li, N., Sioutas, C., Cho, A., Schmitz, D., Misra, C., Sempf, J., Wang, M., et al., 2002. Ultrafine particulate pollutants induce oxidative stress and mitochondrial damage. Environ. Health Perspect. 111 (4), 455–460.
Li, J., Pósfai, M., Hobbs, P.V., Buseck, P.R., 2003. Individual aerosol particles from biomass burning in southern Africa: Compositions and aging of inorganic particles. J. Geophys. Res. Atmos. 108 (D13). http://dx.doi.org/10.1029/2002JD002310.
Li, D., Fan, S., He, A., Yin, F., 2004. Forest resources and environment in China. J. For. Res.-Jpn 9 (4), 307–312.
Li, X., Wang, S., Duan, L., Hao, J., Li, C., Chen, Y., Yang, L., 2007. Particulate and trace gas emissions from open burning of wheat straw and corn stover in China. Environ. Sci. Technol. 41 (17), 6052–6058.
Li, L., Wang, Y., Zhang, Q., Li, J., Yang, X., Jin, J., 2008. Wheat straw burning and its associated impacts on Beijing air quality. Sci. China Ser. D Earth Sci. 51 (3), 403–414.
Li, H., Han, Z., Cheng, T., Du, H., Kong, L., Chen, J., Zhang, R., et al., 2010a. Agricultural fire impacts on the air quality of shanghai during summer harvesttime. Aerosol Air Qual. Res. 10 (2), 95–101.
Li, W.J., Shao, L.Y., Buseck, P.R., 2010b. Haze types in Beijing and the influence of agricultural biomass burning. Atmos. Chem. Phys. 10 (17), 8119–8130.
Li, W.J., Zhang, D.Z., Shao, L.Y., Zhou, S.Z., Wang, W.X., 2011a. Individual particle analysis of aerosols collected under haze and non-haze conditions at a high-elevation mountain site in the North China plain. Atmos. Chem. Phys. 11 (22), 11733–11744.
Li, X., Li, P., Yan, L., Chen, J., Cheng, T., Xu, S., 2011b. Characterization of polycyclic aromatic hydrocarbons in fog-rain events. J. Environ. Monit. 13 (11), 2988–2993.
Li, J., Song, Y., Mao, Y., Mao, Z., Wu, Y., Li, M., Huang, X., et al., 2014a. Chemical characteristics and source apportionment of $PM_{2.5}$ during the harvest season in eastern China's agricultural regions. Atmos. Environ. 92, 442–448.
Li, L., Chen, Y., Zeng, L., Shao, M., Xie, S., Chen, W., Lu, S., et al., 2014b. Biomass burning contribution to ambient volatile organic compounds (VOCs) in the Chengdu-Chongqing Region (CCR). Atmos. Environ. 99, 403–410.
Li, C., Ma, Z., Chen, J., Wang, X., Ye, X., Wang, L., Yang, X., et al., 2015. Evolution of biomass burning smoke particles in the dark. Atmos. Environ. 244-252.
Li, C., Hu, Y., Zhang, F., Chen, J., Ma, Z., Ye, X., Yang, X., et al., 2016a. Multi-pollutants emissions from the burning of major agricultural residues in China and the related health-economic effect assessment. Atmos. Chem. Phys. Discuss. http://dx.doi.org/10.5194/acp-2016-651.
Li, C., Hu, Y., Chen, J., Ma, Z., Ye, X., Yang, X., Wang, L., et al., 2016b. Physiochemical properties of carbonaceous aerosol from agricultural residue burning: density, volatility, and hygroscopicity. Atmos. Environ. 140, 94–105.
Li, X., Chen, M., Le, H.P., Wang, F., Guo, Z., Iinuma, Y., Chen, J., et al., 2016c. Atmospheric outflow of $PM_{2.5}$ saccharides from megacity Shanghai to East China Sea: impact of biological and biomass burning sources. Atmos. Environ. 143, 1–14.
Li, X., Yang, Y., Xu, X., Xu, C., Hong, J., 2016d. Air pollution from polycyclic aromatic hydrocarbons generated by human activities and their health effects in China. J. Clean. Prod. 116, 1360–1367.
Lin, P., Engling, G., Yu, J.Z., 2010. Humic-like substances in fresh emissions of rice straw burning and in ambient aerosols in the Pearl River Delta Region, China. Atmos. Chem. Phys. 10 (14), 6487–6500.
Lin, Y.C., Lin, C.Y., Lin, P.H., Engling, G., Lin, Y.C., Lan, Y.Y., Chang, C.W.J., et al., 2013. Influence of Southeast Asian biomass burning on ozone and carbon monoxide over subtropical Taiwan. Atmos. Environ. 64 (1), 358–365.
Lin, Y., Ma, Y., Qiu, X., Li, R., Fang, Y., Wang, J., Zhu, Y., et al., 2015a. Sources, transformation, and health implications of PAHs and their nitrated, hydroxylated, and oxygenated derivatives in $PM_{2.5}$ in Beijing. J. Geophys. Res. Atmos. 120 (14):7219–7228. http://dx.doi.org/10.1002/2015JD023628.
Lin, Y., Qiu, X., Ma, Y., Ma, J., Zheng, M., Shao, M., 2015b. Concentrations and spatial distribution of polycyclic aromatic hydrocarbons (PAHs) and nitrated PAHs (NPAHs) in the atmosphere of North China, and the transformation from PAHs to NPAHs. Environ. Pollut. 196, 164–170.
Liu, Y., 2005. Atmospheric response and feedback to radiative forcing from biomass burning in tropical South America. Agric. For. Meteorol. 133 (1), 40–53.
Liu, H., Chang, W.L., Oltmans, S.J., Chan, L.Y., Harris, J.M., 1999. On springtime high ozone events in the lower troposphere from Southeast Asian biomass burning. Atmos. Environ. 33 (15), 2403–2410.
Liu, J., Drummond, J.R., Jones, D., Cao, Z., Bremer, H., Kar, J., Zou, J., et al., 2006. Large horizontal gradients in atmospheric CO at the synoptic scale as seen by spaceborne Measurements of Pollution in the Troposphere. J. Geophys. Res. Atmos. 111 (D2). http://dx.doi.org/10.1029/2005JD006076.
Liu, Y., Shao, M., Fu, L., Lu, S., Zeng, L., Tang, D., 2008. Source profiles of volatile organic compounds (VOCs) measured in China: part I. Atmos. Environ. 42 (25), 6247–6260.
Liu, Z., Wang, Y., Gu, D., Zhao, C., Huey, L.G., Stickel, R., Liao, J., et al., 2012. Summertime photochemistry during CAREBeijing-2007: RO_x budgets and O_3 formation. Atmos. Chem. Phys. 12 (16), 7737–7752.
Liu, D., Li, J., Zhang, Y., Xu, Y., Liu, X., Ding, P., Shen, C., et al., 2013. The use of levoglucosan and radiocarbon for source apportionment of $PM_{2.5}$ carbonaceous aerosols at a background site in East China. Environ. Sci. Technol. 47 (18), 10454–10461.
Liu, S., Aiken, A.C., Arata, C., Dubey, M.K., Stockwell, C.E., Yokelson, R.J., Stone, E.A., et al., 2014. Aerosol single scattering albedo dependence on biomass combustion efficiency: laboratory and field studies. Geophys. Res. Lett. 41 (2):742–748. http://dx.doi.org/10.1002/2013GL058392.
Liu, Z., Wang, Y., Hu, B., Ji, D., Zhang, J., Wu, F., Wan, X., et al., 2016. Source appointment of fine particle number and volume concentration during severe haze pollution in Beijing in January 2013. Environ. Sci. Pollut. R. 23 (7), 6845–6860.
Lu, Z., Zhang, Q., Streets, D.G., 2011. Sulfur dioxide and primary carbonaceous aerosol emissions in China and India, 1996-2010. Atmos. Chem. Phys. 11 (18), 9839–9864.
Lyu, X.P., Chen, N., Guo, H., Zeng, L.W., Zhang, W.H., Shen, F., Quan, J.H., et al., 2016. Chemical characteristics and causes of airborne particulate pollution in warm seasons in Wuhan, central China. Atmos. Chem. Phys. 16, 10671–10687.
Martins, J.V., Artaxo, P., Hobbs, P.V., Liousse, C., Cachier, H., Kaufman, Y., Plana-Fattori, A., 1996. Particle Size Distributions, Elemental Compositions, Carbon Measurements, and Optical Properties of Smoke from Biomass Burning in the Pacific Northwest of the United States, Biomass Burning and Global Change. pp. 716–732.
Martins, J.A., Gonçalves, F.L.T., Morales, C.A., Fisch, G.F., Pinheiro, F.G.M., Leal Júnior, J.B.V., Oliveira, C.J., et al., 2009. Cloud condensation nuclei from biomass burning during the Amazonian dry-to-wet transition season. Meteorog. Atmos. Phys. 104 (1–2), 83–93.
Matson, M., Dozier, J., 1981. Identification of subresolution high temperature sources using a thermal IR sensor. Photogramm. Eng. Remote. Sens. 47 (9), 1311–1318.
Mauzerall, D.L., Logan, J.A., Jacob, D.J., Anderson, B.E., Blake, D.R., Bradshaw, J.D., Heikes, B., et al., 1998. Photochemistry in biomass burning plumes and implications for tropospheric ozone over the tropical South Atlantic. J. Geophys. Res. Atmos. 103 (D7), 8401–8423.
May, A.A., Lee, T., McMeeking, G.R., Akagi, S., Sullivan, A.P., Urbanski, S., Yokelson, R.J., et al., 2015. Observations and analysis of organic aerosol evolution in some prescribed fire smoke plumes. Atmos. Chem. Phys. 15 (11), 6323–6335.
McDonald, J.D., Zielinska, B., Fujita, E.M., Sagebiel, J.C., Chow, J.C., Watson, J.G., 2000. Fine particle and gaseous emission rates from residential wood combustion. Environ. Sci. Technol. 34 (11), 2080–2091.
Mcintire, T.M., Ryder, O.S., Gassman, P.L., Zhu, Z., Ghosal, S., Finlayson-Pitts, B.J., 2010. Why ozonolysis may not increase the hydrophilicity of particles. Atmos. Environ. 44 (7), 939–944.
McMeeking, G.R., Kreidenweis, S.M., Baker, S., Carrico, C.M., Chow, J.C., Collett, J.L., Hao, W.M., et al., 2009. Emissions of trace gases and aerosols during the open combustion of biomass in the laboratory. J. Geophys. Res. Atmos. 114 (D19). http://dx.doi.org/10.1029/2009JD011836.
Mellouki, A., Wallington, T.J., Chen, J., 2015. Atmospheric chemistry of oxygenated volatile organic compounds: impacts on air quality and climate. Chem. Rev. 115 (10), 3984–4014.
Meng, Z.Y., Xu, X.B., Yan, P., Ding, G.A., Tang, J., Lin, W.L., Xu, X.D., et al., 2009. Characteristics of trace gaseous pollutants at a regional background station in northern China. Atmos. Chem. Phys. 9 (3), 927–936.
Menon, S., Hansen, J., Nazarenko, L., Luo, Y., 2002. Climate effects of black carbon aerosols in China and India. Science 297 (5590), 2250–2253.
Mielonen, T., Aaltonen, V., Lihavainen, H., Hyvärinen, A., Arola, A., Komppula, M., Kivi, R., 2013. Biomass burning aerosols observed in northern Finland during the 2010 wildfires in Russia. Atmosphere-Basel 4 (1), 17–34.
Moffet, R.C., Henn, T.R., Tivanski, A.V., Hopkins, R.J., Desyaterik, Y., Kilcoyne, A., Tyliszczak, T., et al., 2010. Microscopic characterization of carbonaceous aerosol particle aging in the outflow from Mexico City. Atmos. Chem. Phys. 10 (3), 961–976.

Mohr, C., Huffman, J.A., Cubison, M.J., Aiken, A.C., Docherty, K.S., Kimmel, J.R., Ulbrich, I.M., et al., 2009. Characterization of primary organic aerosol emissions from meat cooking, trash burning, and motor vehicles with high-resolution aerosol mass spectrometry and comparison with ambient and chamber observations. Environ. Sci. Technol. 43 (7), 2443–2449.

Morawska, L., Chen, J., Jayaratne, R., Ye, X., Li, C., 2016. Spatial and Temporal Variation of Airborne Particle Concentration in the Yangtze River Basin.

Mumtaz, M.M., George, J.D., 1995. Toxicological profile for polycyclic aromatic hydrocarbons. Polycyclic Compounds.

Mustard, J.F., Murchie, S.L., Pelkey, S.M., Ehlmann, B.L., Milliken, R.E., Grant, J.A., Bibring, J.P., et al., 2008. Hydrated silicate minerals on Mars observed by the Mars reconnaissance orbiter CRISM instrument. Nature 454 (7202), 305–309.

NBSC (National Bureau of Statistic of China), 2004–2014. China Statistical Yearbook, 480 2003–2013. China Statistics Press, Beijing (in Chinese).

Nel, A., 2005. Air pollution-related illness: effects of particles. Science 308, 804–806.

Ni, H., Han, Y., Cao, J., Chen, L.W.A., Tian, J., Wang, X., Chow, J.C., et al., 2015. Emission characteristics of carbonaceous particles and trace gases from open burning of crop residues in China. Atmos. Environ. 123, 399–406.

Nie, W., Ding, A.J., Xie, Y.N., Xu, Z., Mao, H., Kerminen, V., Zheng, L.F., et al., 2015. Influence of biomass burning plumes on HONO chemistry in eastern China. Atmos. Chem. Phys. 15 (3), 1147–1159.

Niemi, J.V., Saarikoski, S., Tervahattu, H., Mäkelä, T., Hillamo, R., Vehkamäki, H., Sogacheva, L., et al., 2006. Changes in background aerosol composition in Finland during polluted and clean periods studied by TEM/EDX individual particle analysis. Atmos. Chem. Phys. 6 (12), 5049–5066.

Nussbaumer, T., 2003. Combustion and Co-combustion of biomass: fundamentals, technologies, and primary measures for emission reduction. Energy Fuel 17 (6), 1510–1521.

Ohara, T., Akimoto, H., Kurokawa, J., Horii, N., Yamaji, K., Yan, X., Hayasaka, T., 2007. An Asian emission inventory of anthropogenic emission sources for the period 1980–2020. Atmos. Chem. Phys. 7 (16), 4419–4444.

Okada, K., Ikegami, M., Zaizen, Y., Makino, Y., Jensen, J.B., Gras, J.L., 2001. The mixture state of individual aerosol particles in the 1997 Indonesian haze episode. J. Aerosol Sci. 32 (11), 1269–1279.

Omar, A.H., Winker, D.M., Vaughan, M.A., Hu, Y., Trepte, C.R., Ferrare, R.A., Lee, K., et al., 2009. The CALIPSO automated aerosol classification and lidar ratio selection algorithm. J. Atmos. Ocean. Technol. 26 (10), 1994–2014.

Ortega, A.M., Day, D.A., Cubison, M.J., Brune, W.H., Bon, D., de Gouw, J.A., Jimenez, J.L., 2013. Secondary organic aerosol formation and primary organic aerosol oxidation from biomass-burning smoke in a flow reactor during FLAME-3. Atmos. Chem. Phys. 13 (22), 11551–11571.

Ostro, B., Lipsett, M., Reynolds, P., Goldberg, D., Hertz, A., Garcia, C., Henderson, K.D., Bernstein, L., 2010. Long-term exposure to constituents of fine particulate air pollution and mortality: results from the California Teachers Study. Environ. Health Perspect. 118 (3), 363–369.

Ouyang, B., Popoola, L., Jones, R., Li, C., Chen, J., 2016. Portable and low-cost sensors in monitoring air qualities in China. EGU General Assembly Conference Abstracts. 16213.

Paatero, P., Tapper, U., 1994. Positive matrix factorization: a non-negative factor model with optimal utilization of error estimates of data values. Environmetrics 5 (2): 111–126. http://dx.doi.org/10.1002/env.3170050203.

Parikka, M., 2004. Global biomass fuel resources. Biomass Bioenergy 27 (6), 613–620.

Parrington, M., Palmer, P.I., Lewis, A.C., Lee, J.D., Rickard, A.R., Carlo, P.D., Taylor, J.W., et al., 2013. Ozone photochemistry in boreal biomass burning plumes. Atmos. Chem. Phys. 13 (15), 7321–7341.

Pathak, B., Bhuyan, P.K., Gogoi, M., Bhuyan, K., 2012. Seasonal heterogeneity in aerosol types over Dibrugarh-North-Eastern India. Atmos. Environ. 47, 307–315.

Peng, J., Hu, M., Guo, S., Du, Z., Zheng, J., Shang, D., Zamora, M.L., et al., 2016. Markedly enhanced absorption and direct radiative forcing of black carbon under polluted urban environments. Proc. Natl. Acad. Sci. U. S. A. 113 (16), 4266–4271.

Penner, J.E., Dickinson, R.E., O'Neill, C.A., 1992. Effects of aerosol from biomass burning on the global radiation budget. Science 256 (5062), 1432–1434.

Penner, J.E., Chuang, C.C., Grant, K., 1998. Climate forcing by carbonaceous and sulfate aerosols. Clim. Dyn. 14 (12), 839–851.

Perez-Padilla, R., Schilmann, A., Riojas-Rodriguez, H., 2010. Respiratory health effects of indoor air pollution. Int. J. Tuberc. Lung Dis. 14 (9), 1079–1086.

Petters, M.D., Kreidenweis, S.M., 2007. A single parameter representation of hygroscopic growth and cloud condensation nucleus activity. Atmos. Chem. Phys. 7 (8), 1961–1971.

Petters, M.D., Kreidenweis, S.M., 2013. A single parameter representation of hygroscopic growth and cloud condensation nucleus activity-part 3: including surfactant partitioning. Atmos. Chem. Phys. 13 (2), 1081–1091.

Petters, M.D., Carrico, C.M., Kreidenweis, S.M., Prenni, A.J., DeMott, P.J., Collett, J.L., Moosmueller, H., 2009. Cloud condensation nucleation activity of biomass burning aerosol. J. Geophys. Res. Atmos. 114 (D22) (1984–2012). 10.1029/2009JD012353.

Pierce, J.R., Adams, 2007. Efficiency of cloud condensation nuclei formation from ultrafine particles. Atmos. Chem. Phys. 7 (5), 1367–1379.

Pitz, M., Cyrys, J., Karg, E., Wiedensohler, A., Wichmann, H., Heinrich, J., 2003. Variability of apparent particle density of an urban aerosol. Environ. Sci. Technol. 37 (19), 4336–4342.

Pokhrel, R.P., Wagner, N.L., Langridge, J.M., Lack, D.A., Jayarathne, T., Stone, E.A., Stockwell, C.E., et al., 2016. Parameterization of single scattering albedo (SSA) and absorption angstrom exponent (AAE) with EC/OC for aerosol emissions from biomass burning. Atmos. Chem. Phys. 16, 9549–9561.

Pope III, C.A., Dockery, D.W., 2006. Health effects of fine particulate air pollution: lines that connect. J. Air Waste Manage. Assoc. 56 (6), 709–742.

Pope III, C.A., Burnett, R.T., Thun, M.J., Calle, E.E., Krewski, D., Ito, K., Thurston, G.D., 2002. Lung cancer, cardiopulmonary mortality, and long-term exposure to fine particulate air pollution. JAMA 287 (9), 1132–1141.

Popovicheva, O.B., Kozlov, V.S., Rakhimov, R.F., Shmargunov, V.P., Kireeva, E.D., Persiantseva, N.M., Timofeev, M.A., et al., 2016. Optical-microphysical and physical-chemical characteristics of Siberian biomass burning: small-scale fires in an aerosol chamber. Atmos. Oceanic Opt. 29 (4), 323–331.

Pósfai, M., Simonics, R., Li, J., Hobbs, P.V., Buseck, P.R., 2003. Individual aerosol particles from biomass burning in southern Africa: 1. Compositions and size distributions of carbonaceous particles. J. Geophys. Res. Atmos. 108 (D13). http://dx.doi.org/10.1029/2002JD002291.

Pósfai, M., Gelencsér, A., Simonics, R., Arató, K., Li, J., Hobbs, P.V., Buseck, P.R., 2004. Atmospheric tar balls: particles from biomass and biofuel burning. J. Geophys. Res. Atmos. 109 (D6). http://dx.doi.org/10.1029/2003JD004169.

Pratt, K.A., Prather, K.A., 2009. Real-time, single-particle volatility, size, and chemical composition measurements of aged urban aerosols. Environ. Sci. Technol. 43 (21), 8276–8282.

Prins, E.M., Feltz, J.M., Menzel, W.P., Ward, D.E., 1998. An overview of GOES-8 diurnal fire and smoke results for SCAR-B and 1995 fire season in South America. J. Geophys. Res. Atmos. 103 (D24):31821–31835. http://dx.doi.org/10.1029/98JD01720.

Qin, Y., Xie, S.D., 2011. Historical estimation of carbonaceous aerosol emissions from biomass open burning in China for the period 1990–2005. Environ. Pollut. 159 (12), 3316–3323.

Qin, Y., Xie, S.D., 2012. Spatial and temporal variation of anthropogenic black carbon emissions in China for the period 1980–2009. Atmos. Chem. Phys. 12 (11), 4825–4841.

Qin, X., Yan, H., Zhan, Z., Li, Z., 2014. Characterising vegetative biomass burning in China using MODIS data. Int. J. Wildland Fire 23 (1), 69–77.

Raaschou-Nielsen, O., Sørensen, M., Hertel, O., Bo, L.K.C., Vissing, N., Bønnelykke, K., Bisgaard, H., 2011. Predictors of indoor fine particulate matter in infants' bedrooms in Denmark. Environ. Res. 111, 87–93.

Ramana, M.V., Ramanathan, V., Feng, Y., Yoon, S.C., Kim, S.W., Carmichael, G.R., Schauer, J.J., 2010. Warming influenced by the ratio of black carbon to sulphate and the black-carbon source. Nat. Geosci. 3 (8), 542–545.

Ramanathan, V., Carmichael, G., 2008. Global and regional climate changes due to black carbon. Nat. Geosci. 1 (4), 221–227.

Ramanathan, V., Crutzen, P.J., Kiehl, J.T., Rosenfeld, D., 2001. Aerosols, climate, and the hydrological cycle. Science 294 (5549), 2119–2124.

Ramanathan, V., Chung, C., Kim, D., Bettge, T., Buja, L., Kiehl, J.T., Washington, W.M., et al., 2005. Atmospheric brown clouds: impacts on South Asian climate and hydrological cycle. Proc. Natl. Acad. Sci. U. S. A. 102 (15), 5326–5333.

Randerson, J.T., Liu, H., Flanner, M.G., Chambers, S.D., Jin, Y., Hess, P.G., Pfister, G., et al., 2006. The impact of boreal forest fire on climate warming. Science 314 (5802), 1130–1132.

Ravindra, K., Sokhi, R., Van Grieken, R., 2008. Atmospheric polycyclic aromatic hydrocarbons: source attribution, emission factors and regulation. Atmos. Environ. 42 (13), 2895–2921.

Real, E., Law, K.S., Weinzierl, B., Fiebig, M., Petzold, A., Wild, O., Methven, J., et al., 2007. Processes influencing ozone levels in Alaskan forest fire plumes during long-range transport over the North Atlantic. J. Geophys. Res. Atmos. 112 (D10). http://dx.doi.org/10.1029/2006JD007576.

Reid, J.S., Eck, T.F., Christopher, S.A., Koppmann, R., Dubovik, O., Eleuterio, D.P., Holben, B.N., et al., 2005a. A review of biomass burning emissions part III: intensive optical properties of biomass burning particles. Atmos. Chem. Phys. 5, 827–849.

Reid, J.S., Koppmann, R., Eck, T.F., Eleuterio, D.P., 2005b. A review of biomass burning emissions part II: intensive physical properties of biomass burning particles. Atmos. Chem. Phys. 3, 799–825.

Reinhardt, A., Emmenegger, C., Gerrits, B., Panse, C., Dommen, J., Baltensperger, U., Zenobi, R., et al., 2007. Ultrahigh mass resolution and accurate mass measurements as a tool to characterize oligomers in secondary organic aerosols. Anal. Chem. 79 (11), 4074–4082.

Rickards, A.M.J., Miles, R.E.H., Davies, J.F., Marshall, F.H., Reid, J.P., 2013. Measurements of the sensitivity of aerosol hygroscopicity and the κ parameter to the O/C ratio. J. Phys. Chem.: Atmos. 117 (51), 14120–14131.

Rissler, J., Nordin, E.Z., Eriksson, A.C., Nilsson, P.T., Frosch, M., Sporre, M.K., Wierzbicka, A., et al., 2014. Effective density and mixing state of aerosol particles in a near-traffic urban environment. Environ. Sci. Technol. 48 (11), 6300–6308.

Roberts, G.C., Artaxo, P., Zhou, J., Swietlicki, E., Andreae, M.O., 2002. Sensitivity of CCN spectra on chemical and physical properties of aerosol: A case study from the Amazon Basin. J. Geophys. Res. Atmos. 107 (D20). http://dx.doi.org/10.1029/2001JD000583.

Robinson, A.L., Rhodes, J.S., Keith, D.W., 2003. Assessment of potential carbon dioxide reductions due to biomass-coal cofiring in the United States. Environ. Sci. Technol. 37 (22), 5081–5089.

Robinson, A.L., Donahue, N.M., Shrivastava, M.K., Weitkamp, E.A., Sage, A.M., Grieshop, A.P., Lane, T.E., et al., 2007. Rethinking organic aerosols: semivolatile emissions and photochemical aging. Science 315 (5816), 1259–1262.

Robock, A., 1991. Surface cooling due to forest fire smoke. J. Geophys. Res. 96 (D11): 20869–20878, ID020435. http://dx.doi.org/10.1029/91JD02043.

Rollins, A.W., Browne, E.C., Min, K., Pusede, S.E., Wooldridge, P.J., Gentner, D.R., Goldstein, A.H., et al., 2012. Evidence for NOx control over nighttime SOA formation. Science 337 (6099), 1210–1212.

Rose, D., Nowak, A., Achtert, P., Wiedensohler, A., Hu, M., Shao, M., Zhang, Y., et al., 2010. Cloud condensation nuclei in polluted air and biomass burning smoke near the mega-city Guangzhou, China–part 1: size-resolved measurements and implications for the modeling of aerosol particle hygroscopicity and CCN activity. Atmos. Chem. Phys. 10 (7), 3365–3383.

Rose, D., Gunthe, S.S., Su, H., Garland, R.M., Yang, H., Berghof, M., Cheng, Y.F., et al., 2011. Cloud condensation nuclei in polluted air and biomass burning smoke near the mega-city Guangzhou, China-part 2: size-resolved aerosol chemical composition, diurnal cycles, and externally mixed weakly CCN-active soot particles. Atmos. Chem. Phys. 11 (6), 2817–2836.
Ross, A.B., Jones, J.M., Chaiklangmuang, S., Pourkashanian, M., Williams, A., Kubica, K., Andersson, J.T., et al., 2002. Measurement and prediction of the emission of pollutants from the combustion of coal and biomass in a fixed bed furnace. Fuel 81 (5), 571–582.
Russell, L.M., Maria, S.F., Myneni, S.C., 2002. Mapping organic coatings on atmospheric particles. Geophys. Res. Lett. 29 (16). http://dx.doi.org/10.1029/2002GL014874.
Sadezky, A., Muckenhuber, H., Grothe, H., Niessner, R., Pöschl, U., 2005. Raman microspectroscopy of soot and related carbonaceous materials: spectral analysis and structural information. Carbon 43 (8), 1731–1742.
Saffari, A., Daher, N., Samara, C., Voutsa, D., Kouras, A., Manoli, E., Karagkiozidou, O., et al., 2013. Increased biomass burning due to the economic crisis in Greece and its adverse impact on wintertime air quality in Thessaloniki. Environ. Sci. Technol. 47 (23), 13313–13320.
Saikawa, E., Naik, V., Horowitz, L.W., Liu, J., Mauzerall, D.L., 2009. Present and potential future contributions of sulfate, black and organic carbon aerosols from China to global air quality, premature mortality and radiative forcing. Atmos. Environ. 43 (17), 2814–2822.
Sakaeda, N., Wood, R., Rasch, P.J., 2011. Direct and semidirect aerosol effects of southern African biomass burning aerosol. J. Geophys. Res. Atmos. 116 (D12). http://dx.doi.org/10.1029/2010JD015540.
Saleh, R., Robinson, E.S., Tkacik, D.S., Ahern, A.T., Liu, S., Aiken, A.C., Sullivan, R.C., et al., 2014. Brownness of organics in aerosols from biomass burning linked to their black carbon content. Nat. Geosci. 7 (9), 647–650.
Sang, X.F., Chan, C.Y., Engling, G., Chan, L.Y., Wang, X.M., Zhang, Y.N., Shi, S., et al., 2011. Levoglucosan enhancement in ambient aerosol during springtime transport events of biomass burning smoke to Southeast China. Tellus B 63 (1), 129–139.
Schauer, J.J., Kleeman, M.J., Cass, G.R., Simoneit, B.R., 1999. Measurement of emissions from air pollution sources. 1. C1 through C29 organic compounds from meat charbroiling. Environ. Sci. Technol. 33 (10), 1566–1577.
Schkolnik, G., Chand, D., Hoffer, A., Andreae, M.O., Erlick, C., Swietlicki, E., Rudich, Y., 2007. Constraining the density and complex refractive index of elemental and organic carbon in biomass burning aerosol using optical and chemical measurements. Atmos. Environ. 41 (5), 1107–1118.
Schmid, O., Karg, E., Hagen, D.E., Whitefield, P.D., Ferron, G.A., 2007. On the effective density of non-spherical particles as derived from combined measurements of aerodynamic and mobility equivalent size. J. Aerosol Sci. 38 (4), 431–443.
Schmid, O., Chand, D., Karg, E., Guyon, P., Frank, G.P., Swietlicki, E., Andreae, M.O., 2009. Derivation of the density and refractive index of organic matter and elemental carbon from closure between physical and chemical aerosol properties. Environ. Sci. Technol. 43 (4), 1166–1172.
Seaton, A., Godden, D., Macnee, W., Donaldson, K., 1995. Particulate air pollution and acute health effects. Lancet 345 (8943), 176–178.
Seinfeld, J.H., Pandis, S.N., 2012. Atmospheric Chemistry and Physics: From Air Pollution to Climate Change. John Wiley & Sons.
Seinfeld, J.H., Pankow, J.F., 2003. Organic atmospheric particulate material. Annu. Rev. Phys. Chem. 54 (1), 121–140.
Seinfeld, J.H., Pandis, S.N., Seinfeld, J.H., Pandis, S.N., 2008. Atmospheric chemistry and physics: from air pollution to climate change. Phys. Today 51 (2), 212–214.
Semeniuk, T.A., Wise, M.E., Martin, S.T., Russell, L.M., Buseck, P.R., 2007. Hygroscopic behavior of aerosol particles from biomass fires using environmental transmission electron microscopy. J. Atmos. Chem. 56 (3), 259–273.
Shao, J.Z., 2000. The destruction of the forest fire to ecosystem and ecological fireproofing countermeasures. Fire Prev Prod Inform 21–22 in Chinese.
Shen, G., Yang, Y., Wang, W., Tao, S., Zhu, C., Min, Y., Xue, M., et al., 2010. Emission factors of particulate matter and elemental carbon for crop residues and coals burned in typical household stoves in China. Environ. Sci. Technol. 44 (18), 7157–7162.
Shen, G., Tao, S., Chen, Y., Zhang, Y., Wei, S., Xue, M., Wang, B., et al., 2013. Emission characteristics for polycyclic aromatic hydrocarbons from solid fuels burned in domestic stoves in rural China. Environ. Sci. Technol. 47 (24), 14485–14494.
Shi, Y., Yamaguchi, Y., 2014. A high-resolution and multi-year emissions inventory for biomass burning in Southeast Asia during 2001–2010. Atmos. Environ. 98 (98), 8–16.
Shih, S.I., Lee, W.J., Lin, L.F., Huang, J.Y., Su, J.W., Chang-Chien, G.P., 2008. Significance of biomass open burning on the levels of polychlorinated dibenzo-p-dioxins and dibenzofurans in the ambient air. J. Hazard. Mater. 153 (1–2), 276–284.
Shindell, D., Kuylenstierna, J.C., Vignati, E., van Dingenen, R., Amann, M., Klimont, Z., Anenberg, S.C., et al., 2012. Simultaneously mitigating near-term climate change and improving human health and food security. Science 335 (6065), 183–189.
Shrivastava, M.K., Lipsky, E.M., Stanier, C.O., Robinson, A.L., 2006. Modeling semivolatile organic aerosol mass emissions from combustion systems. Environ. Sci. Technol. 40 (8), 2671–2677.
Simoneit, B.R., 2002. Biomass burning-a review of organic tracers for smoke from incomplete combustion. Appl. Geochem. 17 (3), 129–162.
Simoneit, B.R., Schauer, J.J., Nolte, C.G., Oros, D.R., Elias, V.O., Fraser, M.P., Rogge, W.F., et al., 1999. Levoglucosan, a tracer for cellulose in biomass burning and atmospheric particles. Atmos. Environ. 33 (2), 173–182.
Smith, K.R., Mehta, S., Maeusezahl-Feuz, M., 2004. Indoor air pollution from household use of solid fuels. Comparative Quantification of Health Risks, pp. 1435–1493.
Song, Y., Zhang, Y., Xie, S., Zeng, L., Zheng, M., Salmon, L.G., Shao, M., et al., 2006. Source apportionment of $PM_{2.5}$ in Beijing by positive matrix factorization. Atmos. Environ. 40 (8), 1526–1537.
Song, Y., Tang, X., Xie, S., Zhang, Y., Wei, Y., Zhang, M., Zeng, L., et al., 2007. Source apportionment of $PM_{2.5}$ in Beijing in 2004. J. Hazard. Mater. 146 (1), 124–130.
Streets, D.G., Gupta, S., Waldhoff, S.T., Wang, M.Q., Bond, T.C., Yiyun, B., 2001. Black carbon emissions in China. Atmos. Environ. 35 (25), 4281–4296.
Streets, D.G., Yarber, K.F., Woo, J.H., Carmichael, G.R., 2003. Biomass burning in Asia: annual and seasonal estimates and atmospheric emissions. Glob. Biogeochem. Cycles J. 17 (4), 1759–1768.
Streets, D.G., Bond, T.C., Lee, T., Jang, C., 2004. On the future of carbonaceous aerosol emissions. J. Geophys. Res. Atmos. 109 (D24). http://dx.doi.org/10.1029/2004JD004902.
Streets, D.G., Yu, C., Wu, Y., Chin, M., Zhao, Z., Hayasaka, T., Shi, G., 2008. Aerosol trends over China, 1980–2000. Atmos. Res. 88 (2), 174–182.
Su, H., Rose, D., Cheng, Y.F., Gunthe, S.S., Massling, A., Stock, M., Wiedensohler, A., et al., 2010. Hygroscopicity distribution concept for measurement data analysis and modeling of aerosol particle mixing state with regard to hygroscopic growth and CCN activation. Atmos. Chem. Phys. 10 (15), 7489–7503.
Sun, Y., Wang, Z., Dong, H., Yang, T., Li, J., Pan, X., Chen, P., et al., 2012. Characterization of summer organic and inorganic aerosols in Beijing, China with an Aerosol Chemical Speciation Monitor. Atmos. Environ. 51, 250–259.
Sun, Y.L., Wang, Z.F., Fu, P.Q., Yang, T., Jiang, Q., Dong, H.B., Li, J., et al., 2013. Aerosol composition, sources and processes during wintertime in Beijing, China. Atmos. Chem. Phys. 13 (9), 4577–4592.
Sun, L., Xia, X., Wang, P., Zhang, R., Che, H., Deng, Z., Fei, Y., et al., 2015. Surface and column-integrated aerosol properties of heavy haze events in January 2013 over the North China Plain. Aerosol Air Qual. Res. 1514–1524.
Sun, J., Peng, H., Chen, J., Wang, X., Wei, M., Li, W., Yang, L., et al., 2016a. An estimation of CO_2 emission via agricultural crop residue open field burning in China from 1996 to 2013. J. Clean. Prod. 112, 2625–2631.
Sun, Y., Jiang, Q., Xu, Y., Ma, Y., Zhang, Y., Liu, X., Li, W., et al., 2016b. Aerosol characterization over the North China Plain: Haze life cycle and biomass burning impacts in summer. J. Geophys. Res. Atmos. 121 (5). http://dx.doi.org/10.1002/2015JD024261.
Tan, H., Liu, L., Fan, S., Li, F., Yin, Y., Cai, M., Chan, P.W., 2016. Aerosol optical properties and mixing state of black carbon in the Pearl River Delta, China. Atmos. Environ. 131, 196–208.
Tao, S., Li, B., Zhang, Y.X., Yuan, H., 2011. Emission of Polycyclic Aromatic Hydrocarbons in China. Biophysico-chemical Processes of Anthropogenic Organic Compounds in Environmental Systems. :pp. 267–281 http://dx.doi.org/10.1002/9780470944479.ch11.
Tao, J., Zhang, L., Engling, G., Zhang, R., Yang, Y., Cao, J., Zhu, C., et al., 2013. Chemical composition of $PM_{2.5}$ in an urban environment in Chengdu, China: importance of springtime dust storms and biomass burning. Atmos. Res. 122 (3), 270–283.
Tao, J., Gao, J., Zhang, L., Zhang, R., Che, H., Zhang, Z., Lin, Z., et al., 2014. $PM_{2.5}$ pollution in a megacity of southwest China: source apportionment and implication. Atmos. Chem. Phys. 14 (4), 8679–8699.
Tena, A.F., Clarà, P.C., 2012. Deposition of inhaled particles in the lungs. Arch. Bronconeumol. 48 (7), 240–246.
Thrane, K.E., Mikalsen, A., 1981. High-volume sampling of airborne polycyclic aromatic hydrocarbons using glass fibre filters and polyurethane foam. Atmos. Environ. 15 (6), 909–918.
Tian, F., Yu, J., Mckenzie, L., Hayashi, J., Chiba, T., Li, C., 2005. Formation of NO precursors during the pyrolysis of coal and biomass. Part VII. Pyrolysis and gasification of cane trash with steam. Fuel 84 (4), 371–376.
Tian, J., Chow, J.C., Cao, J., Han, Y., Ni, H., Chen, L.A., Wang, X., et al., 2015. A biomass combustion chamber: design, evaluation, and a case study of wheat straw combustion emission tests. Aerosol Air Qual. Res. 15 (5), 2104–2114.
Tian, S.L., Pan, Y.P., Wang, Y.S., 2016. Size-resolved source apportionment of particulate matter in urban Beijing during haze and non-haze episodes. Atmos. Chem. Phys. 16 (1), 1–19.
Tiitta, P., Miettinen, P., Vaattovaara, P., Joutsensaari, J., Petäjä, T., Virtanen, A., Raatikainen, T., et al., 2010. Roadside aerosol study using hygroscopic, organic and volatility TDMAs: characterization and mixing state. Atmos. Environ. 44 (7), 976–986.
Torres, O., Tanskanen, A., Veihelmann, B., Ahn, C., Braak, R., Bhartia, P.K., Veefkind, P., et al., 2007. Aerosols and surface UV products from Ozone Monitoring Instrument observations: an overview. J. Geophys. Res. Atmos. 112 (D24). http://dx.doi.org/10.1029/2007JD008809.
Torres, O., Ahn, C., Chen, Z., 2013. Improvements to the OMI near-UV aerosol algorithm using A-train CALIOP and AIRS observations. Atmos. Meas. Tech. 6 (11), 3257–3270.
Tosca, M.G., Randerson, J.T., Zender, C.S., 2013. Global impact of smoke aerosols from landscape fires on climate and the Hadley circulation. Atmos. Chem. Phys. 13 (10), 5227–5241.
Tritscher, T., Dommen, J., DeCarlo, P.F., Gysel, M., Barmet, P.B., Praplan, A.P., Weingartner, E., et al., 2011. Volatility and hygroscopicity of aging secondary organic aerosol in a smog chamber. Atmos. Chem. Phys. 11 (22), 11477–11496.
Turquety, S., Hurtmans, D., Hadji-Lazaro, J., Coheur, P., Clerbaux, C., Josset, D., Tsamalis, C., 2009. Tracking the emission and transport of pollution from wildfires using the IASI CO retrievals: analysis of the summer 2007 Greek fires. Atmos. Chem. Phys. 9 (14), 4897–4913.
Ulbrich, I.M., Canagaratna, M.R., Zhang, Q., Worsnop, D.R., Jimenez, J.L., 2009. Interpretation of organic components from positive matrix factorization of aerosol mass spectrometric data. Atmos. Chem. Phys. 9 (9), 2891–2918.
Vadrevu, K.P., Lasko, K., Giglio, L., Justice, C., 2015. Vegetation fires, absorbing aerosols and smoke plume characteristics in diverse biomass burning regions of Asia. Environ. Res. Lett. 10:105003. http://dx.doi.org/10.1088/1748-9326/10/10/105003.
Varutbangkul, V., Brechtel, F.J., Bahreini, R., Ng, N.L., Keywood, M.D., Kroll, J.H., Flagan, R.C., et al., 2006. Hygroscopicity of secondary organic aerosols formed by oxidation of cycloalkenes, monoterpenes, sesquiterpenes, and related compounds. Atmos. Chem. Phys. 6 (9), 2367–2388.
Vecchi, R., Bernardoni, V., Cricchio, D., D'Alessandro, A., Fermo, P., Lucarelli, F., Nava, S., et al., 2008. The impact of fireworks on airborne particles. Atmos. Environ. 42 (6), 1121–1132.

Vendrasco, E.P., Dias, P.S., Freitas, E.D., 2009. A case study of the direct radiative effect of biomass burning aerosols on precipitation in the Eastern Amazon. Atmos. Res. 94 (3), 409–421.
Victor, D.G., Zaelke, D., Ramanathan, V., 2015. Soot and short-lived pollutants provide political opportunity. Nat. Clim. Chang. 5, 796–798.
Viktória, K.K., Mihály, P., János, L., 2006. Nanostructure of atmospheric soot particles. Atmos. Environ. 40, 5533–5542.
Volkamer, R., Jimenez, J.L., San Martini, F., Dzepina, K., Zhang, Q., Salcedo, D., Molina, L.T., et al., 2006. Secondary organic aerosol formation from anthropogenic air pollution: rapid and higher than expected. Geophys. Res. Lett. 33 (17). http://dx.doi.org/10.1029/2006GL026899.
Waldheim, L., Monis, M., Verde Leal, M.R., 2000. Biomass power generation: sugar cane bagasse and trash. Progress in Thermochemical Biomass Conversion:pp. 509–523 http://dx.doi.org/10.1002/9780470694954.ch41.
Wang, S.X., Zhang, C.Y., 2008. Spatial and temporal distribution of air pollutant emissions from open burning of crop residues in China. Science Online. 5, pp. 329–333 (in Chinese).
Wang, T., Cheung, T.F., Li, Y.S., Yu, X.M., Blake, D.R., 2002. Emission characteristics of CO, NOx, SO_2 and indications of biomass burning observed at a rural site in eastern China. J. Geophys. Res. Atmos. 107 (D12). http://dx.doi.org/10.1029/2001JD000724.
Wang, T., Guo, H., Blake, D.R., Kwok, Y.H., Simpson, I.J., Li, Y.S., 2005a. Measurements of trace gases in the inflow of South China Sea background air and outflow of regional pollution at Tai O, Southern China. J. Atmos. Chem. 52 (3), 295–317.
Wang, Y., Zhuang, G., Tang, A., Yuan, H., Sun, Y., Chen, S., Zheng, A., 2005b. The ion chemistry and the source of $PM_{2.5}$ aerosol in Beijing. Atmos. Environ. 39 (21), 3771–3784.
Wang, Q., Xu, M., Xia, Y., 2006. Experimental study on transformation of mineral elements of inhaled particulate matters during co-combustion of coal with biomass. Proceedings-Chinese Society of Electricals Engineering. 26(16), p. 103.
Wang, Q., Shao, M., Liu, Y., William, K., Paul, G., Li, X., Liu, Y., et al., 2007a. Impact of biomass burning on urban air quality estimated by organic tracers: Guangzhou and Beijing as cases. Atmos. Environ. 41 (37), 8380–8390.
Wang, Q., Xu, M., Yao, H., Dai, L., 2007b. Co-combustion characteristics of biomass with coal and its effect on inhaled particulate matters emission. Proceedings of the CSEE. 1 (in Chinese).
Wang, G., Kawamura, K., Xie, M., Hu, S., Cao, J., An, Z., Waston, J.G., et al., 2009a. Organic molecular compositions and size distributions of Chinese summer and autumn aerosols from Nanjing: characteristic haze event caused by wheat straw burning. Environ. Sci. Technol. 43 (17), 6493–6499.
Wang, Q., Shao, M., Zhang, Y., Wei, Y., Hu, M., Guo, S., 2009b. Source apportionment of fine organic aerosols in Beijing. Atmos. Chem. Phys. 9 (21), 8573–8585.
Wang, S., Zhao, M., Xing, J., Wu, Y., Zhou, Y., Lei, Y., He, K., et al., 2010. Quantifying the air pollutants emission reduction during the 2008 Olympic Games in Beijing. Environ. Sci. Technol. 44 (7), 2490–2496.
Wang, W., Jariyasopit, N., Schrlau, J., Jia, Y., Tao, S., Yu, T., Dashwood, R.H., et al., 2011. Concentration and photochemistry of PAHs, NPAHs, and OPAHs and toxicity of $PM_{2.5}$ during the Beijing Olympic Games. Environ. Sci. Technol. 45 (16), 6887–6895.
Wang, Z., Hu, M., Yue, D., He, L., Huang, X., Yang, Q., Zheng, J., et al., 2013. New particle formation in the presence of a strong biomass burning episode at a downwind rural site in PRD, China. Tellus B:65 http://dx.doi.org/10.3402/tellusb.v65i0.19965.
Wang, H., An, J., Shen, L., Zhu, B., Pan, C., Liu, Z., Liu, X., et al., 2014. Mechanism for the formation and microphysical characteristics of submicron aerosol during heavy haze pollution episode in the Yangtze River Delta, China. Sci. Total Environ. 490, 501–508.
Wang, H., Qiao, L., Lou, S., Zhou, M., Chen, J., Wang, Q., Tao, S., et al., 2015a. $PM_{2.5}$ pollution episode and its contributors from 2011 to 2013 in urban Shanghai, China. Atmos. Environ. 132, 298–305.
Wang, L., Xin, J., Li, X., Wang, Y., 2015b. The variability of biomass burning and its influence on regional aerosol properties during the wheat harvest season in North China. Atmos. Res. 157, 153–163.
Wang, D., Zhou, B., Fu, Q., Zhao, Q., Zhang, Q., Chen, J., Yang, X., et al., 2016a. Intense secondary aerosol formation due to strong atmospheric photochemical reactions in summer: observations at a rural site in eastern Yangtze River Delta of China. Sci. Total Environ. 571, 1454–1466.
Wang, H., An, J., Shen, L., Zhu, B., Xia, L., Duan, Q., Zou, J., 2016b. Mixing state of ambient aerosols in Nanjing city by single particle mass spectrometry. Atmos. Environ. 132, 123–132.
Wardoyo, A.Y., Morawska, L., Ristovski, Z.D., Marsh, J., 2006. Quantification of particle number and mass emission factors from combustion of Queensland trees. Environ. Sci. Technol. 40 (18), 5696–5703.
Warneke, C., De Gouw, J.A., Goldan, P.D., Kuster, W.C., Williams, E.J., Lerner, B.M., Jakoubek, R., et al., 2004. Comparison of daytime and nighttime oxidation of biogenic and anthropogenic VOCs along the New England coast in summer during New England Air Quality Study 2002. J. Geophys. Res. Atmos. 109 (D10). http://dx.doi.org/10.1029/2003JD004424.
Wehner, B., Berghof, M., Cheng, Y.F., Achtert, P., Birmili, W., Nowak, A., Wiedensohler, A., et al., 2009. Mixing state of nonvolatile aerosol particle fractions and comparison with light absorption in the polluted Beijing region. J. Geophys. Res. Atmos. 114 (D2). http://dx.doi.org/10.1029/2008JD010923.
Wei, S., Shen, G., Zhang, Y., Xue, M., Xie, H., Lin, P., Chen, Y., et al., 2014. Field measurement on the emissions of PM, OC, EC and PAHs from indoor crop straw burning in rural China. Environ. Pollut. 184, 18–24.
Wex, H., Hennig, T., Salma, I., Ocskay, R., Kiselev, A., Henning, S., Massling, A., et al., 2007. Hygroscopic growth and measured and modeled critical super-saturations of an atmospheric HULIS sample. Geophys. Res. Lett. 34 (2). http://dx.doi.org/10.1029/2006GL028260.
Wieser, U., Gaegauf, C.K., 2000. Nanoparticle Emissions of Wood Combustion Processes. Centre of Appropriate Technology and Social Ecology.
Wigder, N.L., Jaffe, D.A., Saketa, F.A., 2013. Ozone and particulate matter enhancements from regional wildfires observed at Mount Bachelor during 2004–2011. Atmos. Environ. 75, 24–31.
Williams, A., Jones, J.M., Ma, L., Pourkashanian, M., 2012. Pollutants from the combustion of solid biomass fuels. Energy Fuels 38 (2), 113–137.
Winker, D.M., Pelon, J.R., McCormick, M.P., 2003. The CALIPSO mission: Spaceborne lidar for observation of aerosols and clouds. Third International Asia-Pacific Environmental Remote Sensing Remote Sensing of the Atmosphere, Ocean, Environment, and Space. International Society for Optics and Photonics, pp. 1–11.
Winker, D.M., Vaughan, M.A., Omar, A., Hu, Y., Powell, K.A., Liu, Z., Hunt, W.H., et al., 2009. Overview of the CALIPSO mission and CALIOP data processing algorithms. J. Atmos. Ocean. Technol. 26 (11), 2310–2323.
Wit, M.D., Faaij, A., 2009. European biomass resource potential and costs. Biomass Bioenergy 34 (2), 188–202.
Witte, J.C., Douglass, A.R., Silva, A.D., Torres, O., Levy, R., Duncan, B.N., 2011. NASA A-Train and Terra observations of the 2010 Russian wildfires. Atmos. Chem. Phys. 11 (17), 9287–9301.
World Health Organization, 2010. WHO Guidelines for Indoor Air Quality: Selected Pollutants. World Health Organization.
Wu, Q.Z., Wang, Z.F., Gbaguidi, A., Gao, C., Li, L.N., Wang, W., 2011. A numerical study of contributions to air pollution in Beijing during CAREBeijing-2006. Atmos. Chem. Phys. 11 (12), 5997–6011.
Xie, Y., Ding, A., Nie, W., Mao, H., Qi, X., Huang, X., Xu, Z., et al., 2015. Enhanced sulfate formation by nitrogen dioxide: implications from in situ observations at the SORPES station. J. Geophys. Res. Atmos. 24:12679–12694. http://dx.doi.org/10.1002/2015JD023607.
Xin, J., Wang, Y., Tang, G., Wang, L., Sun, Y., Wang, Y., Hu, B., et al., 2010. Variability and reduction of atmospheric pollutants in Beijing and its surrounding area during the Beijing 2008 Olympic Games. Chin. Sci. Bull. 55 (18), 1937–1944.
Xu, W.Q., Sun, Y.L., Chen, C., Du, W., Han, T.T., Wang, Q.Q., Fu, P.Q., et al., 2015. Aerosol composition, oxidation properties, and sources in Beijing: results from the 2014 Asia-Pacific Economic Cooperation summit study. Atmos. Chem. Phys. 15 (23), 13681–13698.
Yamaji, K., Li, J., Uno, I., Kanaya, Y., Irie, H., Takigawa, M., Komazaki, Y., et al., 2009. Impact of open crop residual burning on air quality over Central Eastern China during the Mount Tai Experiment 2006 (MTX2006). Atmos. Chem. Phys. 696 (1), 69–80.
Yan, X., Ohara, T., Akimoto, H., 2006. Bottom-up estimate of biomass burning in mainland China. Atmos. Environ. 40 (27), 5262–5273.
Yang, M., Howell, S.G., Zhuang, J., Huebert, B.J., 2009. Attribution of aerosol light absorption to black carbon, brown carbon, and dust in China-interpretations of atmospheric measurements during EAST-AIRE. Atmos. Chem. Phys. 9 (6), 2035–2050.
Yang, Y., Chan, C.Y., Tao, J., Lin, M., Engling, G., Zhang, Z., Zhang, T., et al., 2012. Observation of elevated fungal tracers due to biomass burning in the Sichuan Basin at Chengdu City, China. Sci. Total Environ. 431 (5), 68–77.
Yang, Y.R., Liu, X.G., Qu, Y., An, J.L., Jiang, R., Zhang, Y.H., Sun, Y.L., et al., 2015. Characteristics and formation mechanism of continuous hazes in China: a case study during the autumn of 2014 in the North China plain. Atmos. Chem. Phys. 15 (14), 8165–8178.
Yang, H., Chen, J., Wen, J., Tian, H., Liu, X., 2016. Composition and sources of $PM_{2.5}$ around the heating periods of 2013 and 2014 in Beijing: implications for efficient mitigation measures. Atmos. Environ. 124, 378–386.
Yao, H., Song, Y., Liu, M., Xu, T., Li, J., Wu, Y., Hu, M., et al., 2016a. Direct radiative effect of carbonaceous aerosols from crop residue burning during the summer harvest season in East China. Atmos. Chem. Phys. Discuss.
Yao, L., Yang, L., Chen, J., Wang, X., Xue, L., Li, W., Sui, X., et al., 2016b. Characteristics of carbonaceous aerosols: impact of biomass burning and secondary formation in summertime in a rural area of the North China Plain. Sci. Total Environ. 520-530.
Yin, Z., Ye, X., Jiang, S., Tao, Y., Shi, Y., Yang, X., Chen, J., 2015. Size-resolved effective density of urban aerosols in Shanghai. Atmos. Environ. 133-140.
Yokelson, R.J., Crounse, J.D., DeCarlo, P.F., Karl, T., Urbanski, S.P., Atlas, E., Campos, T., et al., 2009. Emissions from biomass burning in the Yucatan. Atmos. Chem. Phys. http://dx.doi.org/10.5194/acp-9-5785-2009.
Yu, C., Lin, C., Wei, T., 2010. Observations of carbon monoxide mixing ratios at a mountain site in central Taiwan during the Asian biomass burning season. Atmos. Res. 95 (95), 270–278.
Yu, L., Wang, G., Zhang, R., Zhang, L., Song, Y., Wu, B., Li, X., et al., 2013a. Characterization and source apportionment of $PM_{2.5}$ in an urban environment in Beijing. Aerosol Air Qual. Res. 13 (2), 574–583.
Yu, X., Shi, C., Ma, J., Zhu, B., Li, M., Wang, J., Yang, S., et al., 2013b. Aerosol optical properties during firework, biomass burning and dust episodes in Beijing. Atmos. Environ. 475-484.
Yuan, B., Liu, Y., Shao, M., Lu, S., Streets, D.G., 2010. Biomass burning contributions to ambient VOCs species at a receptor site in the Pearl River Delta (PRD), China. Environ. Sci. Technol. 44 (12), 4577–4582.
Yuan, B., Hu, W., Shao, M., Wang, M., Chen, W., Lu, S., Zeng, L., et al., 2013. VOC emissions, evolutions and contributions to SOA formation at a receptor site in eastern China. Atmos. Chem. Phys. 13 (17), 8815–8832.
Zauscher, M.D., Wang, Y., Moore, M.J.K., Gaston, C.J., Prather, K.A., 2013. Air quality impact and physicochemical aging of biomass burning aerosols during the 2007 San Diego wildfires. Environ. Sci. Technol. 47 (14), 7633–7643.
Zeng, X., Ma, Y., Ma, L., 2007. Utilization of straw in biomass energy in China. Renew. Sust. Energ. Rev. 11 (5), 976–987.
Zha, S., 2013. Agricultural fires and their potential impacts on regional air quality over China. Aerosol Air Qual. Res. 3, 992–1001.
Zhang, T., 2011. Prospect of biomass energy and its potential usage in electrical power generation in China. New Energy. 56-58 (in Chinese).
Zhang, Y., Cao, F., 2015a. Fine particulate matter ($PM_{2.5}$) in China at a city level. Sci. Rep.-Uk 5:14884. http://dx.doi.org/10.1038/srep14884.

Zhang, Y., Cao, F., 2015b. Is it time to tackle $PM_{2.5}$ air pollutions in China from biomass-burning emissions? Environ. Pollut. 202, 217–219.
Zhang, J., Smith, K.R., 2007. Household air pollution from coal and biomass fuels in China: measurements, health impacts, and interventions. Environ. Health Perspect. 848–855.
Zhang, Y., Tao, S., 2008. Seasonal variation of polycyclic aromatic hydrocarbons (PAHs) emissions in China. Environ. Pollut. 156 (3), 657–663.
Zhang, R., Suh, I., Zhao, J., Zhang, D., Fortner, E.C., Tie, X., Molina, L.T., et al., 2004. Atmospheric new particle formation enhanced by organic acids. Science 304 (5676), 1487–1490.
Zhang, M., Yuan, Y., Liu, Y., 2005. Research on biomass waste combustion technologies. Energy Research and Information. 2 (in Chinese).
Zhang, Y., Min, S., Zhang, Y., Zeng, L., He, L., Bin, Z., Wei, Y., et al., 2007. Source profiles of particulate organic matters emitted from cereal straw burnings. J. Environ. Sci. 19 (2), 167–175.
Zhang, H., Ye, X., Cheng, T., Chen, J., Yang, X., Wang, L., Zhang, R., 2008a. A laboratory study of agricultural crop residue combustion in China: emission factors and emission inventory. Atmos. Environ. 42 (36), 8432–8441.
Zhang, R., Khalizov, A.F., Pagels, J., Zhang, D., Xue, H., McMurry, P.H., 2008b. Variability in morphology, hygroscopicity, and optical properties of soot aerosols during atmospheric processing. Proc. Natl. Acad. Sci. 105 (30), 10291–10296.
Zhang, T., Claeys, M., Cachier, H., Dong, S., Wang, W., Maenhaut, W., Liu, X., 2008c. Identification and estimation of the biomass burning contribution to Beijing aerosol using levoglucosan as a molecular marker. Atmos. Environ. 42 (29), 7013–7021.
Zhang, Y.H., Hu, M., Zhong, L.J., Wiedensohler, A., Liu, S.C., Andreae, M.O., Wang, W., et al., 2008d. Regional integrated experiments on air quality over Pearl River Delta 2004 (PRIDE-PRD2004): overview. Atmos. Environ. 42 (25), 6157–6173.
Zhang, Y., Dou, H., Chang, B., Wei, Z., Qiu, W., Liu, S., Liu, W., et al., 2008e. Emission of polycyclic aromatic hydrocarbons from indoor straw burning and emission inventory updating in China. Ann. N. Y. Acad. Sci. 1140 (1), 218–227.
Zhang, Q., Streets, D.G., Carmichael, G.R., He, K.B., Huo, H., Kannari, A., Klimont, Z., et al., 2009a. Asian emissions in 2006 for the NASA INTEX-B mission. Atmos. Chem. Phys. 9 (14), 5131–5153.
Zhang, Y., Tao, S., Shen, H., Ma, J., 2009b. Inhalation exposure to ambient polycyclic aromatic hydrocarbons and lung cancer risk of Chinese population. Proc. Natl. Acad. Sci. U. S. A. 106 (50), 21063–21067.
Zhang, Y., Wang, X., Chen, H., Yang, X., Chen, J., Allen, J.O., 2009c. Source apportionment of lead-containing aerosol particles in Shanghai using single particle mass spectrometry. Chemosphere 74 (4), 501–507.
Zhang, G., Li, J., Li, X., Xu, Y., Guo, L., Tang, J., Lee, C., et al., 2010a. Impact of anthropogenic emissions and open biomass burning on regional carbonaceous aerosols in South China. Environ. Pollut. 158 (11), 3392–3400.
Zhang, M., Wang, X., Chen, J., Cheng, T., Wang, T., Yang, X., Gong, Y., et al., 2010b. Physical characterization of aerosol particles during the Chinese New Year's firework events. Atmos. Environ. 44 (39), 5191–5198.
Zhang, Z., Engling, G., Lin, C., Chou, C.C., Lung, S.C., Chang, S., Fan, S., et al., 2010c. Chemical speciation, transport and contribution of biomass burning smoke to ambient aerosol in Guangzhou, a mega city of China. Atmos. Environ. 44 (26), 3187–3195.
Zhang, H., Hu, D., Chen, J., Ye, X., Wang, S.X., Hao, J.M., Wang, L., et al., 2011a. Particle size distribution and polycyclic aromatic hydrocarbons emissions from agricultural crop residue burning. Environ. Sci. Technol. 45 (13), 5477–5482.
Zhang, J., Yao, F., Liu, C., Yang, L., Boken, V.K., 2011b. Detection, emission estimation and risk prediction of Forest fires in China using satellite sensors and simulation models in the past three decades-an overview. Int. J. Environ. Res. Public Health 8 (8), 3156–3178.
Zhang, H., Wang, S., Hao, J., Wan, L., Jiang, J., Zhang, M., Mestl, H.E., et al., 2012. Chemical and size characterization of particles emitted from the burning of coal and wood in rural households in Guizhou, China. Atmos. Environ. 51, 94–99.
Zhang, Y., Shao, M., Lin, Y., Luan, S., Mao, N., Chen, W., Wang, M., 2013. Emission inventory of carbonaceous pollutants from biomass burning in the Pearl River Delta Region, China. Atmos. Environ. 76, 189–199.
Zhang, H., Zhu, T., Wang, S., Hao, J., Mestl, H.E., Alnes, L.W., Aunan, K., et al., 2014a. Indoor emissions of carbonaceous aerosol and other air pollutants from household fuel burning in Southwest China. Aerosol Air Qual. Res. 14 (6), 1779–1788.
Zhang, W., Zhu, T., Yang, W., Bai, Z., Sun, Y.L., Xu, Y., Yin, B., et al., 2014b. Airborne measurements of gas and particle pollutants during CAREBeijing-2008. Atmos. Chem. Phys. 14 (1), 301–316.
Zhang, Y.L., Li, J., Zhang, G., Zotter, P., Huang, R.J., Tang, J.H., Wacker, L., et al., 2014c. Radiocarbon-based source apportionment of carbonaceous aerosols at a regional background site on Hainan Island, South China. Environ. Sci. Technol. 48 (5), 2651–2659.
Zhang, T., Wooster, M.J., Green, D.C., Main, B., 2015a. New field-based agricultural biomass burning trace gas, $PM_{2.5}$, and black carbon emission ratios and factors measured in situ at crop residue fires in Eastern China. Atmos. Environ. 121, 22–34.
Zhang, Y.J., Tang, L.L., Wang, Z., Yu, H.X., Sun, Y.L., Liu, D., Qin, W., et al., 2015b. Insights into characteristics, sources, and evolution of submicron aerosols during harvest seasons in the Yangtze River delta region, China. Atmos. Chem. Phys. 15 (3), 1331–1349.
Zhang, Y.X., Zhang, Q., Cheng, Y.F., Su, H., Kecorius, S., Wang, Z.B., Wu, Z.J., et al., 2015c. Measuring morphology and density of internally mixed black carbon with SP2 and VTDMA: new insight to absorption enhancement of black carbon in the atmosphere. Atmos. Meas. Tech. Discuss. 8 (11), 12025–12060.
Zhang, J.K., Cheng, M.T., Ji, D.S., Liu, Z.R., Hu, B., Sun, Y., Wang, Y.S., 2016a. Characterization of submicron particles during biomass burning and coal combustion periods in Beijing, China. Sci. Total Environ. 812-821.
Zhang, L., Liu, Y., Hao, L., Zhang, L., Liu, Y., Hao, L., 2016b. Contributions of open crop straw burning emissions to PM2.5 concentrations in China. Environ. Res. Lett. 11 (1). http://dx.doi.org/10.1088/1748-9326/11/1/014014.
Zhang, Y., Lin, Y., Cai, J., Liu, Y., Hong, L., Qin, M., Zhao, Y., et al., 2016c. Atmospheric PAHs in North China: spatial distribution and sources. Sci. Total Environ. 565, 994–1000.
Zhao, Y., Nielsen, C.P., Lei, Y., McElroy, M.B., Hao, J., 2011. Quantifying the uncertainties of a bottom-up emission inventory of anthropogenic atmospheric pollutants in China. Atmos. Chem. Phys. 5 (11), 2295–2308.
Zhao, B., Wang, P., Ma, J.Z., Zhu, S., Pozzer, A., Li, W., 2012. A high-resolution emission inventory of primary pollutants for the Huabei region, China. Atmos. Chem. Phys. 12 (1), 481–501.
Zheng, M., Salmon, L.G., Schauer, J.J., Zeng, L., Kiang, C.S., Zhang, Y., Cass, G.R., 2005. Seasonal trends in $PM_{2.5}$ source contributions in Beijing, China. Atmos. Environ. 39 (22), 3967–3976.
Zhou, D., Dai, Y., Yu, C., Guo, Y., Zhu, Y., 2003. China's Sustainable Energy Scenarios in 2020. China Environmental Science Publishing Company.
Zhou, D., Ding, A., Mao, H., Fu, C., Wang, T., Chan, L.Y., Ding, K., Zhang, Y., Liu, J., Lu, A., Hao, N., 2013. Impacts of the East Asian monsoon on lower tropopsheric ozone over coastal South China. Environ. Res. Lett. 8 (4). http://dx.doi.org/10.1088/1748-9326/8/4/044011.
Zhou, D., Ding, A., Mao, H., Fu, C., Wang, T., Chen, L.Y., Ding, K., Zhang, Y., Liu, J., An, L., Hao, N., 2015. Impact of the East Asian monsoon on lower tropospheric ozone over coastal South China. Environ. Res. Lett. 8 (4), 575–591.
Zhu, J., Xia, X., Che, H., Wang, J., Zhang, J., Duan, Y., 2016a. Study of aerosol optical properties at Kunming in southwest China and long-range transport of biomass burning aerosols from North Burma. Atmos. Res. 169, 237–247.
Zhu, Y., Yang, L., Chen, J., Wang, X., Xue, L., Sui, X., Wen, L., et al., 2016b. Characteristics of ambient volatile organic compounds and the influence of biomass burning at a rural site in Northern China during summer 2013. Atmos. Environ. 124, 156–165.
Zhu, Y., Zhang, J., Wang, J., Chen, W., Han, Y., Ye, C., Li, Y., et al., 2016c. Distribution and Sources of Air pollutants in the North China Plain Based on On-Road Mobile Measurements. Atmos. Chem. Phys. Discuss. http://dx.doi.org/10.5194/acp-2016-410.
Zong, Z., Chen, Y., Tian, C., Fang, Y., Wang, X., Huang, G., Zhang, F., et al., 2015. Radiocarbon-based impact assessment of open biomass burning on regional carbonaceous aerosols in North China. Sci. Total Environ. 518-519, 1–7.